

# **Rubber-Layered Clay Nanocomposites**

*Thesis submitted to the  
Cochin University of Science and Technology  
In the partial fulfillment  
of the requirements for the award of the degree of  
**Doctor of Philosophy**  
in Polymer Science  
Under the Faculty of Technology*

*By*

**Ansu Jacob**



**DEPARTMENT OF POLYMER SCIENCE AND RUBBER TECHNOLOGY  
COCHIN UNIVERSITY OF SCIENCE AND TECHNOLOGY  
KOCHI 22, KERALA, INDIA  
MAY 2008**

**DEPARTMENT OF POLYMER SCIENCE AND RUBBER TECHNOLOGY  
COCHIN UNIVERSITY OF SCIENCE AND TECHNOLOGY  
KOCHI-682 022, INDIA.**

**Dr. Philip Kurian**  
Professor

Phone: 0484-2575723 (Off)  
0484-2575590 (Res)  
E-mail: pkurian@cusat.ac.in

**CERTIFICATE**

This is to certify that the thesis entitled “**Rubber-Layered Clay Nanocomposites**” which is being submitted by Mrs. Ansu Jacob in partial fulfillment of the requirements for the award of the degree of Doctor of Philosophy, to the Cochin University of Science and Technology, Kochi-22 is a record of the bonafide research work carried out by her under my guidance and supervision, in the Department of Polymer Science and Rubber Technology, Kochi-22, and no part of the work reported in the thesis has been presented for the award of any degree from any other institution.



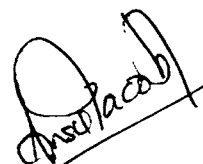
**Dr. Philip Kurian**

Kochi 22  
12 May 2008

## DECLARATION

I hereby declare that the work presented in this thesis entitled “**Rubber-Layered Clay Nanocomposites**” is based on the original research work carried out by me under the guidance and supervision of Dr. Philip Kurian, Professor, Department of Polymer Science and Rubber Technology, Kochi 22 and no part of the work reported in this thesis has been presented for the award of any degree from any other institution.

Kochi -22  
12 May 2008



**Ansu Jacob**

## **Acknowledgements**

*The completion of my thesis would not have been possible without the assistance of many people who gave their support in different ways. I cannot recall how many times I said "thank you" during these years. To these people I would like to express my gratitude and sincere appreciation. Here, I would like to distinguish and express my special thanks*

*To Prof. Dr. Philip Kurian, Professor, Dept. of Polymer Science and Rubber Technology, my supervising guide, for the effective guidance, support, encouragement and understanding throughout the entire work*

*To Dr. Thomas Kurian, Head of the Department, Polymer Science and Rubber Technology, and former Heads of the Department Prof. Dr. K.E. George and Prof. Dr. Rani Joseph for providing me the necessary facilities*

*To the faculty members of the Department of Polymer Science and Rubber Technology, Prof. Dr. Eby Thomas Thachil, Dr. Sunil K Narayanankutty, non-teaching staffs & librarian for their good wishes and support*

*To Dr. Abi Santhosh Aprem, Deputy Manager, Hindustan Latex Ltd., Trivandrum for the support provided to me during early stages of my work*

*To Dr. Chandrasekharan, Professor, Department of Biotechnology, CUSAT for the facilities & my room mate Ms. Jissa for the help provided to me to do the antibacterial studies*

*To Ms. Vijutha, Department of Physics, CUSAT for the XRD results and Mr. Jobin Jose, IIT, Kharagpur for the TEM analysis*

*To all my co-researchers, especially Bipinbal, Saritha, Bhuvaneshwary Teacher, Parameswaran Sir, Leny Teacher, Vijayalekshmi, Julie, Dhanya, Abhilash, Anna, Zeena,*

*Nimmy, Vidya, Neena, Reshmi and Ajilesh for the fruitful interactions and supports provided to me*

*To my senior researchers, Prema Teacher, Mary Teacher, Joshy Sir, Sreenivasan Sir, Raju Sir, Dr. Aswathy K. V, Dr. Maya K.S and Dr. Nisha V. S. for their co-operation, suggestions and support given to me during my research work*

*To my family members especially my parents, my brother, Anish Jacob and my husband, Jim Zachariah for their support, encouragement and love.*

*Above all, I thank God Almighty for His blessings for the successful completion of my research work.*

*Ansu Jacob*

## *PREFACE*

Composites that exhibit a change in composition and structure over a nanometre scale have shown remarkable property enhancements relative to conventional composites. Because of their nanometer size filler dispersion, nanocomposites exhibit markedly improved properties when compared to the pure polymers or their traditional composites. Improved barrier properties, higher mechanical properties, improved flame retardancy and increased dimensional stability have been achieved in polymer nanocomposites. The interest stems not only from their use in the practical applications, such as sporting equipments and under the hood automobile components, but also from the fundamental issues relative to the nanoscale constraints on the polymer and the ultra-large specific interfacial area between the constituents.

Worldwide, there has been a new desire to tailor the structure and composition of materials in nanometre scale. This resulted in the generation of nanocomposites. The design of organic-inorganic nanocomposites is a fascinating topic for science and technology and many applications are expected in the field of optics, mechanics, iono-electronics, biosensors and membranes. Unexpected enhancements of properties such as barrier properties, fire resistance and increase of mechanical properties are reported. The primary goal is to enhance the strength and toughness of polymeric components using molecular or nanoscale fillers. Nanocomposites have been found to exemplify even more positive attributes than the predecessors do and thus we are trying to understand what occurs when nanocomposites of a polymer and inorganic nanomaterial are produced. The field of material science has become quite popular and pragmatic with a tremendous lust for composite materials that exhibit the positive characteristics of both the components.

The thesis is divided into seven chapters.

A comprehensive introduction and review of literature pertaining to reinforcement of rubber, layered clay structure, organophilic modification of nanoclays, polymer clay nanocomposite and rubber clay nanocomposites are presented in **Chapter 1**. The scope and objectives of the study are also included in this chapter.

The specifications of the materials and details of the experimental techniques used in this study are given in **Chapter 2**

Effect of interlayer distance of nanoclays in the cure characteristics, mechanical properties and swelling properties of natural rubber are presented in **Chapter 3**. The polymer intercalation can be made more effective by increasing the interlayer distance. The effect of organosilane coupling in improving the compatibility of clay platelets with the rubber organic phase is investigated. The synergistic effect behaviour of carbon black and organoclay is investigated in NR samples.

The transport properties of the natural rubber nanocomposites are discussed in **Chapter 4**. The sorption, diffusion and permeation coefficients are measured. The barrier properties of latex films have a prominent role in dipped goods. Different gas transport models are also applied to describe the behavior of oxygen through rubber-clay nanocomposites in this Chapter.

**Chapter 5** explains the preparation and characterisation of functionalized montmorillonite (MMT) nanoclays with three different surfactants of the quaternary ammonium compound types. The mechanical and transport properties of natural rubber latex nanocomposites prepared with the synthesized nanoclays is studied. Antibacterial properties of the natural rubber latex films against a Gram positive bacterium and a Gram negative bacterium are evaluated. NR-clay nanocomposites with the modified clays are synthesized via mechanical mixing and the effect of these clays on the properties are studied.

**Chapter 6** discusses the preparation and characterisation of nitrile rubber-clay nanocomposites and the effect of the interlayer distance of the clays in the mechanical and swelling behaviour. Effect of organophilic modification on the cure characteristics and mechanical properties of nitrile rubber based nanocomposite is explained in the same chapter.

The summary and conclusion of the study are presented in **Chapter 7**



# CONTENTS

*Page No.*

## **Chapter I**

<b>Introduction</b>	
1.1 Reinforcement of Rubbers	2
1.2 Filler Characteristics	3
1.3 Carbon black	6
1.4 Clays	8
1.5 Natural Rubber	12
1.6 Nitrile Rubber	16
1.7 Polymer-clay Nanocomposites	17
1.8 Nanocomposite Structure	20
1.9 Characterisation of polymer nanocomposites	22
1.10 Preparation of polymer nanocomposite	24
1.11 Rubber-clay nanocomposite	25
1.12 Thermodynamic aspects of rubber clay nanocomposite	29
1.13 Biomedical application of organoclays	32
1.14 Scope and Objectives	33
References	35

## *Chapter 2*

### **Experimental Techniques**

2.1	Materials	43
2.2	Experimental methods	49
	References	61

## *Chapter 3*

### **Natural Rubber Organoclay Nanocomposites**

3.1	Natural rubber – clay nanocomposites	64
3.2	Effect of silane coupling agent	79
3.3	Effects of carbon black on NR-clay nanocomposites	90
3.4	Conclusion	99
	References	101

## *Chapter 4*

### **Natural Rubber Latex Clay Nanocomposites**

4.1	Preparation of NR latex-clay nanocomposites	109
4.2	Characterisation using X-ray diffraction technique	110
4.3	Transmission electron microscopy	111
4.4	Swelling studies	112
4.5	Gas permeability testing	119
4.6	Mechanical properties	123
4.7	Thermal decomposition	124
4.8	Conclusion	125
	References	127

## **Chapter 5**

### **Modification of Nanoclay with Cationic Surfactants and Preparation of Natural Rubber Latex Clay Nanocomposites with Antimicrobial Properties**

5.1	Modification of nanoclay	134
5.2	Modification of natural rubber latex	140
5.3	NR latex (NRL) - organo modified clay nanocomposites as a microbial barrier	143
5.4	Studies on natural rubber organoclay nanocomposites	156
5.5	Conclusion	171
	References	172

## **Chapter 6**

### **Nitrile Rubber Clay Nanocomposites**

6.1	Preparation of nitrile rubber clay nanocomposites	176
6.2	Modified clay based NBR nanocomposites	189
6.3	Conclusion	200
	References	201

## **Chapter 7**

<b>Conclusion</b>	-	203
<b>List of Abbreviations</b>		
<b>List of Symbols</b>		
<b>List of Publications</b>		

# ***Chapter 1***

---

## ***Introduction***

Rubbers in general are seldom used in their pristine form. They are too weak to fulfill practical requirements because of lack of hardness, strength properties and wear resistance. So they are used with a number of other components called compounding ingredients, which improve the processability, performance properties and life of the final product. In most applications, rubber is normally modified by incorporation of fillers to modify properties so that acceptable engineering properties are obtained. The selection of filler used in rubber formulation is made based on the property requirement of the end-product. Typically, carbon black would be used to enhance strength characteristics while mineral fillers provide a more modest strength enhancement at significantly reduced cost [1]. About 5 million metric tons of carbon black is globally consumed each year while only 250,000 tons of the different silica grades, including the highly dispersible silica are used each year [2]. But due to its polluting nature, the ubiquitous black colour of the compounded rubber and its dependence on petroleum feedstock for the synthesis caused researchers to look out for other “white” reinforcing materials. Since silica is not quite reactive to rubber as carbon black, silane coupling agents are used for surface modification of silica particles. However, the curing time of rubber with silica is longer than with carbon black and thus the production time is extended resulting in reduced productivity. Clay, which has been used as cheap filler in the rubber industry, has poor reinforcing capability because of its large particle size and low surface activity.

Recently, the layered silicates have attracted a great deal of interest as nanocomposite reinforcements in rubbers owing to their intrinsically anisotropic character and swelling capabilities. Moreover, these materials possess a high aspect ratio (500-2000)

and a plate-like morphology. Because of their nanometer size filler dispersion, nanocomposites exhibit markedly improved properties when compared to the pure polymers or their traditional composites. Most notable are increased modulus, increased gas barrier properties, increased heat distortion temperature, resistance to small molecule permeation, improved ablative resistance, increase in atomic oxygen resistance and retention of impact strength [3].

The central theme of this thesis is the studies on rubber clay nanocomposites with special reference to the effect of interlayer distance of nanoclays and the effect of surfactants used for the organophilic modification of nanoclay on mechanical properties, cure characteristics and swelling properties of rubber based nanocomposites. The use of nanofillers in natural rubber latex (NRL) was also investigated in order to find the effect on antibacterial properties, tensile strength, modulus and elongation at break of natural rubber latex films. Therefore, a general introduction is provided in the ensuing sections about filler characteristics, clay structure, organophilic modification of clay, rubber nanocomposites and rubbers used for the study. Finally, the motivation and objectives of the present study are listed.

### **1.1 Reinforcement of rubbers**

It has been well known that particle size, structure and surface characteristics of reinforcing materials were the three factors that influence and help to decide their reinforcing ability, and of these factors, particle size of the filler has the most significant influence [4-8]. In the past, where reinforcement of the polymer was not the main concern, different types of clay minerals have been used as fillers to reduce the cost of the host polymer and provide certain properties useful in rubber compounding. A wide range of non-black, particulate fillers is added to rubber compounds to improve the cured physical properties, reduce cost, and impart colour to the rubber product. The chemical composition and its effect on physical properties of the rubber compound typically result in classifying particulate fillers into three broad categories [6]

1. Non-reinforcing or degrading fillers
2. Semi-reinforcing or extending fillers
3. Reinforcing fillers

The term “reinforcement” refers to an improvement in end-use performance of the rubber compound associated with an increase in modulus and in the so-called ultimate properties including tensile strength, tear resistance and abrasion resistance. Reinforcing filler is a particulate material that is able to increase the tensile strength, the tear strength and abrasion resistance of natural/synthetic rubber. Semi-reinforcing filler is a particulate material that is able to moderately improve the tensile strength and the tear strength, but does not improve the abrasion resistance. Non reinforcing filler is unable to provide any increase on these properties and it function only as a diluent [4].

## **1.2 Filler characteristics**

### **1.2.1 Particle size**

Improvement in the physical properties of the rubber vulcanisate is directly related to the particle size of the filler. The increase of modulus and tensile strength is very much dependent on the particle size of the filler; smaller particle size fillers imparting greater reinforcement to the rubber compound than the coarse ones. Since particle size is directly related to the reciprocal of surface area per gram of filler, an increase in surface area that is in contact with the rubber phase probably leads to the increase in reinforcement. Reducing particle size also simply results in a greater influence in polymer-filler interaction. In addition to average particle size, the particle-size distribution also has a significant effect on reinforcement. Particulate fillers with a broad particle-size distribution have better packing in the rubber matrix, which results in a lower viscosity than that provided by an equal volume of filler with a narrow particle-size distribution. Another important concern in reinforcement is the presence of large particles or agglomerates in the rubber. These agglomerates not only reduce

the contact between filler and rubber matrix but also function as failure initiation sites which would lead to premature failure of materials.

### **1.2.2 Particle structure and anisometry of filler aggregate**

In addition to the surface area, the shape of the filler particle is an important factor that affects the performance of a rubber compound. Inorganic and mineral fillers possess considerable differences in particle geometry, depending on the crystal form of the mineral. The minimum anisometry is found with materials that form crystals with approximately equal dimension in the three directions, i.e. isometric particles. More anisometric are particles in which one dimension is much smaller than the two others, i.e. platelets. The most anisometric are particles which have two dimensions much smaller than the third, so that they are rod-shaped. In compounds containing fillers having identical surface area and chemical nature but differing in shape, modulus increases with increasing anisometry [9]. Particles with a high aspect ratio, such as platelets or fibrous particles have a higher surface-to volume ratio, which results in higher reinforcement of the rubber compound. The greatest hardness is also provided by rod-shaped or plate-like particles, which can line up parallel to one another during processing, compared to spherical particles of similar diameter. Particle shape has a more pronounced effect on processing behaviour than on reinforcement potential and provides important benefits in processing. It can also significantly increase modulus due to occlusion or shielding of some of the rubber phase in highly structured fillers such as structural aggregates of carbon black or silica [7].

### **1.2.3 Surface activity**

The particle size of the filler as discussed earlier may be considered as a physical contribution to reinforcement, while filler surface activity provides the chemical contribution. The ability of the filler to react with the polymer results in chemical bonding, which increases strength significantly. In the absence of strong coupling bonds, the polymer is physically absorbed on the surface of the filler, resulting in a reduced mobility of the rubber molecules near the surface of the filler. Polymer-filler

bonding, particularly in the case of carbon black, develops through active sites on the filler surface resulting in 'bound rubber' attached to the filler surface. Bound rubber is regarded as the result of rubber to filler interactions which can be considered as a measure of the surface activity of the black or white filler. The surface activity of the filler is reflected in the mechanical properties of the rubber such as tensile strength, modulus, abrasion and tear resistance [10]. Adhesion between polymer and filler may also be induced by a coupling agent, which participates in the vulcanisation reaction to form polymer-filler networks. This mechanism of increasing strength is well established with both mineral fillers and carbon blacks [4]. Both mechanisms, interfacial adhesion and formation of networks between filler and polymer, lead to the formation of high modulus compounds, which is a very clear indicator that polymer-filler bonding has taken place. The increased modulus occurs as a result of attachment of the rubber to the filler, which has the effect of reduced mobility of the polymer chain. Organosilane coupling agents have been successfully utilized to further increase the physical properties of a number of non-black fillers including calcium silicate, clay, mica, silica and talc [11].

#### **1.2.4 Surface area**

The most important single factor, which determines the degree of reinforcement, is the development of a large polymer - filler interface. It can be provided only by particle of colloidal dimensions. Spherical particles of 1 $\mu$ m in diameter have a specific surface area of 6 m<sup>2</sup>/cm<sup>3</sup>. This constitutes approximately the lower limit for significant reinforcement. The upper limit of useful surface area is of the order of 300-400 m<sup>2</sup>/cm<sup>3</sup> and it is decided on the basis of considerations of dispensability and processability of the uncured compound and serious loss of rubbery characteristics of the composite [12]. The surface area of particulate solid is related to its particle size. If all the particles are considered as spheres of the same size, the surface area  $A_s$ , per gram of filler can be calculated from the equation

$$A_s = 6/dp$$



where  $d$  is the diameter and  $\rho$  the density of the filler particle. In reality, particles have a distribution of size and are usually far from being spherical. Different fillers of the same particle size may not impart the same reinforcement, e.g., carbon black and silica. The shape of particle also may be different for different fillers, viz., spheroidal, cubic/ prismatic, tubular, flaky or elongated. Non – spherical particles can impart better reinforcement [13].

### **1.2.5 Porosity**

Porosity is a characteristic property of carbon black and can be seen with other particulate type of fillers. Filler porosity can affect the properties of the vulcanisate. However, its effect on reinforcement is secondary. In most-cases, the pores are too small for the polymers to enter although some smaller molecules in the compound may do so.

Particulate fillers used in rubber industry in general can be classified as “Black” and “Non-black”, depending on their origin, the former being mostly produced from petroleum feed stock and the latter from mineral sources. The most important particulate fillers being used in rubber industry are carbon black and silica. Silicates, clays, whiting (calcium carbonate) and other mineral fillers are used extensively where a high degree of reinforcement is not essential [12].

### **1.3 Carbon black**

Carbon black (CB) is a colloidal form of elemental carbon. It owes its reinforcing character to its colloidal morphology, the size and shape of the ultimate units, and to its surface properties. The particles of carbon black are not discrete but are fused clusters of individual particles. Carbon blacks are prepared by incomplete combustion or by thermal cracking of hydrocarbons. Carbon blacks are classified into furnace blacks, channel blacks, thermal blacks, lamp black and acetylene black depending on their method of manufacture.

Table 1.1 Properties of Furnace black

Black		Name	Surface area (m <sup>2</sup> /g)	Average particle size (nm)	DBP absorption (cm <sup>3</sup> /g)
ASTM	Type				
N110	SAF	Super abrasion furnace	140	20-25	1.13
N220	ISAF	Intermediate Super abrasion furnace	120	24-33	1.14
N330	HAF	High abrasion furnace	80	28-36	1.02
N550	FEF	Fast extrusion furnace	45	39-55	1.21
N660	GPF	General purpose furnace	37	50-60	0.91
N774	SRF	Semi-reinforcing furnace	28	70-96	0.70

The major types of rubber reinforcing carbon blacks are manufactured by the furnace process. The predominant purpose of furnace type carbon blacks in elastomers is the reinforcement they impart to the vulcanisates [12, 14]. Carbon blacks have reactive organic groups on the surface that cause affinity to rubber. Incorporation of carbon black into rubber gives enhanced modulus, improved fatigue, abrasion resistance and better overall technological properties. Details of a range of furnace blacks generally used for rubber reinforcement are given in table 1.1 [15].

## 1.4 Clays

Clays represent the largest volume of non-black filler used in rubber industry [11]. They are second to carbon black in this respect. Clay minerals are widely used in rubber compounding because of their cost effectiveness in terms of providing beneficial reinforcing and processing properties at a modest cost. The main clay mineral of importance is kaolin (china clay) and the derivative produced by chemical and heat (calcining) treatment. Clay is classified as hard clay if it reinforces rubber and also imparts high modulus, tensile strength, and resistance to abrasion. Clay is considered “soft” if it produced compound with lower physical properties. Several commercial clays have been treated with silane coupling agents to improve their performance in rubber. Since the silane coupling agent provides a means to bond the clay particles to the rubber, increased modulus and tensile strength are obtained. Clay can be formulated to rather high loadings in most elastomers, with soft clays allowing somewhat higher loadings than hard clays. Viscosity builds moderately with loading of clay, but formulations with 150-200 phr (part per hundred rubber) are reported to be feasible [16]. The main factor to be considered in adding clay to most formulations is the reduction in cure rate. This reduction will require the addition of an activator and/or an increase in the dosage of accelerator.

### 1.4.1 Clay structure and cation exchange with surfactants

Clay minerals consist of a group of hydrated layered magnesium or aluminum silicates (phyllosilicates). Each phyllosilicate is essentially composed of two types of sheets, octahedral and tetrahedral, designated O and T, respectively [17-20]. In the corners, three of the four oxygen are attached to adjacent tetrahedrons. These connecting oxygen atoms are arranged in-plane so as to create a net of surfaces with six tetrahedrons arranged in rings. The tetrahedral layers are interlinked at their vertices by metal ions such as Al tetrahedron,  $\text{Si}^{4+}$  is surrounded by four  $\text{O}^{2-}$ ,  $\text{Al}^{3+}$  and  $\text{Mg}^{2+}$ . The connecting cations are arranged in octahedral coordination, with free valences saturated by  $\text{O}^{2-}$  and/or  $\text{OH}^-$  ions. The tetrahedral and octahedral sheets can be stacked

on top of each other to form two basic types of clay structure: TO or TOT. Kaolinite is a common mineral of the non-expanding TO type group. In the kaolinite clay layer, oxygen atoms located at the apices of the silicate tetrahedron of the tetrahedral sheet and hydroxyls of one of the two OH planes of the octahedral sheet are condensed, forming a single plane common to both sheets. In the other basic clay structure, TOT, four main groups can be distinguished: talc-pyrophyllite, smectite (montmorillonite), vermiculite, and kaolinite. Only smectite and vermiculites are expanding type clays. Smectite family includes montmorillonite, hectorite and saponite and they possess excellent intercalation capabilities. Their chemical formulae are shown in table 1.2 [21]. This type of clay is characterized by a moderate negative surface charge. The charge of the layer is not locally constant as it varies from layer to layer and must rather be considered as an average value over the whole crystal. Proportionally, even if a small part of the charge balancing cations is located on the external crystallite surface, the majority of these exchangeable cations are located inside the galleries. When the hydrated cations are ion-exchanged with organic cations such as more bulky alkylammoniums, it usually results in a larger interlayer spacing.

**Table 1.2 Chemical structures of commonly used 2:1 phyllosilicates [21, 22]**

2:1 Phyllosilicate	General formula
Montmorillonite	$M_x[Al_{4-x}M_{gx}](Si_8)O_{20}(OH)_4$
Hectorite	$M_x[Mg_{6-x}Li_x](Si_8)O_{20}(OH)_4$
Saponite	$M_x[Mg_6](Si_{8-x}Al_x)O_{20}(OH)_4$

M = monovalent charge compensating cation in the interlayer

x = degree of isomorphous substitution (between 0.5-1.3)

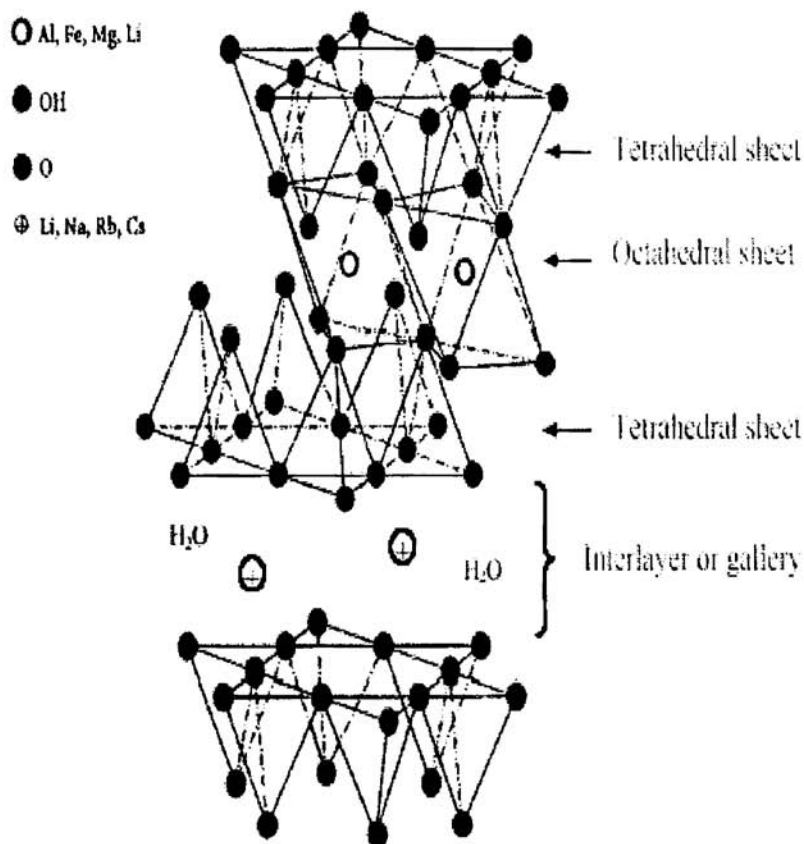


*Figure 1.1 Structure of layered nanoclay*

The most commonly used layered silicates for the preparation of polymer-clay nanocomposites belong to the TOT family, in particular montmorillonite (MMT), shown in figure 1.1. The layer thickness is around 1 nm, and the lateral dimensions of these layers can vary from 100 nm to several microns. Stacking of the layers leads to a regular van der Waals gap between the layers called interlayer or gallery. The isomorphous substitution within the layers, Al<sup>3+</sup> in the aluminate sheet with Mg<sup>2+</sup>,

generates negatively charged layers, which are then balanced by alkali and alkaline earth cations ( $\text{Na}^+$ ,  $\text{K}^+$ ,  $\text{Ca}^{2+}$ ) to maintain charge neutrality [17]. These cations are arranged in between the parallel-superimposed layers. One particular characteristic of these silicate layers is a moderate surface charge known as cation exchange capacity (CEC), generally expressed as meq/100 g. This charge is not locally constant; it varies from layer to layer, and must be considered as an average value over the whole crystal [23].

#### **1.4.2 Organophilic modification of clay**

Montmorillonite is originally hydrophilic, and must be converted to hydrophobic or organophilic type in order to make it compatible with polymer matrices. Normally, this can be done through ion exchange of the inorganic cations for organic ones such as from surfactants and polyelectrolytes. Ion exchange reactions depend on the CEC of the clay. The organic cations lower the surface energy, and improve the wetting and intercalation of the polymer matrix, resulting in a larger interlayer spacing. Additionally, the organic cations may provide functional groups that can react with monomer or polymer to enhance interfacial adhesion between the clay nanolayers and polymer matrix [24, 25].

After the clay is organically modified, the most common technique used to analyze the clay is X-ray diffraction (XRD) technique, which allows the interlayer 'd' spacing, the distance between the basal layers of the montmorillonite (MMT) clay or any layered material, to be measured. In organoclays, a displacement of the peak to lower angles, which corresponds to an increase in interlayer distance, is obtained. Other important techniques used are Fourier Transmission Infrared spectroscopy (FTIR), which gives some additional peaks due to organoclay and Thermogravimetric analysis (TGA), which also give some additional peaks attributed to the liberation of the modifying groups.

## 1.5 Natural rubber (NR)

Natural rubber is chemically cis 1, 4 polyisoprene; its structure is given in figure 1.2. Cis 1, 4 polyisoprene is the only natural product in the rubber family. It has been identified in about 200 plant species, but only the species *Hevea brasiliensis* is of commercial significance. From the tree, it is collected in the form of latex by tapping. This rubber contains more than 99% of its double bonds in the cis configuration which is essential for elasticity in polyisoprene. Even though there is a synthetic analogue of NR, over 90% of the cis - 1, 4 - polyisoprene used industrially is natural Hevea rubber [26]. 1, 4 polymerization of the conjugated diene system of isoprene monomer leads to a polymer structure with a repeating alkene double bond in the polymer chain (figure 1.2).

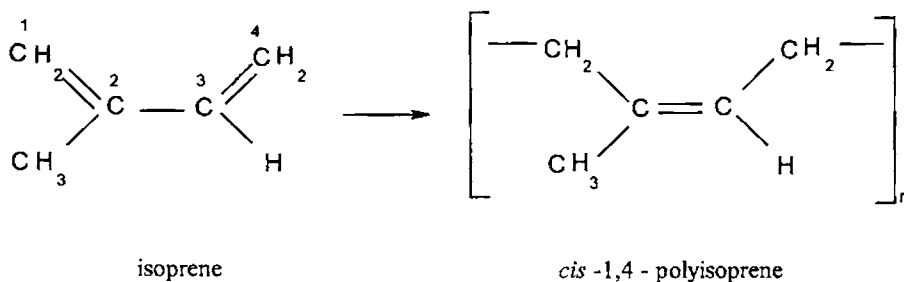


**Figure 1.2 Structure of natural rubber**

Rubber is separated from the latex by coagulation usually by acidification. The resultant coagulum is then processed into different marketable forms of NR such as sheet rubber, technically specified rubber and crepe rubber.

The molecular weight of polymer ranges from 200,000 to 600,000 with a relatively broad molecular weight distribution. Today more than 80% of the total world production of natural rubber comes from Southeast Asia. Malaysia is the largest producer, followed by Indonesia. Thailand accounts for much of the remainder in this area [27]. Rubber is collected in the form of latex that extrudes from the bark of the tree when it is cut. The average rubber content of field latex may range between 30-

45%. This fresh 'field' latex is not utilized in its original form due to its high water content and susceptibility to bacterial attack. It is necessary both to preserve and concentrate the latex, so that the end product is stable and contains 60 % or more of dry rubber. Latex concentrates are differentiated by the method of concentration, and type of preservative used. Concentration is achieved by centrifugation (most common), creaming or evaporation. Currently, about 50% of all latex concentrate is consumed by the dipped goods industry. About 63% of this is contributed by natural rubber latex (table1.3). Other uses of latex are in foam matrices, carpet backing, thread and adhesives.

*Table1.3 Global usage of materials for dipping (%)*

---

Natural rubber latex	63%
Polyvinyl chloride	15%
Carboxylated nitrile rubber latex	7.5%
Polyurethane dispersions	6%
Polychloroprene latex	3.5%
Silicone rubber	2.8%
Heat sensitive latex	1.5%
Styrene butadiene latex	0.5%
Polycarbonate	0.1%
Cellulose	0.1%

---



### **1.5.1 Latex properties**

Natural rubber latex basically consists of a dispersed phase containing rubber particles (cis 1, 4 polyisoprene) and other non-rubber components in minor quantities, and the dispersing medium, water, which contains several organic substances and mineral salts. Rubber particles are formed by aggregation of molecules of rubber hydrocarbon and they have a spherical, oval, pear-like and various other constricted forms [7].

Particle sizes range from 0.1 to 4  $\mu\text{m}$ . These latex particles are stabilized in the aqueous system by the presence of a film of adsorbed carboxylic anions from fatty acid soaps and protein molecules. The adsorbed anions cause the particle surface to have a net negative electrical charge which produces inter-particle repulsive forces and hence ensures absence of aggregation and stability of the latex. Natural rubber latex concentrates are highly specified materials and are characterized by a number of properties that are significant to the user [28].

#### **1.5.1.1 Total solid content (TSC)**

TSC is the amount of rubber and all non-rubber constituents determined by evaporation of latex and expressed as a weight percentage of the weight of latex.

#### **1.5.1.2 Dry rubber content (DRC)**

Amount of rubber and part of the non-rubber constituents determined by precipitation of latex with acid under standardized conditions and expressed as a weight percentage of the weight of latex is the DRC.

#### **1.5.1.3 Alkalinity**

The total alkalinity of the latex is expressed as grams of ammonia per 100 g of water in the latex.

#### **1.5.1.4 Potassium hydroxide (KOH) number**

In ammonium-preserved latex, KOH number is defined as the number of grams of potassium hydroxide equivalent to the acids present as ammonium salts in a quantity

of latex containing 100 g of total solids. The KOH number has a twofold significance. First, it is regarded as a general index of quality of the latex. The higher the KOH number means poorer the quality of the latex. Activity of microorganisms tends to produce acids which, in the presence of ammonia, form ammonium salts. Second, the KOH number gives the minimum quantity of potassium hydroxide which must be added to the latex in order to ensure the virtual absence of ammonium ions.

#### **1.5.1.5 Volatile fatty acids (VFA) number**

Volatile fatty acids measured in the VFA test consist primarily of acetic and formic acids. These are present as a result of bacterial activity in the latex. The VFA number of latex is defined formally as the number of grams of potassium hydroxide equivalent to the steam-volatile fatty acids which are produced by the acidification of latex containing 100 g of solids. The VFA number also provides a good guide to latex quality.

#### **1.5.1.6 Mechanical stability time (MST)**

The mechanical stability time of latex is one of the most important measures of latex stability and indicates the resistance of the latex to aggregation destabilization by shear forces. Shear forces are encountered in operations such as pumping, transportation, compounding and processing of the latex. The general procedure for mechanical stability determination is to stir a defined amount of latex under given conditions of dilution, temperature and speed of stirring, then measure the time which elapses before signs of incipient agglomeration appear. The mechanical stability time is expressed in seconds.

#### **1.5.1.7 Sludge content**

Sludge content refers to non-polymer impurities which tend to sediment under the influence of gravity. They are dirt, sand, bark fragments and magnesium ammonium phosphate.

The rubber solid content and the alkalinity are considered relatively fixed properties, if properly stored, these properties should remain largely unchanged. In contrast, properties such as KOH number, VFA number and MST are time dependent and also depend on the effectiveness of preservation, handling procedures and storage.

### **1.5.2 Latex types**

In principle, Hevea latex has been classified according to the methods used for their concentration and stabilization. High ammonia (HA) latex, containing 0.7% ammonia in the latex, is still the most frequently used material. More than 60 percent of centrifuged latex is of the high ammonia type. However, in recent years, the trend has been toward the use of low ammonia (LA) lattices, in particular the LA-TZ (low ammonia-tetramethylthiuram disulfide, TMTD-zinc oxide) which ensure good colour and chemical stability of the films and a low toxicity of the latex. The two-component system serves as a secondary stabilizing agent, in which one component zinc oxide acts as an enzyme poison and the other component TMTD has bactericidal properties. The low ammonia latex contains 0.2% of ammonia, with the addition of 0.2% of sodium pentachlorophenolate (LASPP latex), 0.2% of boric acid (LA-BA latex) or 0.1% of zinc diethyldithiocarbamate (LA-ZDC latex). The use of LA latex should reduce ammonia in the factory environment and also eliminate the deammoniation step required in some latex processing, resulting in cost saving. These merits are now increasingly being recognized.

### **1.6 Nitrile rubber (NBR)**

Nitrile rubber (NBR) is a copolymer of acrylonitrile and butadiene and it is a polar rubber. NBR has good resistance to a wide variety of oils and solvents and hence is widely used for the manufacture of products like oil seals, oil hoses, pipe protectors, blow out preventors etc [15]. Nitrile rubbers are manufactured by emulsion copolymerisation of butadiene with acrylonitrile. Major properties of NBR depend on the acrylonitrile content (ACN) and usually vary from 20-50% by weight.

Commercially available nitrile rubbers differ from one another in three respects: acrylonitrile content, polymerization temperature and Mooney viscosity.

### **1.7 Polymer-clay nanocomposites**

Composites with more than one solid phase with a dimension in the 1-20 nm range are defined as nanocomposites [22, 29-31]. Nanometer is an atomic dimension and hence the properties of nanoclusters or particles are reflective of atoms rather than bulk materials. Moreover adjusting the size can control the energy level spacing and other properties, but it is still large compared to the atomic limit. Recent studies show that it may be possible to combine the nanocrystal into nanocrystal molecules and nanocrystal solids in the same way as one does with real atoms; and these solids comprise tens to thousand of atoms and have dimensions in nanometer (<10 nm) range. An example for nanocomposite in nature is the natural bone consisting of approximately 30% matrix material and 70% nanosized mineral. Here the matrix material is collagen fibers (polymer) and the mineral is hydroxyapatite crystals of 50 nm x 25 nm x 3 nm size (ceramic). In conventionally filled polymers, the constituents are immiscible and this results in a coarsely blended macrocomposite with chemically distinct phases. This results in poor physical attraction between the organic and inorganic components, leading to the agglomeration of the latter and therefore weaker materials. In addition, the microscale particles act as stress concentrates, whereas in nanocomposites, chemically dissimilar components are combined on a nanoscale and the nanofillers are too small to be stress concentrators.

Nanoscale materials have currently attracted a great deal of attention due to their interesting chemical and physical properties. The modified nano-sized systems are nanocomposites, nanocrystals, nanotubes, cluster assembled materials, quantum boxes, etc [32, 33]. All these systems improve the interest of scientists in this field. Polymer nanocomposites have been making a splash in the media and throughout several industries of late. In nanoparticles, the matrix encloses randomly distributed particles or randomly composed aggregates of particles. Here, the matrix is usually

polymer, which is able to passivate various materials and prevent particle aggregation, while maintaining a good spatial dispersion of the particles. Polymers are expected to provide good mechanical properties, conferring high kinetic stability to nanoparticles [34].

The outstanding reinforcement of nanocomposites is primarily attributed to the large interfacial area per unit volume or weight of the dispersed phase (e.g.  $750 \text{ m}^2/\text{g}$ ). The nanolayers have much higher aspect ratio than typical microscopic aggregates [22, 17, 18]. Mineral clays which can be dispersed as silicate nanolayers of high aspect ratio are attractive for polymer reinforcements. Polymer-clay nanocomposites have shown considerable enhancements in mechanical properties (modulus and strength) [35-38], thermal properties (heat resistance and flammability) [39, 40] barrier properties [30, 41-46], and biodegradability [47, 48] of the pure polymer. Their unique properties stem from a combination of factors: the platelet structure of nanolayer clay, the high aspect ratio (width to thickness) of the platelets with thicknesses of the order of a nanometer and widths and lengths of the order of 500-2000, and the molecular bonds formed between the platelets and the polymer during compounding that may modify polymer properties.

Some polymer-clay nanocomposite products have already been developed that are being used commercially for certain applications. These include automotive [49] and packaging film [50] applications with nylon nanocomposites. Other nanocomposite systems that have been extensively reported in the literature include polymer matrices such as polystyrene, poly (methyl methacrylate), polyolefins, poly(ethylene oxide), polyimide, poly(vinyl pyrrolidone) and epoxy.

The three major advantages that nanocomposites have over conventional composites are as follows:

1. Lighter weight due to low filler loading,
2. Low cost due to fewer amounts of filler use and

3. Improved properties (includes mechanical, thermal, optical, electrical, barrier, etc.) compared with conventional composites at very low loading of filler.

Three types of nanocomposites can be distinguished depending upon the number of dimensions of the dispersed particles in the nanometer range [22] as follows:

1. Isodimensional nanofillers result when the three dimensions are in the order of nanometers, such as spherical silica nanoparticles obtained by in-situ solgel methods [51, 52] or by polymerization promoted directly from their surface [53].
2. When two dimensions are in the nanometer scale while the third is larger, an elongated structure result, as for example, carbon nanotubes [54, 55] or cellulose whiskers [56, 57], which are extensively studied as reinforcing nanofillers yielding materials with exceptional properties.
3. The third type of nanocomposites is characterized by only one dimension in the nanometer range. Here the filler is in the form of sheets of one to a few nanometer thick to hundreds to thousands nanometers long. Clays and layered silicates belong to this family and the composites are known as polymer-clay nanocomposites (PCNs) or polymer-layered silicate nanocomposites.

The fundamental principle of polymer clay nanocomposite formation is that the polymer should penetrate into the intergalleries of the clay i.e., the space between the platelets (layered galleries) of the silicate should be made accessible for the polymer chains. As the distance between the layers of pristine clays is less than 1nm it does not allow the penetration of the polymer molecules therein. The layer distance can be enlarged by cation exchange with suitable intercalant because the silicate layers are negatively charged. To support intercalation and exfoliation (i.e., further and complete layer expansion respectively) the layer distance should be greater than 1.5 nm. This is usually achieved with ammonium salts, which render the surface of the silicate organophilic. The hydrophilic nature of the layered silicates requires that the surface of the clay be modified to improve the wettability and dispersibility in the polymer

matrix. Because of the weak interactions between the nanolayers, the cations can be easily exchanged with alkylammonium cations, thus making the layered silicate compatible with the polymer matrix. Replacement of alkali cations by long chain alkyl groups containing onium ions introduces hydrophobic character into the clay surfaces and reduces the electrostatic interaction between clay layers which encourages the penetration of polymer precursor into the interlayer galleries leading to the formation of nanocomposites [58]. The inorganic relatively small (sodium) ions are exchanged against more voluminous organic onium cations. It was also reported that morphology and properties of nanocomposites are often greatly influenced by the properties of the modifying group. The length of the alkyl ammonium cations (modifying groups) [59] and the presence of double bonds [60] are crucial factors for the preparation of exfoliated polymer clay nanocomposites.

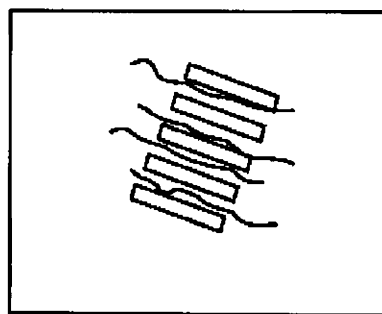
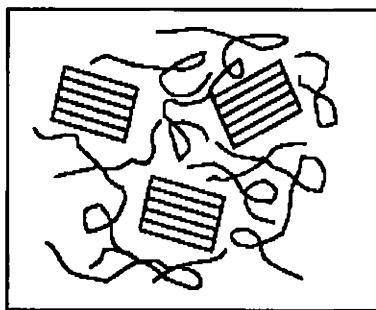
Extensive research has been devoted to the understanding of ion exchange and adsorption of surfactant molecules into the clay surface and gallery since organoclays are used in many industrial applications. This technique is applied in applications like thickeners in paints, oil-based glue, grease and cosmetic products [17, 61]. The negatively charged clay layers attract the organic cations primarily by electrostatic forces. In addition, van der Waals forces act between the flat oxygen planes and the organic species located in the interlayers. With increasing size of the adsorbed organic cation, there is an increase in the sorption energy as the van der Waals contribution to the adsorption process becomes more significant [17]. Due to the increase in the van der Waals interactions, montmorillonites have high affinity towards long chain organic cations. Many surfactants including primary, secondary, tertiary and quarternary alkylammonium cations are water soluble and most cation exchange reactions are performed in aqueous suspensions.

### **1.8 Nanocomposite structure**

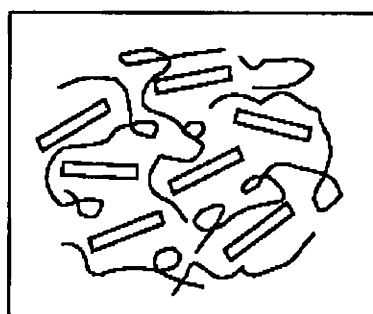
Three main types of composites may be obtained when layered clay is associated with a polymer [22, 30]. These primarily depend on the method of preparation and the

nature of components used such as layered silicates, organic cation and polymer matrix. When the polymer is unable to intercalate between the silicate layers, a phase separated polymer-silicate composite is obtained (figure 1.3a). This conventional composite contains clay tactoids of stacked layers in a coplanar orientation, that are associated in aggregates and agglomerates dispersed as a segregated phase. Their properties stay in the same range as those seen for traditional microcomposites. Beyond this classical family of composites, two types of nanocomposites are possible, intercalated and exfoliated.

a) Phase separated



b) Intercalated



c) Exfoliated

**Figure 1.3 Schematic representations of different polymer-silicate hybrid structures**



Intercalated structures in which typically more extended polymer chains are pictured as occupying the interlayer space between silicate layers resulting in a well ordered multilayer morphology of alternating polymeric and inorganic layers (figure 1.3b). When the silicate layers (1 nm thick) are completely and uniformly dispersed in a continuous polymer matrix, an exfoliated or delaminated structure is obtained (figure 1.3c).

Favourable interactions between the polymer matrix and clay surface and the resulting energy reduction are critical for the formation of exfoliated nanocomposites. Although highly desirable, exfoliation is challenging and requires fine tuning of the clay surface chemistry as well as synthesis and processing conditions. The less desirable but more attainable structure is intercalated particle dispersion where the polymer chains penetrate into the interlayer region of clay layers to form nanocomposites without totally disrupting the crystallites. Along with partial exfoliation and partial intercalation, partial confined structures are also possible for rubber clay nanocomposites. This may be due to formation of coordination complex, which occurs in accelerated sulphur vulcanisation in presence of zinc oxide. Note that zinc oxide is prone to form coordination complex in which amine groups of the intercalant and sulphur of the sulphuric curatives may participate [62-65]. The amine functionality of the intercalant when removed from the interlayer to participate in the formation of a Zn-based complex along with sulphur results in close-up of the silicate galleries.

### **1.9 Characterisation of polymer nanocomposites**

The improvement in properties for nanocomposites is related to the dispersion and nanostructure of the layered silicate in the polymer. Therefore, it is of paramount importance to determine whether or not the exfoliation and intercalation of pristine layered silicates can be achieved. There are several techniques that are used to elucidate the nanostructure of polymer layered silicate nanocomposites including atomic force microscopy (AFM) [66], Nuclear magnetic resonance spectroscopy (NMR) [67, 68], neutron scattering method [69], Scanning electron microscopy

(SEM), Transmission electron microscopy (TEM) and X-ray diffraction techniques. However TEM and XRD are the most commonly used techniques. With the help of these techniques immiscible, intercalated, exfoliated and confined structures can be characterised.

X rays like visible light exhibit a wave nature. The wavelength of light can be measured using a diffraction grating, which consists of a series of lines separated by a distance of roughly one wavelength ( $\lambda$ ) of the monochromatic light. When a monochromatic beam of light falls on the grating, the light waves emerging from the grating interfere with one another, to either amplify or eliminate the light in a particular direction and finally give alternately dark and bright bands on the screen. In a crystal lattice, the molecules are seated in a well-defined and repetitive pattern and can act as a diffraction grating. Similarly in an intercalated nanocomposite, the galleries form a periodic structure and their periodicity can be measured by XRD technique. The 'd' spacing observed by XRD for the nanocomposites have been used to describe the nanoscale dispersion of the clay in the polymer. XRD parameter 'd' is calculated using the Bragg formula

$$n\lambda = 2d \sin \theta$$

where  $\lambda$  corresponds to the wave length of the X - ray radiation used in the diffraction experiment, 'd' the spacing between diffraction lattice planes and  $\theta$  is the measured diffraction angle or glancing angle. The aim of the XRD results is to show the presence or the absence of Bragg diffraction peaks characteristic of intercalation, that is only the layer period measured on the nanocomposite are compared to those of the organoclay alone. This structure and properties of layered silicate nanocomposites are usually studied by wide angle X-ray diffraction (WAXD). WAXD is usually considered to be at angles ( $2\theta$ ) of  $1^\circ$  or higher. Angles below  $1^\circ$  are measured with small angle XRD. Bragg peaks in the WAXD curve with greater Bragg periods with respect to the organoclay are the indicators of the presence of intercalated structures. Intercalated nanocomposites with gallery height up to about 4 nm (with resolution

limit of typical instruments used) can be resolved using this technique [70]. Exfoliated nanocomposite shows no peak by XRD, suggesting that a great amount of polymer has entered the gallery space, expanding the clay layers so far apart that the difference cannot be observed with wide angle ( $2\theta > 1^\circ$ ) XRD technique [60]. Exfoliated structures are formed when the lamellae are fully dispersed in the matrix polymer. Here the polymer matrix separates the individual galleries of the clay mineral and they are not characterised by a regular, periodic arrangement. But in it, the inorganic lamellae covered by the surface modifying organic layer form particles with different electron densities with respect to that of the matrix polymer therefore they can be detected from the lowest angle fraction of the X-ray scattering curve, small angle X-ray diffraction (SAXS) [71]. Immiscible materials give no change in 'd' spacing meaning that no polymer has entered the gallery and thus the spacing between the clay layers is unchanged. In confinement the distance between the layers is reduced and hence 'd' spacing lower than the initial value will be obtained.

### **1.10 Preparation of polymer nanocomposite**

Clays have been extensively used in the polymer industry as fillers to reduce the amount of the polymers used to shape structures thereby lowering the high cost of the polymer systems. The efficiency of clay as a reinforcing agent to modify the physicomechanical properties of the polymer is determined by the degree of dispersion in the polymer matrix, which in turn depends on the particle size. However, the hydrophilic nature of the clay surfaces impedes their homogeneous dispersion in the organic polymer phase. Several attempts have been done to improve the dispersion of clay in the polymer matrix, which include:

1. Impregnation of the clay by monomers followed by their polymerization.
2. Direct adsorption of uncharged linear polymers onto a clay surface.
3. Grafting of polymers onto the available hydroxyl group on clay surfaces through coupling agents.

However these methods are based on physical adsorption which depends on the desorption of the hydration water molecules, or surface grafting processes [72]. Thus the polymers do not penetrate between the clay interlayer and do not homogeneously disperse with each other, because the enthalpy change of the process is commonly very small which does not lead to high adsorption. The nanoscale materials that often exhibit different physical and chemical properties from their bulk counterparts have recently received considerable interest.

Polymer clay nanocomposites are currently prepared in the following ways

- solution blending
- latex compounding
- direct intercalation of the molten polymer (melt intercalation) and
- in-situ polymerization

As most of the rubbers are available in solid (dry) and latex (solution) forms, melt and latex intercalations are considered to be the industrially feasible methods for preparing rubber nanocomposites. Although the in-situ polymerization route is viable, it is not used with rubbers at present.

### **1.11 Rubber-clay nanocomposite**

Until recently research involving layered silicates of synthetic and natural origin for the property modification of polymers was mostly devoted to thermoplastics, [22,73-77] and thermosetting resins [22,73,76,78,79] However, elastomers and rubbers are very promising polymeric matrices for the preparation of polymer clay nanocomposites because of the following reasons [80]

1. It is well known that amine compounds act as curing reaction activators in sulfur containing rubber recipes [81]. Thus, polymer clay nanocomposites intercalated by amine compounds may interact with the sulfur curatives thereby promoting thermodynamically favoured interactions between the

rubber chains and the silicate layers leading to increased intercalation/exfoliation.

2. Rubbers exhibit high melt viscosities during melt mixing because of their high molecular weight and this paves the path for generation of high shear stresses for the shearing and peeling apart of the silicate layers.
3. Further, the swelling of pristine and organophilic clays in both aqueous and organic solutions makes it amenable for the preparation of rubber clay nanocomposites via the latex and solution routes.

Nanocomposites have some unique outstanding mechanical property with respect to their conventional microcomposite counterparts.

Arroyo et al. reinforced natural rubber with 10 phr of unmodified clay and octadecylamine -modified MMT (organoclay) and compared the results with natural rubber loaded with 10 and 40 phr carbon black (Spheron 6400) [82]. The organoclays behaved as an effective reinforcement agent for NR and showed a stronger reinforcing effect than carbon black while retaining the elasticity of the rubber. The mechanical behaviour of natural rubber with 10 phr organoclay was comparable with the compound with 40 phr carbon black. Sadhu and Bhowmick prepared a series of nanocomposites by mixing nitrile rubber (19, 34, and 50 weight % of acrylonitrile), styrene butadiene rubber (23% bound styrene) and polybutadiene rubber (BR) with unmodified and octadecylamine modified clays [83]. The mechanical properties of the rubber-clay nanocomposites were correlated with TEM and XRD. In all the cases, the nanocomposites showed improved mechanical properties and the extent of the increase in strength varied from 38 to 166% depending on the nature of the base rubber and its polarity, packing and orientation of the rubber chains and the clay particles. Joly et al. observed that organically modified galleries of MMT were easily penetrated by natural rubber chains and led to intercalated structures along with partial exfoliation [84]. Modulus increase comparable to that achieved by high loadings of conventional micrometersized fillers was observed at 10 wt% organically modified

MMT loading demonstrating the advantages of high surface area of the filler and the better interface adhesion between the polymer and clay.

Evaluation of the cure characteristics of rubber nanocomposites with organoclays shows the prominent accelerating effect of the modifying group [82, 85-87]. Lopez-Manchado et al. studied the effect of incorporation of unmodified and organically modified bentonite clay on the vulcanisation kinetics of NR by Cure Meter testing and Differential scanning calorimetry (DSC) under dynamic and isothermal conditions [87]. The cure kinetic studies performed by both techniques demonstrated that the clay hardly affected the crosslinking reaction of NR, but a strong increase in cure rate was observed when the organically modified clay was added to the rubber. A significant decrease in the induction time and optimum cure time of the elastomer were observed in the NR-organoclay nanocomposite. In a recent study, onium ion-modified MMT (organoclay) at 2–10 phr loading was shear mixed with NR in an internal mixer [88]. Both scorch time and cure time was reduced with the incorporation of the organoclay. The increment in maximum torque, minimum torque, and increase in torque with increasing filler content indicated the enhancement of stiffness of the nanocomposite.

Application of a small amount of intercalated clay to the rubber matrix can provide considerable improvement in barrier performance. This behaviour is observed for various rubber articles containing highly compressed air, such as inner tubes for pneumatic tyres, air springs, curing bladders for tyre curing presses [89]. Toyota group synthesized intercalated NBR-clay nanocomposites (4% clay by volume) which had hydrogen and water vapor permeability 30% lower than pure rubber [90]. Nah et al. [91] prepared an intercalated clay-acrylonitrile butadiene copolymer nanocomposite having better barrier properties by melt intercalation method. The air permeability decreases considerably with increasing clay content. NBR clay nanocomposite having better barrier performance was reported to be prepared from their latex very easily and cheaply by following a latex method. Compared to gum NBR vulcanisate, the nitrogen permeability of the NBR clay nanocomposite, prepared from compounded latex, with

10, 20 and 30 phr of clay was reduced by 29 %, 41% and 48 %, respectively. Similar barrier properties were also observed by Wu et al. [92] with 10% clay by volume, nitrogen permeability decreased by almost 50%. The nanocomposites also showed enhanced tensile strength and modulus [93].

Zhang et al [94] first introduced a latex route for the preparation of nanocomposites. The molecular weight of the rubber is higher than plastic; it had a very high viscosity in the processing stage. Most of the rubbers had latex forms and could blend with clay dispersion in water without coagulation. Some layered silicates are suitable additives for latex provided that they can form dispersions adequate for latex compounding. In aqueous dispersions, the clay swells, its layers are separated by hydration, which makes its good dispersion in the rubber possible. Varghese and Karger-Kocsis prepared NR based nanocomposites with 10 wt% natural (sodium bentonite) and synthetic (sodium fluorohectorite) layered silicates by the latex compounding method [95]. Wang et al. prepared NR-MMT and chloroprene rubber (CR) -MMT nanocomposites by coagulating the rubber latex and the aqueous clay suspension [96]. TEM showed that the clay layers were dispersed in the NR matrix at the nano level but XRD studies indicated that there were some nonexfoliated MMT layers in the NR matrix. The presence of more than 10 phr nanoclay inhibited the strain-induced crystallization of NR. Compared with the carbon black filled NR composites, NR-MMT nanocomposites exhibited high hardness, high modulus, high tear strength, and excellent antiaging and gas barrier properties.

Stephen et al. studied the impact of layered silicates such as sodium bentonite and sodium fluorohectorite on the rheological behaviour of NR, carboxylated SBR (CSBR) lattices, and their blends with special reference to shear rate, temperature and filler loading [97]. They observed that the viscosity of the layered silicates increased with increasing filler concentration and also exhibited pronounced shear thinning behaviour. Viscosity enhancement due to the addition of the nanofillers indicated a

more uniform distribution of clay particles and higher extent of silicate exfoliation on a nano scale.

### **1.12 Thermodynamic aspects of rubber clay nanocomposite**

To achieve reinforcement, partial exfoliation or intercalation, the layers of the silicates have to be completely separated from one another in the matrix polymer. Major driving force for this is of thermodynamic origin [101]. This is governed by terms of Gibbs equation,

$$\Delta H - T\Delta S < 0$$

where H, T and S denote the enthalpy, temperature and entropy respectively. For small favourable internal energy changes, intercalated states are expected. As the change in internal energy becomes more negative the tendency to form exfoliated hybrids increases. One would expect that the interaction between silicates and polymer chains occurs via entropy loss. This is because the size of the polymer molecules is almost close to the distance between the silicate platelets and thus the penetration of the polymer into the interlayer occurs. Penetration of polymer molecule into the interlayer is associated with some “ordering”, resulting an entropy loss and polymer chains which are initially in an unconstrained environment must enter the constrained environment of the narrow silicate interlayer [99]. This results in a decrease in the overall entropy of the polymer chains as shown in figure 1.4. The entropy loss of the polymer (3-D coil will be transferred into a 2-D structure) is approximately compensated by the entropy gain of surfactant chains attached on the sheet surface [58].



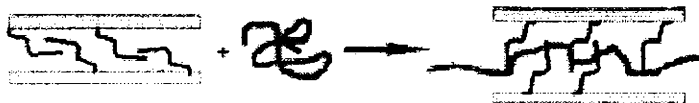


*Figure 1.4 Schematic picture of the situation when a polymer chain is entering the gap between two clay sheets [58]*

But the entropy change per interlayer volume is comprised of two factors: an entropy decrease per interlayer volume associated with confinement of the polymer upon intercalation and an entropy increase per interlayer volume associated with conformational freedom of the aliphatic chains upon layer separation. In earlier works [100], it has been reported that the organic chains gain configurational freedom as the interlayer distance increases and this may compensate for the entropic penalty of the polymer confinement. The interaction between the organic modifiers and the molecules of the polymer matrix will favour the intercalation process of polymer molecules into the interlayers of silicates. Enthalpy reduction can be achieved by special interactions with the matrix molecules like hydrogen bonding, chemical reactions etc. A lattice based mean field theory has been developed by 'Vaia' [100] to understand the impact of the different enthalpies onto the possibility of dispersion of particles in a polymer matrix. Here three different interactions come into focus, namely the polymer-surfactant interaction, the surfactant-filler surface interaction and the polymer-filler surface interaction. The calculations lead to the conclusion that even when the surfactant chains are miscible with the matrix polymer, a complete layer separation depends on the establishment of very favourable polymer surface interactions to overcome the penalty of polymer confinement. By comparing the experimental results with the theoretical predictions of the mean field 'Vaia' later proposed [101] that

1. an optimal interlayer structure of the organically modified silicates, with respect to the number per area and size of the alkyl ammonium chains, is most favourable for hybrid formation and

2. polymer interaction depends on the existence of polar interactions between the organically layered silicates and the polymer.

Initially, the interlayer structure of the organically layered silicates should be optimized to maximize the configurational freedom of the functionalizing chains upon layer separation. The authors suggested that this is because, for small increases in the gallery height, the entropy gain associated with the aliphatic chains approximately nullifies the entropy loss due to polymer confinement. Here, small favourable internal energy changes will lead to free energy decrease and thus hybrid formation. As the gallery height increases, the magnitude of the entropy loss due to polymer confinement increases and the total entropy change decreases. As the number of the aliphatic chains increases, the initial gallery height increases, resulting in a smaller entropic penalty for polymer confinement. Secondly polar polymers containing groups capable of associative-type interactions, such as Lewis-acid/base interaction or hydrogen bonding, lead to intercalation. The greater the polarizability or hydrophilicity of the polymer, the shorter the functionalizing groups in the modified silicates should be to minimize unfavourable interactions between the aliphatic chains and the polymer.

In addition to the above, some other factors favours entropy change of rubber compounds 1) amine compounds is widely used in sulfur curing rubber recipes as accelerators and they are reported to enhance the mobility of the intercalating compounds and 2) the layered structure of silicates can be broken up due to high acting shear forces [102-104]. The breakdown of the layered structure is obviously higher for higher molecular weight polymer and lower mixing temperature. Rubbers are very high molecular weight materials showing extremely high viscosities during melt compounding. High shear stresses support the peel off and thus the delamination of the silicate layers. Thus the production of organophilic silicates using amine intercalants as the organic modifier and the use of high shear stresses for the formation

of rubber nanocomposites can be considered as a thermodynamically favoured process.

### **1.13 Biomedical application of organoclay**

Organoclay based nanocomposites exhibit remarkable improvements in properties when compared with virgin polymer or conventional micro and macro composites. Another important application of organoclays is in adsorption for example, in pollution prevention and environmental remediation such as treatment of chemical spills, waste water and hazardous waste landfills and others [105,106]. Meanwhile, the synthesis and application of clay-based antibacterial materials have attracted great interest due to the worldwide concern about public health [107]. According to the type of antibacterial ions used, antibacterial materials could be divided into two basic types, i.e., inorganic and organic antibacterial materials. In the synthesis of clay-based inorganic antibacterial materials, most antibacterial inorganic cations used are heavy metal such as  $\text{Ag}^+$ ,  $\text{Cu}^{2+}$  and  $\text{Zn}^{2+}$  [108-112]. Each of these cations can function as an antibacterial agent. However, a lot of problems and/or disadvantages arise in the synthesis and application of inorganic antibacterial materials with heavy metals, including 1) accumulation of heavy metals will result in serious environmental problems and may be harmful to humans in the case of high metal concentration; 2)  $\text{Ag}^+$  is not stable in aqueous solution. It tends to be reduced to  $\text{Ag}^0$  when exposed to light or heat or to react with anions (e.g.  $\text{Cl}^-$ ,  $\text{HS}^-$ ,  $\text{SO}_4^{2-}$ ) in water, forming insoluble compounds and losing their antibacterial activity [111]. 3) Heavy metals are easy to be fixed into the hexagonal cavities and the octahedral vacancies in montmorillonite [113], resulting in a decrease of the antibacterial activity.

Although several types of polymer-layered silicate nanocomposite products with different shapes and applications including food packaging films and containers, engine parts, dental materials, etc. are now available in markets [114] polymer-layered

silicate nanocomposites with antimicrobial activity, which will be very much favourable to the nanocomposites applications are rarely seen.

#### **1.14 Scope and objectives**

Today one of the most promising arenas of science and technology is nano technology. Polymer nanocomposites represent a new alternative to conventionally filled polymers, thereby providing the possibility of atomic-level manipulation in materials. Materials that possess nano structures have properties different from those of bulk systems in factors including dimensionality, composition and in their performance. These include modulus and strength, outstanding barrier properties, improved solvent and heat resistance and decreased flammability. Thus they can provide considerable improvement in barrier performance to various rubber articles that contains highly compressed air such as inner tubes for tyres, pneumatic springs for automobiles, curing bladders and rubber bladders for sports goods.

It is reported that acrylic fibers that contain antimicrobial agents such as quaternary ammonium salts has numerous applications including incontinence and sanitary products, mattress covers, wound dressing, hospital drapes and gowns. Since polymer nanocomposites possess active positive cations it can efficiently sterilize bacteria. Thus the scope of polymer nanocomposites in biomaterial applications requires much attention.

The objectives of the present work are

- To prepare and characterise natural rubber-clay nanocomposite
- To study the effect of interlayer distance of layered clays on mechanical properties and swelling resistance of natural rubber-clay nanocomposites
- To study the effect of silane coupling agent on the mechanical properties of natural rubber-clay nanocomposites
- To study the effect of carbon black on natural rubber-clay nanocomposites

## ***Chapter 1***

---

- To prepare and characterise natural rubber latex-unmodified clay nanocomposite
- To study the effect of nanoclays on transport properties of natural rubber latex-unmodified clay nanocomposite
- Organophilic modification of nanoclays using different cationic surfactants
- To study the effect of modified clays on mechanical properties and swelling resistance of dry natural rubber and natural rubber latex based nanocomposites
- To investigate the antibacterial property of natural rubber latex based nanocomposites
- To prepare nitrile rubber based nanocomposites
- To study the effect of interlayer distance of layered clays on mechanical properties and swelling resistance of nitrile rubber-clay nanocomposites
- To study the effect of modified clays on mechanical properties and swelling resistance of nitrile rubber-clay nanocomposites
- Correlation of results

## **References**

1. Katz, H. S. and Milewski, J. V., Handbook of Fillers and Plastics, Van Nostrand Reinhold Co., New York, p 459, 1987.
2. Donnet, J. B., Compos. Sci. Technol., 63, 1085, 2003
3. Messermith, P. B., Ginnaleis, E. P., J. Polm. Sci. Part A Polym. Chem., 33, 1047, 1995.
4. Rothon, R., Editor, Particulate-Filled Polymer Composites, Longman Scientific & Technical, New York, p 371, 1995.
5. Blow, C. M., Editor, Rubber Technology and Manufacture, The Chemical Rubber Co., Ohio, p 509, 1971.
6. Dick, J. S., Editor, Rubber Technology: Compounding and Testing for Performance, Hanser Publishers, p 523, 2001.
7. Eirich, F. R., Editor, Science and Technology of Rubber, Academic Press, NewYork, p 633, 1978.
8. Franta, I., Editor, Elastomers and Rubber Compounding Materials, Elsevier, New York, p 588, 1989.
9. Wang, M. J., Rubber Chem. Technol., 71, 520, 1998.
10. Wolff, S., Rubber Chem. Technol., 69, 325, 1996.
11. Morton, M., Editor, Rubber Technology, 3<sup>rd</sup> ed., Van Nostrand Reinhold Co., New York, p 631, 1987.
12. Medalia, A. I., Kraus, G., In: Science and Technology of Rubber, Eds., Mark J. E., Erman, B. and Eirich R. F., Academic Press, New York, p 387, 1994.

13. Blow, S., In: Handbook of Rubber Technology, Editor, Blow, S., Galgotia Publication Ltd, New Delhi, p 483, 1998.
14. Kraus, G., In: Reinforcement of Elastomers, Editor, Kraus, G., Interscience Publishers, John Wiley & Sons, New York, p 329, 1965.
15. Werner Hofmann, In: Rubber Technology Handbook, Editor, Werner Hofmann, Hanser Publishers, Munich, p 284, 1989.
16. Bateman, L., Chemistry and Physics of Rubber-like Substances, John Wiley & Sons, p 777, 1963.
17. Yariv, S. and Cross, H., Eds., Organo-Clay Complexes and Interactions, Marcel Dekker, New York, 2002.
18. Van Olphen, H., An introduction to Clay Colloid Chemistry, 2<sup>nd</sup> ed., Wiley, New York, 1973.
19. Avena, M. and De Pauli, C., Effect of Structural Charges on Proton Adsorption at Clay Surfaces, Geochemical and Hydrological Reactivity of Heavy Metals in Soils, Eds., Selim, H. and Kingery, W., Lewis Publishers, p 79, 2003.
20. Rohl, W., Rybinski, W. and Schwuger, M., Prog. Coll. Polym. Sci., 84, 206, 1991.
21. Giannelis, E. P. et al., Adv. Polym. Sci, 138, 107, 1999.
22. Alexandre, M. and Dubois, P., Mater. Sci. Eng., 28, 1, 2000.
23. Ray, S. and Okamoto, M., Prog. Polym. Sci., 28, 1539, 2003.
24. Qutubuddin, S. and Fu, X., Polymer-Clay Nanocomposites: Synthesis and Properties, Nano-Surface Chemistry, Editor, Rosoff, M., Marcel Dekker, p 653, 2001.
25. Theng, B. K. G., Formation and properties of clay-polymer complexes., Elsevier, New York, 1979.

26. Odian, G., Principles of Polymerization, John Wiley & Sons, p 749, 1991.
27. Robert, A. D., Editor, Natural Rubber Science and Technology, Oxford Science Publications, p 1078, 1988.
28. Blackley, D. C. High Polymer Lattices: Their Science and Technology:Vol. 2: Testing and Applications, Palmerton Publishing Co., New York, p 843, 1966.
29. Komarneni, S. J., J. Mater. Chem., 2, 1219, 1992.
30. Giannelis, E. P., Adv. Mater., 8, 29, 1996.
31. Ziolo, R. F., Giannelis, E. P., Weinstein, B. A., O' Horo, M. P., Granguly, B. N., Mehrota, V., Russell, M. W. and Hoffman, D. R., Science, 257, 219, 1992.
32. Parson, Cupnik . T. and Davis . J ; M . Phy. Rev., B, 1988, 38, 282.
33. Gauthier, C., Chazeau, L., Prasse, T. and Cavaille, J. Y., Comp. Sci. Tech., 65 (2), 335, 2005.
34. Chun-Wei Chen, Mie Higashi, Taichi Naito and Mitsure Akashi, Chem. Lett., 9, 870, 2001.
35. Kojima, Y., Kawasumi, M., Usuki, A., Okada, A., Fukushima, Y., Kurachi, T. and Kamigaito, O., J. Mater. Res., 8 (5), 1185, 1993.
36. Fu, X. and Qutubuddin, S., Mater. Lett., 42, 12, 2000.
37. LeBaron, P., Wang, Z. and Pinnavaia, T., Appl. Clay Sci., 15, 11, 1999.
38. Vaia, R. Price, G., Ruth, P., Nguyen, H. and Lichtenhan, J. Appl. Clay Sci., 15, 67, 1999.
39. Messersmith, P. B. and Giannelis, E. P., Chem. Mater., 6, 1719, 1994
40. Giannelis, E., Appl. Organomet. Chem., 12, 675, 1998.
41. Yano, K., Usuki, A., Okada, A., Kurauchi, T. and Kamigaito, O., J. Polym. Sci. A: Polym. Chem. 31, 2493, 1993.



42. Lan, T., Kaviratna P. and Pinnavaia, T., *Chem. Mater.*, 6, 573, 1994.
43. Strawhecker, K. E. and Manias, E., *Chem. Mater.*, 12, 2943, 2000.
44. Matayabas, J. and Turner, S., In Pinnavaia T. and Beall, G., Eds., *Polymer-clay Nanocomposites*, Wiley, New York, p 207, 2001.
45. Yano, K., Usuki, A. and Okada, A., *J. Polym. Sci. A: Polym. Chem.*, 35, 2289, 1997.
46. Bharadwaj, R., Mehrabi, A., Hamilton, C., Trujillo, C., Murga, M. Fan, R., Chavira, A. and Thompson, A., *Polymer*, 43, 3966, 2002.
47. Ray, S, Okamoto, K. and Okamoto, M., *Macromolecules*, 36, 2355, 2003.
48. Ray, S., Yamada, K., Okamoto, M., Fujimoto, Y., Ogami, A. and Ueda, K., *Polymer*, 44, 6633, 2003.
49. Nanocomposites showing promise in automotive and packaging roles, *Modern Plastics Magazine*, Feb., 26, 1998.
50. Lange, J. and Wyser, Y., *Packag. Techn. Sci.*, 16, 149, 2003.
51. Mark, J.E., *Polym. Eng. Sci.*, 36, 2905, 1996.
52. Wen, J. and Wilkes, G. L., *Chem. Mater.*, 8, 1667, 1996.
53. Von Werne, T., and Patten, T.E., *J. Am. Chem. Soc.*, 121, 7409, 1999.
54. Calvert, P., In: *Carbon Nanotubes*, Editor, Ebbesen, T.W., CRC Press, Boca Raton, 1992.
55. *Carbon Nanotubes: Synthesis, Structure, Properties and Applications*, Topics of Applied Physics, vol. 80, Eds., Dresselhaus, M.S., Dresselhaus, G. and Avouris, P., Springer-Verlag, Heidelberg, 2001.
56. Favier, V., Canova, G. R., Shrivastava, S. C. and Cavaille, J.Y., *Polym. Eng. Sci.*, 37, 1732, 1997.

57. Chazeau, L., Cavaille, J.Y., Canova, G., Dendievel R. and Bouterin B., *J. Appl. Polym. Sci.*, 71, 1797, 1999.
58. Fischer H., *Polymer nanocomposites: from fundamental research to specific applications*, *Materials Science and Engineering*, C 23, 763, 2003.
59. Vaia, R A., *Polymer melt intercalation in mica-type layered silicates*, PhD Thesis, Cornell University, USA, 1995.
60. Zhang, W. A., Chem, D. Z., Xu, H. Y., Shen, X. F. and Fang, Y. E., *European Polymer Journal*, 39, 2323, 2003.
61. Jones, T. R., *Clay Minerals*, 18, 399, 1983.
62. Chapman, A. V. and Porter, M., In: *Natural Rubber Science and Technology*, Editor, Roberts, A. D., Oxford Science, Oxford, p 511, 1990
63. Krejsa, M. R. and Koenig, J. L., In: *Elastomer Technology Handbook*, Editor, Cheremisinoff, N. P., CRC Press, Boca Raton, FL, p 475, 1993.
64. Karger Kocsis, J., Gremmels, J., Mousa, A., Ishiaku. U. S. and Mohd Ishak, Z. A., *Kautsch Gummi Kunstst*, 53, 528, 2000.
65. Kumar, C. R. and Karger Kocsis, J., *Eur. Polym. J.*, 38, 2231, 2002.
66. Gunter, M., Reichert, P., Mulhaupt, R. and Gronski, W., *Polym. Mater. Sci. Eng.*, 82, 228, 2000.
67. Davis, R. D., Jarrett, W. L. and Mathias, L., *J. Polym. Mater. Sci. Eng.*, 82,272, 2000.
68. VanderHart, D. L., Asano, A. and Gilman, J. W., *Chem. Mater.*,13, 3781, 2001.
69. Krishnamoorti, R., Vaia, R. A. and Giannelis, E. P., *Chem. Mater.*, 8, 1728, 1996.
70. Wagener, R. and Reisinger, T. J. G., *Polymer*, 44, 7513, 2003.
71. Bhattacharya, S. N. and Cser. F., *J. Appl. Polym. Sci.*, 90, 3026, 2003.

72. Akelah, A., El-Deen, S. N., Hiltner, A., Baer, E. and Moet, A., *Mater. Lett.*, 22, 97, 1995.
73. Pinnavaia, T. J., and Beall, G.W., Eds., *Polymer Clay Nanocomposites*, Wiley, New York, 2000.
74. Dennis, H. R., Hunter, D. L., Chang, Kim, S., White, J. L., Cho, J. W. and Paul, D.R., *Polymer*, 42, 9513, 2001.
75. Fornes, T.D., Yoon, P.J., Keskkula, H. and Paul, D.R., *Polymer*, 42, 9929, 2001.
76. Sinha Ray, S. and Okamoto, M., *Prog. Polym. Sci.*, 28, 1539, 2003.
77. Kawasumi, M., Hasegawa, N., Kato, M., Usuki, A. and Okada, A., *Macromolecules*, 30, 6333, 1997.
78. Biswas, M. and Sinha Ray, S., *Adv. Polym. Sci.*, 155, 167, 2001.
79. Karger-Kocsis, J., Gryshchuk, O., Frohlich, J. and Mulhaupt, R., *Compos. Sci. Technol.*, 63, 2045, 2003.
80. Karger-Kocsis, J. and Wu, C.M., *Polym. Eng. Sci.*, 44, 1083, 2004.
81. Roberts A.D., Editor, *Natural Rubber Science and Technology*, Oxford Science Publishers, Oxford, 1990.
82. Arroyo, M., Lopez-Manchado, M.A. and Herrero, B., *Polymer*, 44, 2447, 2003.
83. Sadhu, S. and Bhowmick, A.K., *J. Polym. Sci. Part B: Polym. Phys.*, 42, 1573, 2004.
84. Joly, S., Garnaud, G., Ollitrault, R. and Bokobza, L., *Chem. Mater.*, 14, 4202, 2002.
85. Mousa A. and Karger Kocsis, J., *Macromol. Mater. Eng.*, 286 (4), 260, 2001.
86. Varghese, S. and Karger-Kocsis, J., *J. Appl. Polym. Sci.*, 91, 813, 2004.

87. Lopez Manchando, M. A., Arroyo, M., Herrero, B. and Biagiotti, J., *J. Appl. Polym. Sci.*, 89, 1, 2003.
88. Teh, P. L., Mohd Isak, Z.A., Hashim, A. S., Karger-Kocsis, J. and Ishiaku, U. S., *J. Appl. Polym. Sci.*, 100, 1083, 2006.
89. Gent, A. N. Editor, *Engineering with Rubber; How to Design Rubber Components.*, Chapter 1 and 8, Hanser, 1992.
90. Kojima, Y., Fukumori, K., Usuki, A., Okada, A. and Kurauchi, T., *J. Mater. Sci. Lett.*, 12, 889, 1993.
91. Nah, C., Ryu, H. J., Kim, W. D. and Choi, S. S., *Polym. Adv. Technol.* 13, 649, 2002.
92. Wu, Y., Jia, Q., Yu, D. and Zhang, L., *J. Appl. Polym. Sci.*, 89, 3855, 2003.
93. Kim, J., Oh, T. and Lee, D., *Polym. Int.*, 52, 1058, 2003.
94. Zhang, L., Wang, Y., Suri, Y., Yu, D., *J. Appl. Polym. Sci.* 78, 1873, 2000.
95. Varghese, S. and Karger-Kocsis, J., *Polymer*, 44, 4921, 2003.
96. Wang, Y., Zhang, H., Wu, Y., Yang, J. and Zhang, L., *J. Appl. Polym. Sci.*, 96, 318, 2005.
97. Stephen, R., Alex, R., Cherian, T., Varghese, Joseph, K. and Thomas, S., *J. Appl. Polym. Sci.*, 101, 2355, 2006.
98. Giannelis, E. P., *SPE-ANTEC*, 45, 3966, 1999.
99. Ko, M. B., *Polym. Bull. (Berlin)*, 45, 183, 2000.
100. Vaia, R. and Giannelis, E., *Macromolecules*, 30, 7990, 1997.
101. Vaia, R. and Giannelis, E., *Macromolecules*, 30, 8000, 1997.
102. Fornes, T. D., Yoon, P. J., Keskkula, H. and Paul, D. R., *Polymer*, 42, 9929, 2001.

103. Ko, M. B., Jho, J. Y., Jo, W. H., Lee, M. S., *Fibers Polym.*, 3 (3), 103, 2002.
104. Schon, F., Thomann, R. and Gronski, W., *Macromol. Symp.*, 189, 105, 2002.
105. Zhu, L. Z., Chen, B. L. and Shen, X. Y., *Environ. Sci. Technol.*, 34, 468, 2000.
106. Adebajo, M.O., Frost, R. L., Klopogge, J. T. and Carmody, O., *J. Porous Mater.*, 10,159,2003.
107. Ma, Y. L., Xu, Z. R., Guo, T. and You, P., *J. Colloid Interface Sci.*, 280, 283, 2004.
108. Ohashi, F. and Oya, A., *Appl. Clay Sci.*, 6, 301, 1992.
109. Ohashi, F., Oya, A., Duclaux, L and Beguin, F., *Appl. Clay Sci.*, 12, 435,1998.
110. Li, B. W., Yu, S. H., Hwang, J. Y. and Shi, S. Z., *J. Miner. Mater. Characterisation. Eng.*, 1, 61, 2002.
111. Zhou, Y. H., Xia, M. S., Ye, Y. and Hu, C. H., *Appl. Clay Sci.*, 27, 215,2004.
112. Osinaga, P. W. R., Grande, R. H. M., Ballester, R. Y., Simionato, M. R. L., Rodrigues, C.R.M. and Muench, A., *Dental Mater.*, 19, 212, 2003.
113. He, H. P., Guo, J. G., Xie, X. D. and Pen, J. L., *Environ. Int.*, 26, 347, 2001.
114. Pinnavaia, T. J. and Beal, G. W., *Polymer clay nanocomposites*. 1<sup>st</sup> ed., Wiley, England, 2001.

## *Chapter 2*

---

### *Experimental Techniques*

The materials used for the study, the experimental techniques, and analytical methods employed for characterisation of the nanocomposites are discussed in this chapter.

#### **2.1 Materials**

##### **2.1.1 Natural rubber**

ISNR-5 grade of natural rubber with a Mooney viscosity (ML 1+4, 100 °C) 85 supplied by Rubber Research Institute of India, Kottayam was used for the study. Bureau of Indian Standards (BIS) specification for ISNR-5 is given in table 2.1 [1].

*Table 2.1 BIS specifications of ISNR-5*

<b>Sl. No</b>	<b>Parameters</b>	<b>Limit</b>
1	Dirt content, % by mass, max	0.05
2	Volatile matter, % by mass, max	0.8
3	Nitrogen, % by mass, max	0.6
4	Ash, % by mass, max	0.6
5	Initial plasticity, Po, Min	30
6	Plasticity retention index (PRI), min	60

Natural rubber from the same lot has been used for the entire study since it is known that the molecular weight, molecular weight distribution and type and amount of non rubber constituents present are affected by clonal and seasonal variations, use of yield stimulants and method of preparation [2].

### **2.1.2 Natural rubber latex**

Centrifuged natural rubber latex concentrate with minimum 60% dry rubber content (DRC), preserved with high ammonia (HA) preservative system and conforming to the BIS 5430-1981 specifications was used in the study. BIS specification for the high ammonia latex is given in table 2.2.

*Table 2.2 BIS specifications for natural rubber latex (HA) concentrate*

Sl. No	Parameters	Limit
1	Dry rubber content, % by mass min.	60.040
2	Total solids content, % by mass max.	61.050
3	Coagulum content, % by mass max.	0.030
4	Sludge content, % by mass max.	0.007
5	Alkalinity as ammonia, % by mass	0.730
6	KOH number	0.496

### **2.1.3 Acrylonitrile butadiene rubber (NBR)**

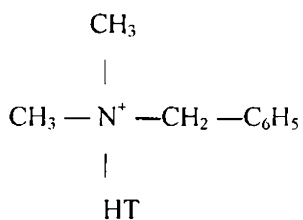
Nitrile Rubber (N-03868) with acrylonitrile content 40 weight percentage supplied by M/s Gujarat Apar polymers Ltd, Mumbai, India was used for the study.

### 2.1.4 Nanoclay

Montmorillonite clays used in this study were provided by Southern clay Products Inc., USA. Unmodified clay used was sodium montmorillonite clay (cloisite Na<sup>+</sup>), which has an ion exchange capacity of 92.6meq/100g clay and an interlayer distance of 11.7Å. Two different types of organically modified nanoclays differing in the interlayer distance and in modifying groups were also used for this study. The interlayer distance of the clays used were 18.3Å, and 30.6Å for cloisite 10A [2MBHT: dimethyl, benzyl, hydrogenated tallow, quaternary ammonium], cloisite 15A [2M2HT: dimethyl, dihydrogenated tallow, quaternary ammonium] respectively.

#### 2.1.4.1 Cloisite 10A

Quaternary ammonium salt with the following structure is used as the modifier for cloisite 10A clay



HT : Hydrogenated Tallow (~65% C18, ~30% C16, ~5% C14)

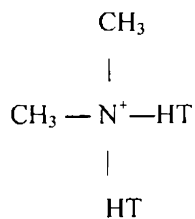
Anion :Chloride

2MBHT: dimethyl, benzyl, hydrogenated tallow, quaternary ammonium

#### 2.1.4.2 Cloisite 15A

Quaternary ammonium salt with the following structure is used as the modifier for cloisite 15A clay





HT : Hydrogenated Tallow (~65% C18, ~30% C16, ~5% C14)

Anion :Chloride

2M2HT: dimethyl, dihydrogenatedtallow, quaternary ammonium

Properties of nanoclay used for the study are given in table 2.3

**Table 2.3 Properties of nanoclays**

Nanoclay	Organic modifier	Ion exchange capacity	% Moisture	% Weight Loss on ignition	Specific Gravity,g/cc
Cloisite 10A	2MBHT	125 meq/100g clay	<2%	39%	1.90
Cloisite 15A	2M2HT	125 meq/100g clay	<2%	43%	1.66
Cloisite Na <sup>+</sup>		92.6 meq/100g clay	<2%	7%	2.86

### **2.1.5 Carbon black**

High Abrasion Furnace black (N330), a product of M/s. Philips Carbon Chemicals Ltd Kochi was used. It had the following specifications

***Table 2.4 Specifications for N330 (HAF) black***

Sl.No	Parameters	Limit
1	Appearance	Black granules
2	DBP absorption (cc/100g)	102
3	Pour density (Kg/m <sup>3</sup> )	376
4	Iodine adsorption number	82
5	Loss on heating (%)	2.5

### **2.1.6 Coupling agent**

The coupling agent used was Si69, a product of Degussa AG, Germany. Chemically Si69 is bis (triethoxysilyl propyl) tetrasulphide and the molecular formula is  $(C_2H_5O)_3-Si(CH_2)_3-S_4-CH_2)_3-Si(OC_2H_5)$ . The specification of Si69 is given in table 2.5 [3].

**Table 2.5 Properties of Silane coupling agent (Si69)**

Sl.No	Parameters	Limit
1	Molecular weight	539.06
2	Sulphur content	22±1%
3	Viscosity at 25 °C	<16.0 cps
4	Flash point	>156 °C
5	Density at 25 °C	1.080-1.10
6	Refractive Index	>1.480

**2.1.7 Other chemicals**

Compounding ingredients used for the study were zinc oxide (activator) supplied by M/s Meta Zinc Ltd. Mumbai; Stearic acid (co-activator) supplied by Godrej Soap (P) Ltd. Mumbai; N-Cyclohexyl-2-Benzothiazole Sulphenamide (CBS) (accelerator) of the class I sulphenamide supplied by Polyolefins Industries Ltd. Mumbai and N (1,3-dimethylbutyl) N-phenyl-*p*- phenylene diamine (anti-oxidant) called Vulkanox PPD supplied by Bayer India Ltd. Mumbai. Quaternary ammonium surfactants viz, Cetyl trimethyl ammonium bromide (CTAB), Cetyl pyridinium chloride (CPC), Benzalkonium chloride (BAC) used for the organophilic modification of the clay were obtained from Loba chemie Pvt. Ltd, Mumbai.

Toluene and Methyl ethyl ketone used in the present investigation were of analytical grade. Methyl methacrylate (MMA) used for the preparation of MMA grafted NR was obtained from Loba chemie Pvt. Ltd, Mumbai.

## **2.2 Experimental methods**

### **2.2.1 Characterisation techniques**

#### **2.2.1.1 Characterisation using X-ray diffraction technique**

X-ray diffraction (XRD) was used to study the nature and extent of dispersion of the clay in the composite. XRD were collected using Bruker, D8 Advance diffractometer at the wavelength  $\text{CuK}\alpha = 1.54 \text{ \AA}$ , a tube voltage of 40 KV and tube current of 25 mA. Bragg's law defined as  $n\lambda = 2d\sin\theta$ , was used to compute the crystallographic spacing (d) for the clay. The samples were scanned in step mode by  $1.0^\circ/\text{min}$ , scan rate in the range of 2 to  $12^\circ$ .

#### **2.2.1.2 Scanning electron microscopy (SEM)**

In SEM, the electron beam incident on the specimen surface causes various phenomena of which the emission of secondary electrons is used for the surface analysis. Emitted electron strikes the collector and the resulting current is amplified and used to modulate the brightness of the cathode ray tube. There is a one to one correspondence between the number of secondary electrons collected from any particular point on the specimen surface and the brightness of the analogous point on the screen and thus an image of the surface is progressively built up on the screen. Scanning electron microscopic studies of the vulcanisates were carried out on the freshly cut surface in a Hitachi SE Microscope (model H 6010). The sample surface was gold coated prior to the examination.

#### **2.2.1.3 Transmission electron microscopy**

The transmission electron microscopy was performed using a JEOL JEM - 2010 (Japan) transmission electron microscope, operating at an accelerating voltage of 200 KV. The samples for TEM analysis were prepared by ultra-cryomicrotomy using a Leica Ultracut UCT. Freshly sharpened glass knives with cutting edge of  $45^\circ$  were used to get the cryosections of 50 - 70 nm thickness. Since these samples were elastomeric in nature, the temperature during ultra cryomicrotomy was kept at  $-70^\circ\text{C}$ .

The cryosections were collected individually on sucrose solution and directly supported on a copper grid of 300-mesh size.

### **2.2.2 Preparation of rubber clay nanocomposites**

The mixing was done on a laboratory size two roll-mixing mill (16 × 33 cm) at a friction ratio of 1:1.25 for natural rubber 1:1.1 for nitrile rubber as per ASTM D 3182-89. A nip gap of 0.2mm was set and the temperature maintained at  $70 \pm 5$  °C. For the mixing of rubber with compounding ingredients, the rubber was passed through the rolls and it was banded over the front roll. After the nerve had disappeared, the compounding ingredients were added as per the procedure given in ASTM D 3184-89 (2001). After mixing, the stock was homogenised by passing through the tight nip of the mill for six times and sheeted out at a nip gap of 3 mm. Mixing time and temperature were controlled during the process.

### **2.2.3 Cure characteristics**

Cure characteristics of the mixes were determined as per ASTM D 2084-1995 using Rubber Process Analyzer, RPA 2000<sup>®</sup>, which is a computer controlled torsional dynamic rheometer with a unique test gap design, an advanced temperature control system and fully automated operation modes. Testing environments employed in the present work are given in table 2.6.

**Table 2.6 Testing parameters used for RPA**

---

Sl.No.	Parameters	Limit
1	Frequency	50 cpm
2	Strain angle	0.20 °
3	Temperature	150 °C
4	Time	30 min.
5	Die Type	Biconical
6	Die Gap	0.487 mm
7	Angle of oscillation of the Die	3°

---

To determine the cure characteristics of the rubber compound, approximately 5 g of the sample was placed in a sealed biconical cavity under pressurized conditions and submitted to harmonic torsional strain by the oscillation of the lower die through a small deformation angle of about 3° and the transmitted torque is measured on the upper fixed wall [4]. The torque transducer on the upper die senses the force being transmitted through the rubber sample. A typical RPA cure curve is shown in the figure 2.1 and the following data can be obtained.

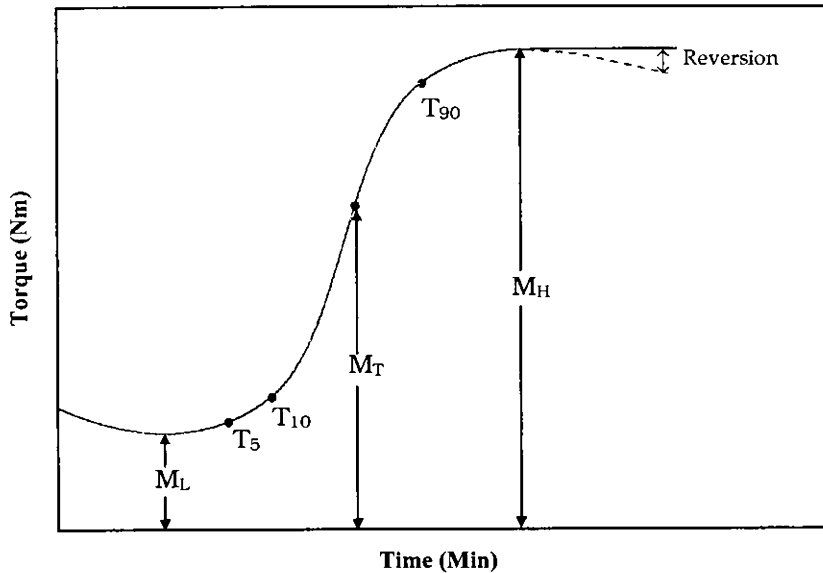


**Figure 2.1 Typical cure curve obtained from the Rubber Process Analyzer, RPA 2000**

Minimum torque,  $M_L$

Torque obtained by mix after homogenising at the test temperature and before the onset of cure.

Maximum torque,  $M_H$

Maximum torque recorded after the curing of the mix is completed.

Torque,  $M_T$

Torque at any given time  $T$

Optimum Cure time,  $T_{90}$

This is the time taken for obtaining 90% of the maximum torque

Scorch time,  $T_{10}$

Time for attaining 10% of the maximum torque

Induction time,  $T_5$

It is the time taken for about 5 % vulcanisation.

Cure rate index

Cure rate index is calculated from the following equation.

$$\text{Cure rate index} = 100 / T_{90} - T_{10}$$

Where,  $T_{90}$  and  $T_{10}$  are the times corresponding to the optimum cure and scorch respectively.

The computer software analyses the cure curve and prints out the data after each measurement.

#### **2.2.4 Moulding**

The test specimens for determining the physical properties were moulded in standard moulds by compression moulding on an electrically heated hydraulic press having 45 cm x 45 cm platen at a pressure of 200 Kg cm<sup>-2</sup>. The rubber compounds were vulcanized up to their respective optimum cure time at 150 °C. Mouldings were cooled quickly in water at the end of the curing cycle and stored in a cool and dark place for 24 hours and were used for subsequent physical tests. Additional curing time based on the sample thickness for samples having thickness higher than 6 mm (hardness) was given to obtain satisfactory cure for the entire thickness of the sample.

#### **2.2.5 Physical testing**

Physical tests such as tensile strength, tear strength, hardness, etc have been carried out on vulcanised rubber to standardize the rubber compounds used in the rubber industry to meet various service requirements and to investigate product or process failures. Physical tests are also utilized for the quality assurance and the quicker prediction of quality of the prepared rubber products. For each tests at least six specimens were tested and the mean values are reported.



### **2.2.5.1 Tensile properties**

The tensile strength is defined as the force per unit area of cross section, which is required to break the test specimen, the condition being such that the stress is substantially uniform over whole of the cross section. The cure conditions giving the highest tensile strength are being widely adopted as optimum cure. The elongation at break (EB) is the maximum value of elongation expressed as a percentage of the original length. The value of tensile stress (force/ unit area) required to stretch the test piece from the unstrained condition to a given elongation is called modulus or more accurately tensile stress at a given strain.

The tensile properties of the vulcanisates were determined on a 'Shimadzu Autograph AG-I series' universal testing machine (UTM), using a crosshead speed of 500 mm/min as per ASTM D 412-1998 (Method A). All the tests were carried out at  $28 \pm 2^{\circ}\text{C}$ . Dumbbell specimens for the test were punched out of the moulded sheet along the mill grain direction using a dumb bell die (C-type). The thickness of the narrow portion was measured using a digital thickness gauge. The sample was held tight by the two grips or jaws of the UTM, the upper grip being fixed. The tensile strength, elongation at break and modulus were evaluated and printed out after each measurement by the microprocessor.

### **2.2.5.2 Tear resistance**

This test was carried out as per ASTM D 624 -1998 using unnicked,  $90^{\circ}$  angle test pieces. The samples were cut from the compression-moulded sheets parallel to the mill grain direction. The test was carried out on the Shimadzu Autograph AG-I series universal testing machine (UTM). The speed of extension was 500 mm/min and the test temperature was  $28 \pm 2^{\circ}\text{C}$ . The thickness of the narrow portion was measured using a digital thickness gauge. The sample was held tight by the two grips or jaws of the UTM, the upper grip being fixed. The tear resistance of the samples was reported in N/mm.

### **2.2.5.3 Hardness**

The hardness (Shore A) of the moulded samples was determined using Zwick 3114 hardness tester in accordance with ASTM D 2240 -1997. The tests were performed on unstressed samples of 30 mm diameter and 6 mm thickness. Readings were taken after 15 seconds of the indentation after a firm contact has been established with the specimens.

### **2.2.5.4 Heat build up**

The Ektron flexometer conforming to ASTM D 623-1999 was used for measuring the heat build-up. A cylindrical sample of 25 mm in height and 19 mm in diameter was used for the test. The oven temperature was maintained at 100 °C. The samples were placed in the preconditioning oven for 20 minutes at 100 °C. After preconditioning the test samples were subjected to a flexing stroke of 4.45 mm under a load of 10.9 kg and the temperature rise at the end of 20 minutes was taken as the heat build up.

### **2.2.5.5 Abrasion resistance**

The abrasion resistances of the samples were measured with a DIN Abrader (DIN 53516). Moulded samples of  $6 \pm 0.2$  mm diameter and 12 mm thickness were prepared as per ASTM D3183 and abrasion loss was measured as per ASTM D5963-04. The sample is kept on a rotating sample holder and 10 N load was applied. Initially a pre run is given for the sample and its weight taken. The weight after the final run is also noted. The difference in weight is the weight loss on abrasion. The volume loss on abrasion was calculated using the equation

Volume loss on abrasion = (weight loss on abrasion/ specific gravity of the sample)

Abrasion resistance is the reciprocal of volume loss on abrasion.

#### **2.2.5.6 Strain sweep studies**

The strain sweep measurements on green compound were conducted to study the rubber-filler interaction. Rubber Process Analyzer (RPA 2000-Alpha Technologies) is a purposely modified commercial dynamic rheometer [5]. Such instrument was modified for capturing strain and torque signals, through appropriate software. Filled rubber compounds exhibit strong non-linear viscoelastic behaviour, the well-known Payne effect, i.e. the reduction of elastic modulus with increasing strain amplitude [6]. RPA can do strain sweep tests in which the variation of storage modulus ( $G'$ ), loss modulus ( $G''$ ) and complex modulus ( $G^*$ ) with change in strain amplitude are measured. With respect to its measuring principle, the RPA cavity must be loaded with a volume excess of test material. In agreement with ASTM 5289, the manufacturer recommends to load samples of about 5.0 g ( $4.4 \text{ cm}^3$ ) for a standard filled rubber compound with a specific gravity of  $1.14 \text{ g/cm}^3$ . Samples for RPA testing were consequently prepared by die cutting 46 mm diameter disks out of around 2 mm thick sheets of materials. The testing temperature was selected as  $100^\circ\text{C}$ ; a temperature below the curing temperature and the shear strain was varied from 0.5 to 100% keeping the frequency measurements at 0.5 Hz.

#### **2.2.5.7 Dynamic mechanical analysis (DMA)**

DMA works by applying an oscillating force to the material and the resultant displacement of the sample is measured. From this, the stiffness can be determined and  $\tan \delta$  can be calculated.  $\tan \delta$  is the ratio of the loss component to the storage component. By measuring the phase lag in the displacement compared to the applied force it is possible to determine the damping properties of the material.  $\tan \delta$  is plotted against temperature and glass transition is normally observed as a peak since the material will absorb energy as it passes through the glass transition. Dynamic mechanical thermal analysis (DMTA) spectra were recorded on rectangular specimens (length  $\times$  width  $\times$  thickness =  $5 \text{ cm} \times 4 \text{ cm} \times 2.11 \text{ cm}$ ) in the tensile mode at a frequency of 1 Hz with a TRITEC2000B DMA 1L dewar (Triton-technology, U K).

DMTA spectra [i.e., the storage modulus and mechanical loss factor ( $\tan \delta$ )] were measured from -120 to 30 °C at a heating rate of 1°C/min.

### **2.2.6 Cross link density and swelling studies**

Circular specimen of 20 mm diameter and 1mm thickness were cut using a sharp edged circular disc shaped die from the vulcanized rubber sheet. The samples were immersed in airtight test bottles containing about 20 ml of toluene maintained at constant temperature. Samples were removed periodically and the surface absorbed solvent drops were wiped off carefully by placing them between filter wraps. The mass of the sorbed sample was determined immediately on a digital balance with an accuracy of  $\pm 0.01$ mg. As the weighing was done within 30-40 seconds the error due to evaporation of other than surface adsorbed liquid is considered insignificant. The weighing of the sample is continued till the equilibrium swelling is attained. For calculating the crosslink density, desorbed weights of the samples were also taken after complete removal of the solvent.

The mole percent uptake of the sample is calculated from the diffusion data. The  $Q_t$  values were determined as

$$Q_t = \frac{(\text{Wt. of the solvent sorbed at a given time}) / (\text{Mol. wt. of the solvent})}{(\text{Initial wt. of the rubber specimen} \times 100)}$$

At equilibrium swelling  $Q_t$  becomes  $Q_\infty$ .

The mechanism of diffusion was investigated using the equation

$$\log Q_t / Q_\infty = \log k + n \log t$$

The value of  $k$  depends on the structural features of polymer, whereas the value of  $n$  determines diffusion mechanism. For the Fickian mode, case 1, the value of  $n$  is 0.5 and it occurs when the rate of diffusion of penetrant molecules is much less than the relaxation rate of the polymer chains. For case 2 or non-Fickian transport, where the  $n$  value is 1, the diffusion is rapid when compared with the simultaneous relaxation

process. However in the case of anomalous transport where the  $n$  value is in between 0.5 and 1, both solvent diffusion and polymer relaxation rate are comparable.

The effective diffusivity,  $D$  of the rubber solvent system was calculated from the initial portion of the sorption curves using the equation [7, 8]

$$D = \pi \left[ \frac{h\theta}{4Q_{\infty}} \right]^2$$

Where  $h$  is the initial thickness of rubber sample,  $\theta$  the slope of the linear portion of the sorption curve  $Q_t$  versus  $t^{1/2}$

The permeation of a solvent into a polymer membrane will also depend on the sorptivity of the penetrant in the membrane. Hence sorption coefficient  $S$  has been calculated using the relation [9]

$$S = \frac{W_s}{W}$$

Where  $W_s$  is the weight of the solvent at equilibrium swelling and  $W$  the initial weight of the polymer sample.

Since the permeability depends on both diffusivity and sorptivity, the permeation coefficient has been determined using the relation [9]

$$P = D \times S$$

As diffusion is influenced by polymer morphology, the molar mass between cross links  $M_c$  from the sorption data is also determined. The rubber solvent interaction parameter, which is needed for the estimation, has been calculated using the equation [9]

$$\chi = \beta + \frac{V_s}{RT} (\partial_s - \partial_p)^2$$

Where  $V_s$  is the molar volume of the solvent and  $\delta$  and  $\delta_p$  are solubility parameters of solvent and polymer taken from the polymer handbook.  $R$  is the universal gas constant and  $T$  the absolute temperature,  $\beta$  is the lattice constant and is 0.38 in the calculation.

Using  $\chi$  values the molar mass between crosslinks ( $M_c$ ) of the polymer was estimated from the Flory Rehner equation [10, 11]

$$M_c = \frac{-\rho_p V_s (V_r)^{1/3} \chi}{\ln(1 - V_r) + (V_r) + \chi(V_r)^2}$$

The volume fraction of rubber in the deswollen network was then calculated using the equation. [12]

$$V_r = \frac{(d - fw)\rho_p^{-1}}{(d - fw)\rho_p^{-1} + A_o \rho_s^{-1}}$$

Where  $d$  is the desorbed weight of the polymer,  $f$  the weight percent of filler,  $w$  the initial weight of the polymer,  $\rho_p$  and  $\rho_s$  the density of polymer and the solvent respectively and  $A_o$  the net solvent uptake of the polymer. The monomeric molecular weight of NR being  $68 \text{ g mol}^{-1}$ , the average number of monomeric units between crosslinks can be calculated. A decrease in the value is observed. Using the  $M_c$  values crosslink density can be calculated using the equation  $\nu = 1/2M_c$

The expansion of the rubber in the presence of a solvent will significantly modify the conformational entropy ( $\Delta S$ ) and the elastic Gibbs free energy ( $\Delta G$ ). The elastic gibbs free energy can be determined from the Flory- Huggins equation [13]

$$\Delta G = RT [\ln(1 - V_r) + (V_r) + \chi(V_r)^2]$$

### **2.2.7 Gas permeability testing**

The air permeability of the rubber vulcanisates were measured using Lyssy Manometric Gas Permeability Tester L100-2402. The test gas used was oxygen at a rate of 500ml/minute. Permeability of the samples is calculated using the equation,  $P_m = (T_r X P_r) / t_m$ , where  $P_m$  is the permeability of the test sample,  $t_m$  is the interval time constant for the test sample,  $P_r$  is the permeability of the reference (standard Polyethylene terphthalate (PET) sample) and  $T_r$  is the interval time constant for standard PET.

### **2.2.8 Infrared spectroscopy**

Fourier transform infrared spectra are generated by the absorption of electromagnetic radiation in the frequency range 400 to 4000  $\text{cm}^{-1}$  by organic molecules. Different functional groups and structural features in the molecules absorb energy at characteristic frequencies. The frequency and intensity of absorption are the indication of the bond strength and structural geometry in the molecule. The IR spectra of the modified clays and methacrylated natural rubber latex were recorded with Fourier Transform Infrared Spectroscopy, Bruker, Tensor 27 model.

### **2.2.9 Thermal analysis**

The thermogram of modified clays and rubber vulcanisates are recorded with a Thermo Gravimetric Analyzer Q-50, TA instruments. It is a computer-controlled instrument that permits the measurement of the weight changes in the sample material as a function of temperature. The sample placed in a temperature programmed furnace is subjected to temperature in the ranges 30 °C to 800 °C with a heating rate of 10 °C/minute and the corresponding weight changes was noted with the help of an ultra sensitive microbalance. Air and nitrogen were used as purge gases.

**References**

1. Babu, P.S.S., Gopalakrishnan, K.S. and Jacob J. In: Natural Rubber; Agromanagement and Crop Processing. Eds. George, P. J. and Jacob C. K, Rubber Research Institute of India, Kottayam. Ch. 24 p 434, 2000.
2. Subramanyam, A., Proc. of R. R. L. M. Planters Conference, Kuala Lumpur, 255, 1971.
3. Degussa, Product Information Sheet on Ultrasil VN3, PI 203. IE- from the website [www.degussa-fp.com](http://www.degussa-fp.com)
4. Jean L. Leblanc. and Anne Mongruel., Progress in Rubber and Plastics Technology, 17, 3, 2001.
5. Jean L. Leblanc. and Marie Cartault., J. Appl. Polym. Sci., 2001, 80(11), 2093.
6. Payne, A. R. and Whittaker, W.E., Rubber Chem. Technol., 1971, 44,440.
7. Crank, J. In: The mathematics of diffusion. 2<sup>nd</sup> Ed. Oxford: Clarendon Press., p 244, 1975.
8. Britton, L. N., Ashman, R .B., Aminabhavi, T. M. and Cassidy, P. E., J. Chem. Edn., 65, 368, 1988.
9. Aprem, A. S., Joseph, K., Mathew, A. P. and Thomas, S., J Appl Polym Sci., 78, 941, 2000.
10. Khinnava, R. S. and Aminabhavi, T. M., J Appl Polym Sci. 42, 2321,1991.
11. Flory, P. J. and Renner, Jr., J Chem Phys., 11, 521, 1943.
12. Cassidy, P.E., Aminabhavi, T.M. and Thompson, C.M., Rubber Chem. Tech., 56, 594, 1983.
13. Kojima, Y., Usuki, A., Kawasumi, M., Okada, A., Fukushima, Y., Kurauchi, T. and Kamigaito, O., J Mater Res., 8, 1174, 1993.



## ***Chapter 3***

---

### ***Natural Rubber Organoclay Nanocomposites***

Polymer nanocomposites have been intensely researched in the last decade since the addition of a small quantity of reinforcing fillers, up to 10 weight percentage, such as nanoclays in the polymer matrix have led to improvements of mechanical, thermal, and barrier properties [1-4]. The enhancement of such properties is strongly influenced by the nanostructure of the dispersed clay and by its interfacial interaction with the polymer. The fundamental principle of polymer clay nanocomposite formation is that the polymer should penetrate into the intergalleries of the clay. The development of 'reactive' organoclays in which the intercalants, participate in the polymer building/crosslinking reactions [5, 6] is a recent strategy to facilitate the nanocomposite formation. They include the modification of the surface of the clay layers and/or the polymeric chains [7-11]. Further important factors were the length of the organophilic intercalant [12] and its number of alkyl tails [13], the molecular mass of the polymer matrix [14] and its polarity [15, 16], as well as, the type of the layered silicate [17, 18]. The layered silicates commonly used in polymer nanocomposites belong to the structural family known as the 2:1 montmorillonite (MMT). In the pristine state, MMT is made up of stack of platelets resulting in a much smaller aspect ratio in the range of 50-200. The layer thickness is around 1nm and lateral dimensions of their layers may vary from 300Å to several microns and even larger depending on the particular silicates. The startling property of montmorillonite is its ability to expand and contract its interlayer structure while maintaining two-dimensional crystallographic integrity. By this means, a large active surface area (700-800 m<sup>2</sup> /g) is potentially exposed, allowing an enormous range of guest molecules to be intercalated [19].

As the distance between the layers is less than 1nm, it does not allow the penetration of the polymer molecules therein. So the space between the platelets or layered galleries of the silicate should be made accessible for the polymer chains. To support intercalation and exfoliation, the interlayer distance should be greater than 1.5 nm [20] and the layered structure should be broken down [21]. Thus the polymer intercalation might be made more effective by increasing the interlayer distance. In this study, two organoclays having different interlayer distance and modifying groups were used and their influence on the cure characteristics, mechanical properties, and transport properties on natural rubber were investigated. Morphological studies using TEM was also carried out to ascertain the formation of intercalated and exfoliated structures in nanocomposites.

### **3.1 Natural rubber- clay nanocomposites**

#### **3.1.1 Preparation of the nanocomposites**

Natural rubber of grade ISNR-5 obtained from Rubber Research Institute of India, Kottayam, India was used for the study. Two different types of nanoclay differing in the interlayer distance and in modifying groups were used for the study and were obtained from Southern Clay Products, USA. The interlayer distance of the clays used were 18.3Å and 30.6Å for cloisite 10A [2MBHT: dimethyl, benzyl, hydrogenated tallow, quaternary ammonium], and cloisite 15A [2M2HT: dimethyl, dihydrogenated tallow, quaternary ammonium], respectively. Other chemicals used were of commercial grade. Compounds were prepared in a two roll mill with various filler loadings from 1 to 15 phr for the two clays according to the recipe given in table 3.1.

The mixed compounds were matured for a period of 24 hrs and the cure characteristics like cure time, scorch time, maximum and minimum torque were determined using rubber process analyzer at a temperature of 150 °C. From the respective cure curves, the optimum cure time for the vulcanisation were determined. Sheets for preparing the test specimens were moulded to a thickness of 2 mm using, an electrically heated hydraulic press at 150 °C and 200 kgcm<sup>-2</sup> pressure up to their respective cure times.

For determining the abrasion resistance cylindrical shaped test specimens with 16 mm diameter and 6 mm thickness were moulded using suitable moulds.

**Table 3.1 Compound formulation**

Ingredients	Sample Code		
	Gum	10A	15A
Natural Rubber	100	100	100
ZnO	5	5	5
Stearic acid	2	2	2
Sulphur	2.5	2.5	2.5
CBS	0.6	0.6	0.6
Antioxidant-HS	1	1	1
Cloisite 10A	–	X	–
Cloisite 15A	–	–	Y

X = 1, 3, 5, 10 & 15 parts of cloisite 10A for hundred parts of rubber

Y = 1, 3, 5, 10 & 15 parts of cloisite 15A for hundred parts of rubber

### **3.1.2 Characterisation of NR-Clay nanocomposites using X-ray diffraction technique**

X-ray diffraction (XRD) was used to study the nature and extent of dispersion of the clay in the nanocomposite. XRD patterns were obtained using Bruker, D8 advance diffractometer at the wavelength  $\text{CuK}\alpha = 1.54^\circ$ , a tube voltage of 40 KV and tube

current of 25 mA. Bragg's law defined as  $n\lambda = 2d\sin\theta$ , was used to compute the crystallographic spacing ( $d$ ) for the clay. The samples were scanned in step mode by  $1.0^\circ/\text{min}$ , scan rate in the range of  $2$  to  $12^\circ$ .

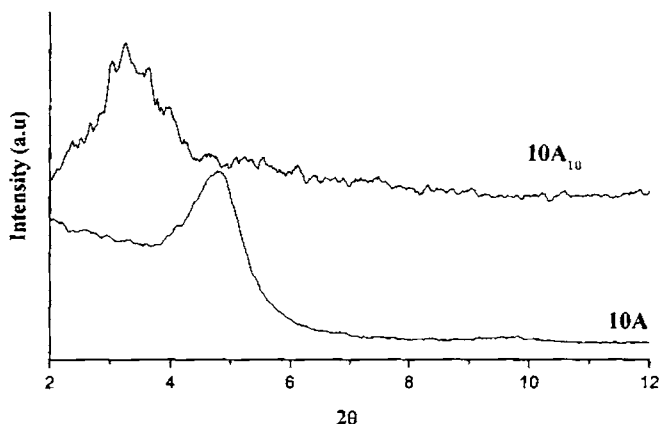


**Figure 3.1 XRD patterns of cloisite 10A & nanocomposite with 10 phr of cloisite 10A in natural rubber (10A<sub>10</sub>)**

Figure 3.1 shows the X-ray diffraction patterns of the cloisite 10A (10A) and nanocomposite with 10 phr of clay (10A<sub>10</sub>). The cloisite 10A clay shows a diffraction peak at  $2\theta = 4.80^\circ$  that is assigned to an interlayer platelet spacing (001 diffraction peak) of  $18.39 \text{ \AA}$ . For natural rubber based nanocomposites with 10 phr of cloisite 10A clay, the  $2\theta$  shifts to a lower value,  $3.16^\circ$  that is assigned to an interlayer spacing of  $27.93 \text{ \AA}$ . Two more peaks at  $24.66 \text{ \AA}$  and  $22.07 \text{ \AA}$ , which are also higher than the interlayer distance of the clay, are observed. This increase in interlayer distance of the clay by approximately  $9 \text{ \AA}$  confirms the formation of intercalated nanocomposite.

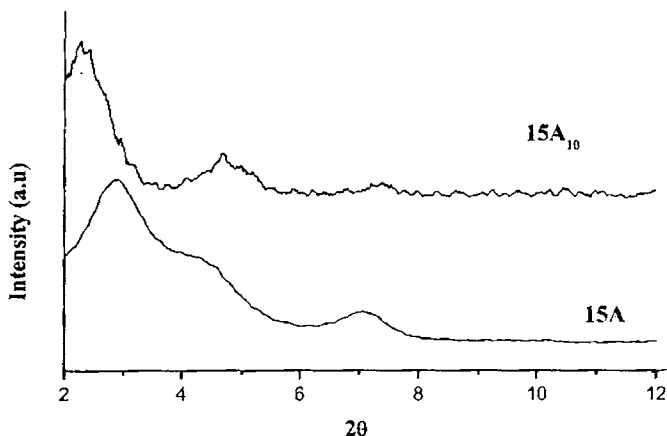


***Figure 3.2 XRD patterns of cloisite 15A & NR based nanocomposites containing 10 phr of cloisite 15A (15A<sub>10</sub>)***

Figure 3.2 depicts the XRD trace of cloisite 15A(15A) and NR nanocomposite with 10 phr of cloisite 15A clay(15A<sub>10</sub>), which possess two peaks at  $2\theta = 2.23^\circ$  and  $2.42^\circ$  corresponding to the interlayer distance of  $39.58 \text{ \AA}$  and  $36.49 \text{ \AA}$ , respectively. These peaks are also displaced from the original  $2\theta$  value of cloisite 15A,  $2.88^\circ$  and interlayer distance  $30.6 \text{ \AA}$ . This increase in  $d$  spacing suggests the intercalation of the polymer chains between the clay layers.

### **3.1.3 Transmission electron microscopy**

The Transmission electron microscopy (TEM) imaging for the rubber nanocomposites was carried out using a Transmission Electron Microscope CM-200 of Philips Technology. TEM was used in order to visualize the morphology of the clay layers in the nanocomposites. Figure 3.3 shows TEM micrographs for sample with 10 phr of nanoclay having higher interlayer distance. Even though, X-ray diffraction indicated all intercalated structures, exfoliated layers can also be observed in the TEM pictures.

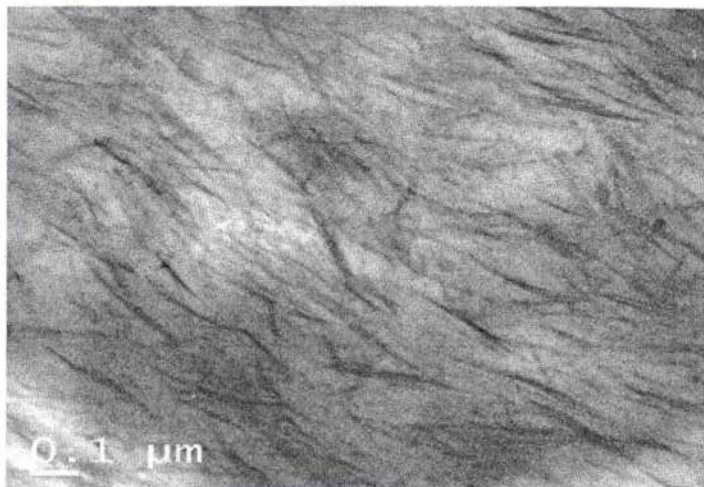


*Figure 3.3 TEM micrograph of nanocomposite with 10phr cloisite 15A*

#### **3.1.4 Cure characteristics of the compound**

Rubber nanocomposites with organoclays show prominent accelerating effect on the cure characteristics [22- 25]. This effect is essentially attributed to the amine groups in the nanosilicate structure, which came from the organofication of the clay. A transition complex formation with amines and sulphur containing compounds, which facilitates the development of elemental sulphur, is suggested. This aspect however has not been studied yet. It is well known that amine group facilitates the curing reaction of SBR and NR stocks [23]. Although the amine itself accelerates the vulcanisation process, the amine modified clay give rise to a further noticeable increase in the vulcanisation rate, which could be attributed to a synergetic effect between the filler and amine. The cure parameters derived from the rubber process analyzer is given in table 3.2.

**Table 3.2 Cure characteristics of nanocomposites**

Sample code	Min Torque (dNm)	Max Torque (dNm)	T <sub>10</sub> (minutes)	T <sub>50</sub> (minutes)	T <sub>90</sub> (minutes)
Gum	0.15	2.229	4.55	6.07	9.71
10A <sub>1</sub>	0.013	2.916	2.31	3.83	6.98
10A <sub>3</sub>	0.072	3.040	1.56	3.03	6.39
10A <sub>5</sub>	0.029	3.115	1.16	2.60	6.34
10A <sub>10</sub>	0.069	3.291	0.97	2.52	6.78
10A <sub>15</sub>	0.023	3.154	0.79	2.21	6.83
15A <sub>1</sub>	0.032	3.262	1.97	3.41	6.96
15A <sub>3</sub>	0.055	3.22	1.18	2.63	6.29
15A <sub>5</sub>	0.170	3.540	1.07	2.37	5.60
15A <sub>10</sub>	0.035	3.736	0.92	2.42	6.31
15A <sub>15</sub>	0.032	4.354	0.72	2.24	6.35

Samples 10A<sub>1</sub>, 10A<sub>3</sub>, 10A<sub>5</sub>, 10A<sub>10</sub>, & 10 A<sub>15</sub> represents nanocomposite with 1, 3, 5, 10 and 15 phr of cloisite 10A clay, respectively

Samples 15A<sub>1</sub>, 15A<sub>3</sub>, 15A<sub>5</sub>, 15A<sub>10</sub>, & 15 A<sub>15</sub> represents nanocomposite with 1, 3, 5, 10 and 15 phr of cloisite 15A clay, respectively

In presence of organoclays both the cure time and scorch time are considerably reduced. The cure time is reduced by almost three minutes for compounds containing 10 phr of nanoclay. This effect is attributed to the ammonium groups of the organic cations. This reduction in cure time is slightly boosted with the increase in interlayer distance of the clay. The cure activation of organoclays is reported in the literature [26]. The intercalation of the organically modified clay within the silicate galleries facilitates the vulcanisation reaction.

A dramatic increase in maximum torque value with increase in clay content is also observed for the nanocomposites prepared using the two different clays. The maximum torque value increased by 1.5 times for the nanocomposite prepared with 10 phr clay having higher interlayer distance. This increase in maximum torque value directs to the increase in modulus of the composites.

Maximum torque increases during vulcanisation in the case of filled compounds. The ratio between the increase in torque of the filled compound to that of the gum compound was found to be directly proportional to filler loading. The slope of the linear plot showing the relative torque increase with filler loading was defined by Wolf [26] as  $\alpha_f$

$$\frac{D_{\max} - D_{\min}}{D_{\max}^0 - D_{\min}^0} - 1 = \alpha_f \frac{m_f}{m_p}$$

where  $D_{\max} - D_{\min}$  is the change in torque during vulcanisation for filled compound,  $D_{\max}^0 - D_{\min}^0$  is the change in torque during vulcanisation for gum compound,  $m_p$  and  $m_f$  are the mass of the polymer and mass of the filler in the compound, respectively.



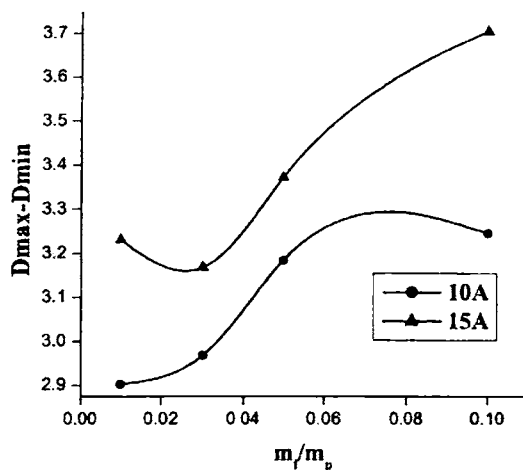


Figure 3.4 Variation of  $\Delta$  torque against filler loading

Figure 3.4 depicts the relation between  $D_{max} - D_{min}$  against loading of nanoclay. The increase in  $\Delta$  torque indicates that the incorporation of nanoclay affects the crosslinking between the polymer chains.

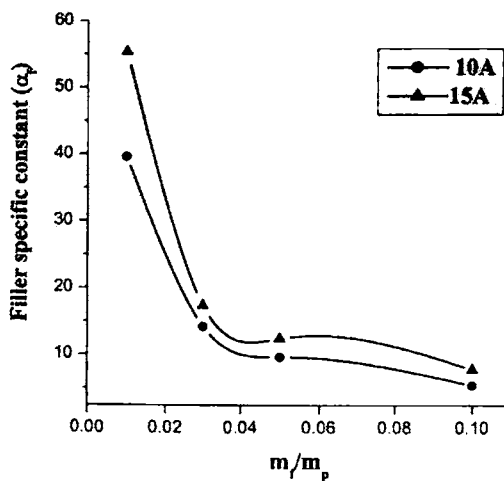
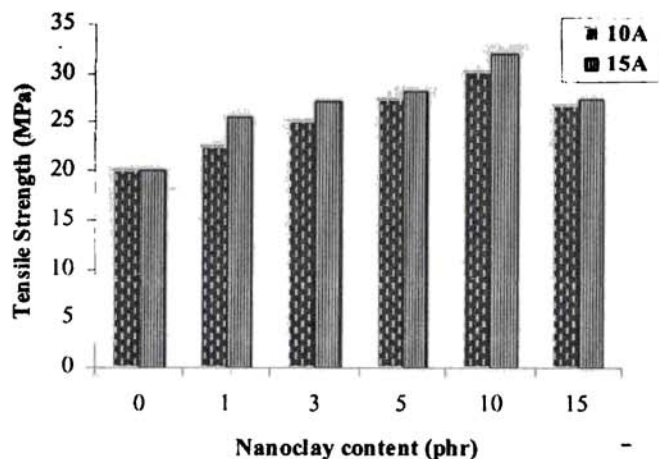


Figure 3.5 Variation of filler specific constant ( $\alpha_f$ ) against filler loading

In figure 3.5, the values of  $\alpha_f$  of the two clays are plotted against filler concentration. Since  $\alpha_f$  is a measure of the in-rubber structure of fillers, the decrease of  $\alpha_f$  with filler loading can be attributed to the decrease in the distance between aggregates. These results are attributed to the intercalation of the polymer within the silicate galleries. Consequently, a better interaction between the rubber and the filler is obtained. The minimum torque value is a measure of viscosity of the compound. The values do not vary much with clay content suggesting that the processability of the composites is not affected.

### 3.1.5 Mechanical properties of nanocomposites

The mechanical properties of the nanocomposites were studied and are analyzed in the following section.



**Figure 3.6 Tensile strength of nanocomposites with nanoclay loading**

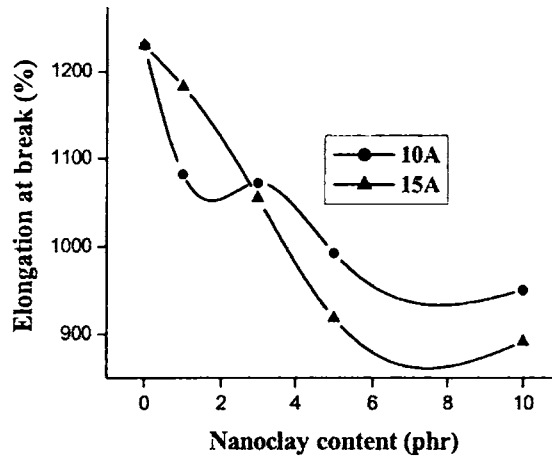


Figure 3.7 Elongation at break of nanocomposites with nanoclay loading

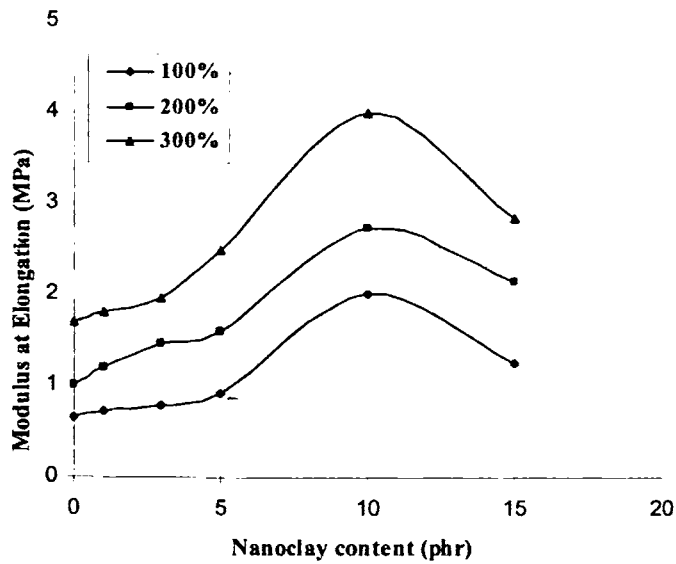
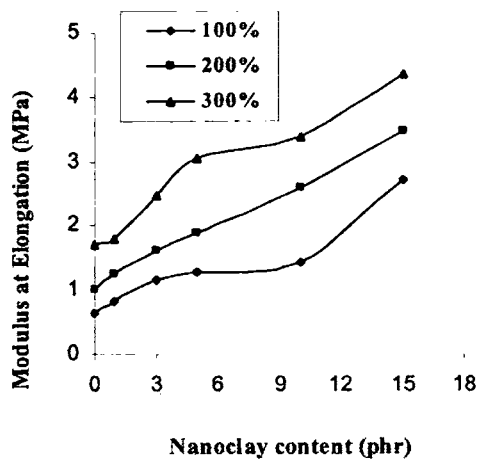
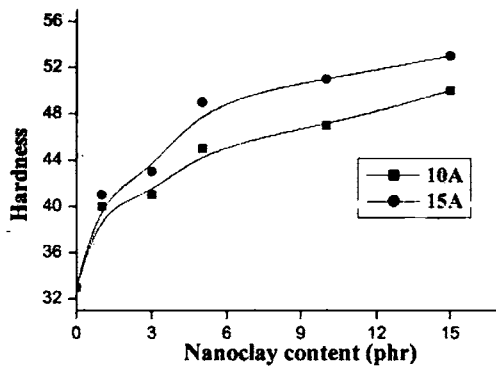


Figure 3.8 Tensile modulus of cloisite 10A nanocomposites



**Figure 3.9 Tensile modulus of cloisite 15A nanocomposites**



**Figure 3.10 Hardness of nanocomposites**

As expected, the silicate reinforced systems prepared by mixing organoclay in natural rubber show superior modulus and strength relative to conventional rubber vulcanisates. It is obvious from the figures 3.6, 3.8 and 3.9 that even with the addition

of such a low loading of nanoclay (1 phr-10 phr), the tensile strength and modulus increases considerably.

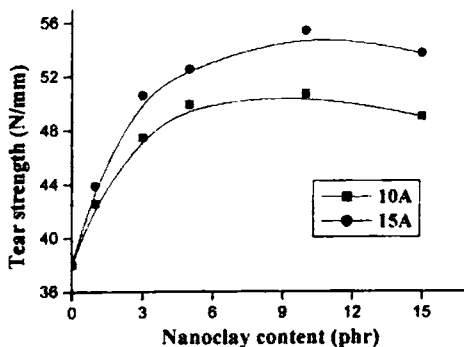


**Figure 3.11 Tear strength of nanocomposites**

For example, compared to unfilled rubber, 15 phr of cloisite 15A clay nanocomposite has 156% higher tensile modulus than the gum vulcanisate. A sixty percentage increase in tensile strength is obtained for the nanocomposite with 10 phr of cloisite 15A clay. From figures 3.10 and 3.11, it can be observed that hardness and tear strength of the nanocomposites also show the same trend. However, the elongation at break is observed to decrease on addition of clay. Generally, rigid fillers cause a dramatic decrease in elongation at break [27], whereas the composite with 10 phr loading of nanoclay, shows only 14% reduction in elongation at break (figure 3.7). It is seen that the nanocomposite with the clay having higher interlayer distance shows better mechanical properties. This suggests that interlayer distance play a major role in the intercalation of the rubber matrix.

The mechanical properties increase with increase in clay content up to 10 phr. A further decrease is observed at higher clay loading, which may be due to agglomeration of the clay.

### **3.1.6 Strain sweep measurements for uncured compounds**

The complex modulus ( $G^*$ ) values obtained for the uncured compounds are plotted and shown in figures 3.12 and 3.13. The elastic modulus of a filled rubber is strongly dependent on the deformation and decreases substantially at higher strains. This phenomenon is known as the Payne effect and is attributed to the presence and breakdown of the filler network during deformation. But investigations performed with both experimental and theoretical approaches shows that the decrease in  $G^*$  with amplitude of deformation (strain) is attributed to the destruction – reformation of a percolating network of filler that can also involve polymer bonded filler [28]. The complex modulus values at low strains (15%) are a measure of the filler polymer interactions [29]. The limiting values at high strains are due to polymer networks and hydrodynamic effect. Polymer networks are the same for a fixed mass of rubber. But the hydrodynamic effect varies with the filler content and nature of the filler. The theoretical meaning of hydrodynamic effect is given by the modified form of Guth and Gold equation [30, 31].

The addition of the filler increases the shear modulus of the pure elastomer,  $G_0$  and results in a shear modulus,  $G_f$  for the filled compound

$$G_f = G_0 (1 + 0.67 f_s \Phi + 11.62 f_s^2 \Phi^2)$$

where  $\Phi$  is the volume fraction of the particles and the shape factor  $f_s$  represents the ratio of the longest dimension to the shortest dimension of the particle. The modulus as calculated by the equation is independent of the applied strain [32].

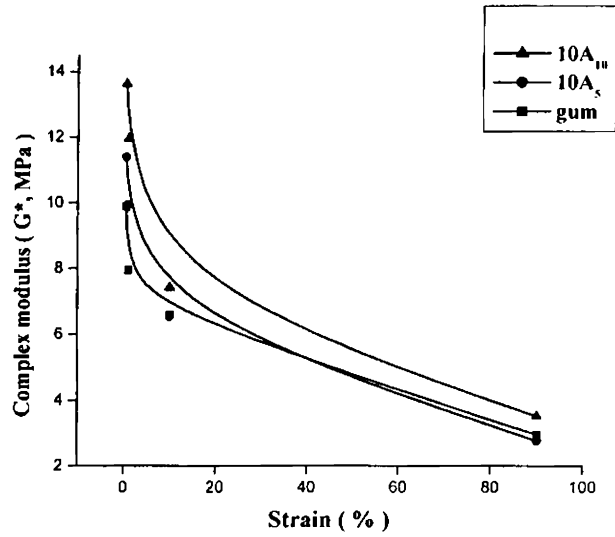


Figure 3.12 Variation of complex modulus with filler content for cloisite 10A nanocomposites

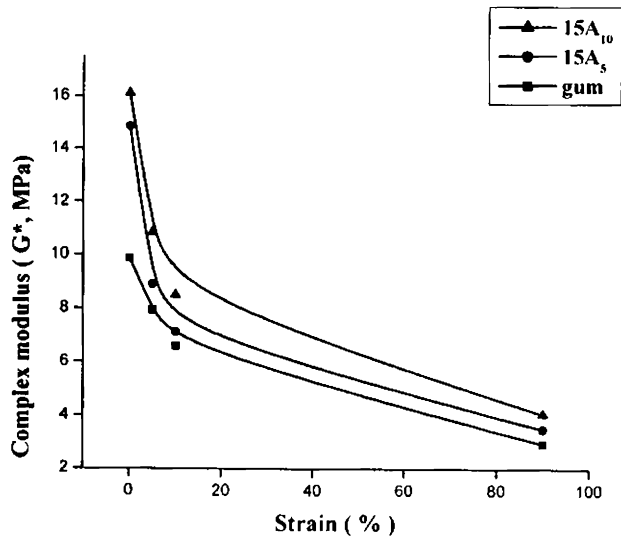


Figure 3.13 Variation of complex modulus with filler content for cloisite 15A nanocomposites

The variation of complex modulus ( $G^*$ ) with strain for the composites with the two clays are presented in figures 3.12 and 3.13. The graphs show that the complex modulus values at low strain increases with filler concentration. The complex modulus values at low strains (<15 %) are a measure of the filler polymer interaction. The high values of  $G^*$  is due to higher filler-filler or filler polymer interactions. Variation in mechanical properties of the composites explained earlier shows that the network formed are mainly between filler and polymer.

### **3.1.7 Gas permeability measurement**

The air permeability of the natural rubber layered silicate membranes were measured using Lyssy Manometric Gas Permeability Tester L100-2402. The test gas used was oxygen at a flow rate of 500 ml/minute. Permeability of the samples is calculated using the equation,  $P_m = (T_r \times P_r)/t_m$ , where  $P_m$  is the permeability of the test sample,  $t_m$  is the interval time constant for the test sample,  $P_r$  is the permeability of the reference (standard PET) sample and  $T_r$  is the interval time constant for standard PET.

The oxygen permeability of the gum and nanoclay filled vulcanisate having 2 mm thickness are given in table 3.3. It is clearly seen that the oxygen permeability decreased substantially by incorporation of 5 phr of layered silicate. Higher permeation resistance is offered by the nanoclay having higher interlayer distance. This supports the better exfoliation, which resulted in the permeation resistance obtained by the incorporation of lower silicate loadings.

Gas barrier in polymer clay nanocomposites was traditionally explained in terms of Nielson model, originally adopted to describe the tortousity effect of plate like particulates on gas permeability of filled polymer composite structures [33]. This model system consists of uniform platelets homogeneously dispersed in the polymer matrix and oriented parallel to the polymer film surface. The model can be applied using the equation,



$$\frac{P}{P_0} = \frac{1 - \phi_f}{1 + \frac{L}{2W} \phi_f}$$

to obtain the clay aspect ratio from the permeability data of these nanocomposites. In the equation, P is the permeability of the nanocomposite, P<sub>0</sub> is the permeability of the gum vulcanizate and φ<sub>f</sub> is the volume fraction of the clay. L and W are length and width of the clay sheets, respectively, its ratio L/W, defines the aspect ratio α, of the fillers. The model assumes that the fillers are impermeable to the diffusing gas or liquid molecule and are oriented to the diffusion direction. Aspect ratios calculated are given in the table 3. 3. The samples with better dispersion presented the highest aspect ratio as suggested by the permeability data. Thus, the presence of the filler particles creates tortuous path for the permeant to travel through the composites.

**Table 3.3 Oxygen Permeability of the rubber vulcanisates and aspect ratio of clay from Nielson's model**

Sample code	Oxygen Permeability (mL / m <sup>2</sup> day)	Aspect ratio from Nielson's model
gum	824.19	—
10A <sub>5</sub>	740.55	2.31
15A <sub>5</sub>	693.63	5.14

### 3.2 Effect of silane coupling agent

The compatibility of clay platelets with the rubber organic phase, in terms of wetting and dispersion, may be substantially improved by, for instance the covalent addition

of some organics to the reactive surface of the clay. Organosilane coupling agents may be used to help the dispersion and to improve clay-rubber adhesion.

Several commercial clays have been treated with silane coupling agents to improve their performance in rubber. Adhesion between polymer and filler may be induced by a coupling agent, which participates in the vulcanisation reaction to form polymer-filler crosslinks. This mechanism of increasing strength is well established with both mineral fillers and carbon blacks [34]. Both mechanisms lead to the formation of high modulus compounds, which is a very clear indicator that polymer-filler bonding has taken place. Organosilane coupling agents have been successfully utilized to further increase the physical properties of a number of non-black fillers including calcium silicate, clay, mica, silica and talc [35]. In this part of the study organoclays treated with 3 weight percentage of silane coupling agent is used to prepare rubber clay nanocomposites.

### 3.2.1 Cure characteristics

An increase in maximum torque value with increase in clay content is observed for the nanocomposites prepared using the two different clays treated with silane coupling agent.

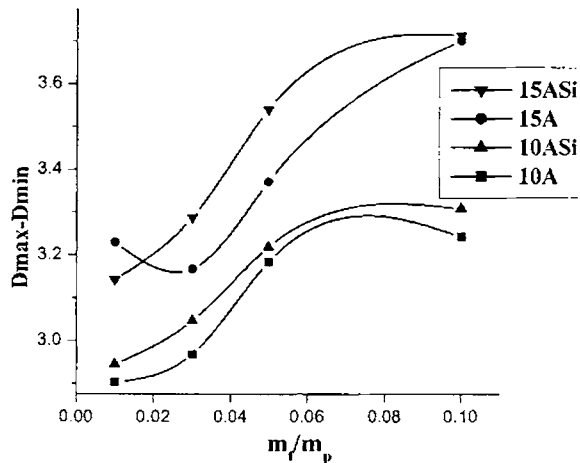
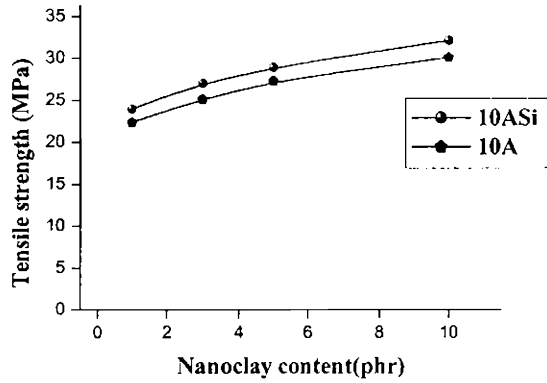


Figure 3.14 Variation of  $\Delta$  torque against filler loading

This increase in maximum torque value is a direct measure of the increase in modulus of the composites. Figure 3.14 represents the relation between  $D_{\max} - D_{\min}$  and nanoclay loading. The  $\Delta$  torque value is higher for the composites with silane treated nanoclay and it increases with the clay loading. This is because of the formation of a higher number of crosslinks, which is attributed to the confinement of the rubber chains within the clay galleries and hence, better interactions between the filler and the elastomers.

### **3.2.2 Mechanical properties**

The effect of silane coupling agent on the mechanical properties of the nanocomposites was studied and is depicted in figures 3.15 to 3.20. An improvement in mechanical properties like tensile strength, tear strength and modulus is observed for the nanocomposites prepared with nanoclay treated with organosilane coupling agent. Silane coupling agent, Si69 improves the dispersion of the clay in the rubber matrix. The interfacial adhesion between the clay layers and the rubber chains is enhanced as a result of the sulfur atom of Si69 participating in the vulcanisation reaction of NR. The increased modulus occurs as a direct result of attachment of the rubber to the filler, which has the effect of reducing polymer mobility. Improved mechanical properties are obtained for nanocomposite with clay having higher interlayer distance.



*Figure 3.15 Tensile strength of cloisite 10A & 10A Si nanocomposites*

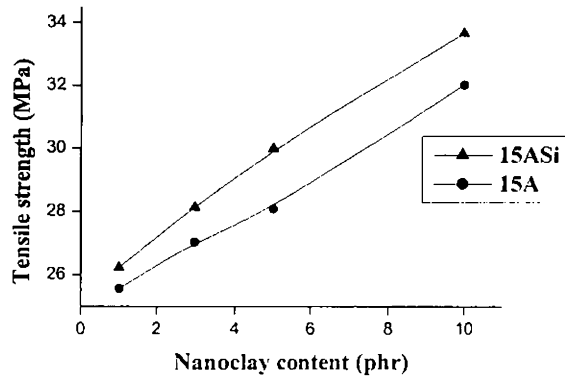


*Figure 3.16 Tensile strength of cloisite 15A & 15A Si nanocomposites*

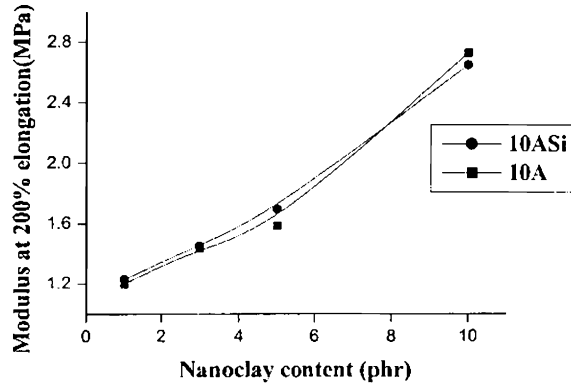


*Figure 3.17 Modulus at 200% elongation of 10A & 10A Si nanocomposites*

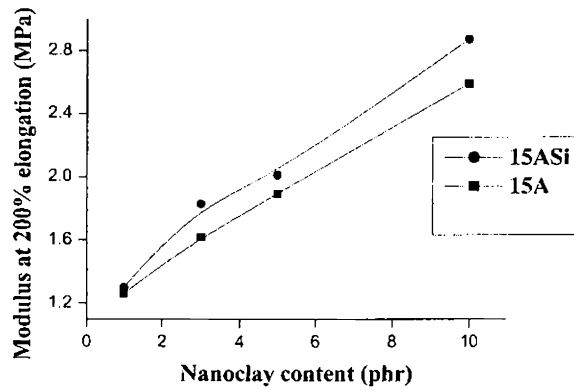


*Figure 3.18 Modulus at 200% elongation of 15A & 15A Si nanocomposites*

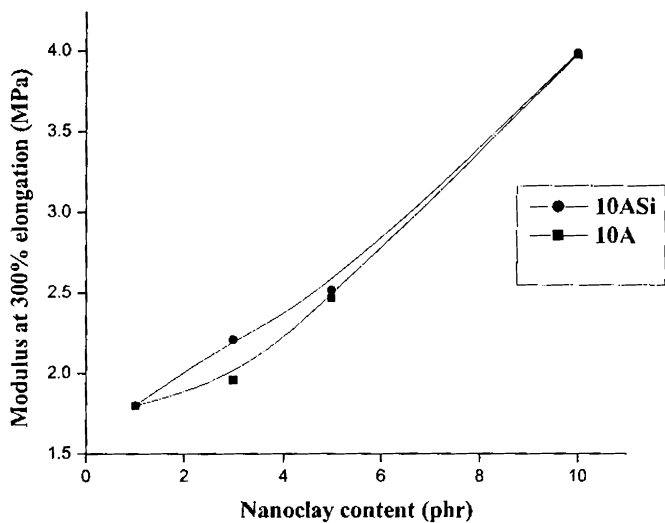


Figure 3.19 Modulus at 300% elongation of 10A & 10A Si nanocomposites

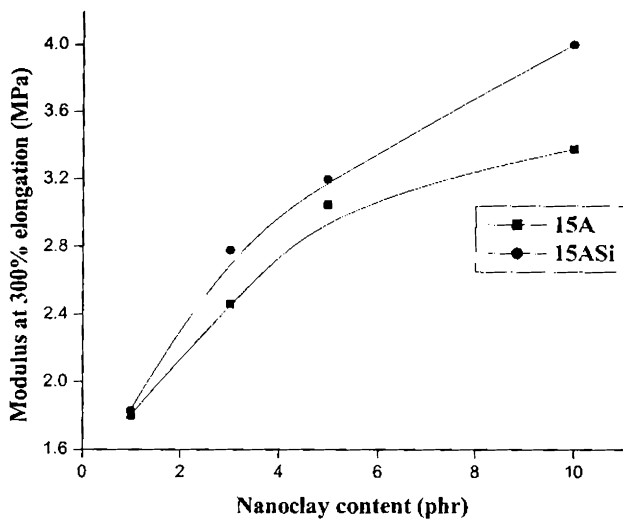


Figure 3.20 Modulus at 300% elongation of 15A & 15A Si nanocomposites

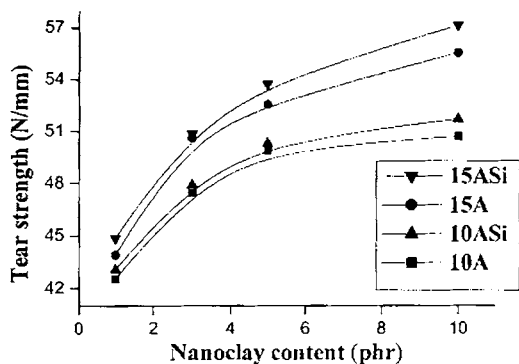


Figure 3.21 Tear strength of nanocomposites

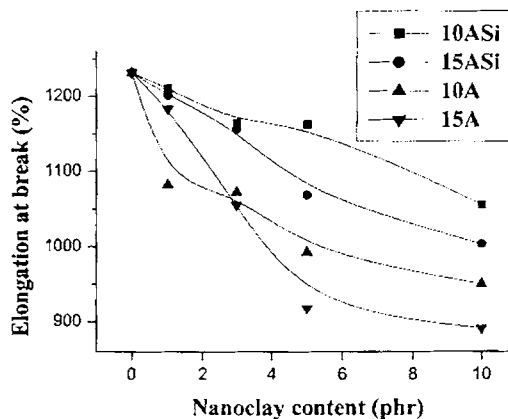


Figure 3.22 Elongation at break of nanocomposites

From figure 3.22, it is clear that elongation at break is decreasing with increase in nanoclay content, but the decrease is less for the organosilane modified nanocomposites than that without the silane coupling agent. The organoclay, treated with the silane coupling agent behaves as effective reinforcing filler for NR. The silane treated clays improve the mechanical properties of the nanocomposite without adversely affecting the elasticity of the rubber matrix.

### 3.2.3 Swelling studies

Swelling studies of the vulcanisates prepared with two clays in different concentrations were done in toluene at 303 K. Detailed procedure for the measurement is given in section 2.2.6. Sorption curves of the vulcanisates that are obtained by plotting  $Q_t$  (mole% uptake per 100 g of the solvent) against time are shown in figures 3.23 and 3.24. For all compositions, the uptake is rapid in the initial zone. After this, the sorption rate decreases leading to a plateau corresponding to equilibrium swelling. Note that the gum has maximum toluene uptake at equilibrium swelling. The swelling of the material is strongly reduced in the presence of clay within the NR matrix. The presence of impermeable clay layers decreases the rate of transport by increasing the average diffusion path length in the specimen.

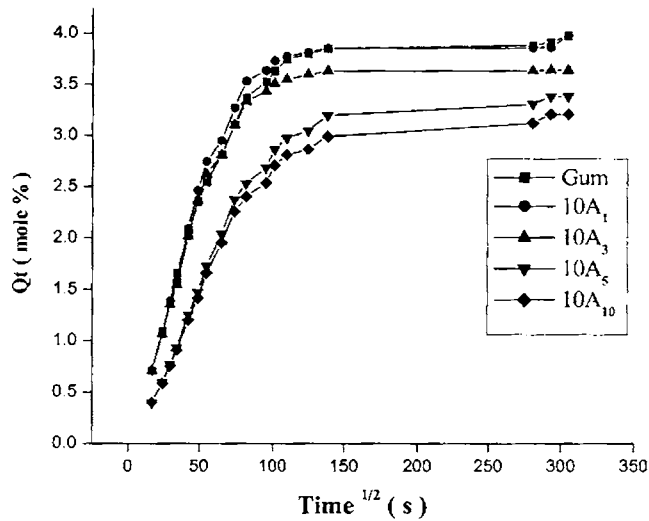


Figure.3.23 Sorption curves of the 10A vulcanisates at 303 K



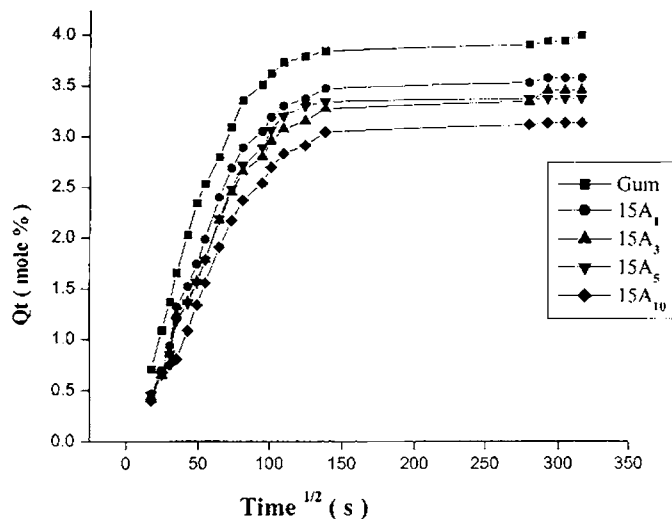


Figure 3.24 Sorption curves of the 15A vulcanisates at 303 K

In order to determine how the clay content affects the permeability, the transport properties like diffusion coefficient, permeation coefficient and sorption coefficient of the samples were calculated using the relations given in section 4.4.

The values of diffusion coefficient,  $D$  for the two clay filled samples are given in the table 3.4 and figure 3.25. The variation of  $D$  depends on the solvent uptake, which shows a maximum for the gum vulcanisate. Adding clay to the natural rubber matrix results a progressive decrease of  $D$  value and a substantial decrease with increase in clay content. Changes in diffusivity and permeability of nanocomposites with clay content are conventionally explained within the concept of tortuous paths. According to this approach, the path that a small molecule of a penetrant must travel in a polymeric matrix substantially increases in the presence of intercalated and/or exfoliated clay layers. This result in a noticeable decrease in the diffusion coefficient, estimated as the mean value of the square of the end-to-end distance passed per unit time. This also shows the strong interaction between the filler and the matrix, which limits the toluene diffusivity within the entangled polymer matrix.

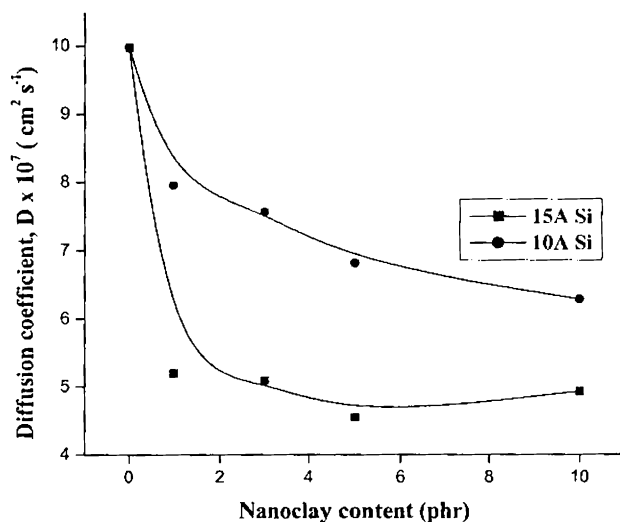


Figure 3.25 Variation of Diffusion coefficient ( $D$ ) with nanoclay content

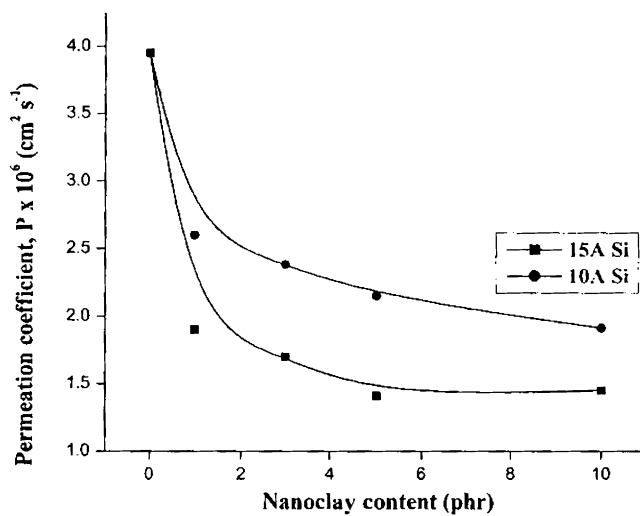


Figure 3.26 Variation of Permeation coefficient ( $P$ ) with nanoclay content

**Table 3.4 Variation of Diffusion coefficient (D), Sorption coefficient (S) and Permeation coefficient (P) with loading of nanoclay**

Sample code	Diffusion coefficient, D $\times 10^7 (\text{cm}^2 \text{s}^{-1})$	Sorption coefficient S	Permeation coefficient, P $\times 10^6 (\text{cm}^2 \text{s}^{-1})$	Crosslink density, $\nu \times 10^5$ (moles $\text{gm}^{-1}$ )	$\Delta G$ (J $\text{mol}^{-1}$ )
Gum	9.98	3.96	3.95	4.7	-14.05
10A <sub>1</sub>	7.96	3.26	2.6	5.51	-16.18
10A <sub>3</sub>	7.57	3.14	2.38	5.86	-16.97
10A <sub>5</sub>	6.82	3.14	2.15	5.54	-17.13
10A <sub>10</sub>	6.29	3.03	1.91	5.59	-18.11
15A <sub>1</sub>	5.2	3.64	1.9	5.03	-15.17
15A <sub>3</sub>	5.09	3.34	1.7	5.44	-16.61
15A <sub>5</sub>	4.55	3.1	1.41	6.06	-18.8
15A <sub>10</sub>	4.41	2.94	1.3	6.04	-18.74

The permeation of a solvent into a polymer membrane will also depend on the sorptivity of the penetrant in the membrane. Hence sorption coefficient,  $S$  has been calculated using the relation

$$S = w_s/w$$

where  $w_s$  is the weight of the solvent at equilibrium swelling and  $w$ , the initial weight of the polymer sample. The numerical values of sorption coefficient are also given in

table 3.4. The values are slightly higher in the gum than in the nanocomposites because of the higher contribution of the layered silicates.

Since the permeability depends on both diffusivity and sorptivity, the permeation coefficient has been determined using the relation

$$P = D \times S$$

The permeation coefficient is the net effect of sorption and diffusion process. The values obtained for P are given in the table 3.4 and figure 3.26. It is seen that the decreasing value of the permeability of the nanocomposites is largely dominated by the diffusion phenomenon, as shown by the respective values of sorption and diffusion. The thermodynamical parameter,  $\Delta G$  of the studied material is reported in table 3.4. It should be noted that  $\Delta G$  increases in the presence of clay. It is assumed that  $\Delta G$  is closely related to the elastic behaviour of the material i.e., the nanocomposites shows a better elasticity than the gum compound and it increases with increase in clay content. These results can be attributed to better compatibility between the silicate and rubber. The rubber molecules can penetrate into the galleries more easily giving rise to a process of exfoliation of the silicate layer.

### **3.3 Effects of carbon black on NR-clay nanocomposites**

Carbon black (CB) is the most important reinforcing filler used in the rubber industry. About 90% of the worldwide production of carbon black is used in the tyre industry; carbon black improves tear strength, modulus and wear characteristics of the tyres [36]. Carbon black consists essentially of elemental carbon in the form of nearly spherical particles of colloidal size, coalesced into particle aggregates and agglomerates, which are obtained by the partial combustion or thermal decomposition of hydrocarbons. The carbon black aggregates are built from primary particles tightly fused together so that the particles cannot be separated by normal processing techniques used for rubber. A group of aggregate together forms agglomerate, but the aggregate is the smallest dispersible unit of carbon black, not the primary particle. The

unique ability of carbon black to enhance the physical properties of elastomers is associated with the size, shape and surface chemistry of the primary aggregates [37].

Since the origin of carbon black is from petroleum, it causes pollution and gives the rubber a black colour. In the past two decades, research was aimed to develop other reinforcing agents to replace carbon black in rubber compounds such as sepiolite, kaolin and precipitated silica. These fillers are inorganic in nature and incompatible with organic polymer matrices. Thus, the reinforcing effect was much lower than with carbon black. However, with the development of nanocomposites, it is possible to tailor the surface of the silicate layers to become organophilic, which can enhance the properties of the polymer significantly. Indeed, some rubber-clay nanocomposites reported in the literature have mechanical properties similar to or better than rubber filled with carbon black [23, 38-40]. Arroyo et al. [23] prepared natural rubber nanocomposites with 10 phr organoclay with similar modulus, tensile strength and hardness as natural rubber with 40 phr carbon black. Magaraphan et al. [38] also prepared natural rubber nanocomposites with 7 phr of MMT functionalized with octadecylamine, which presented higher tensile strength and elongation than NR with 20 phr carbon black. Meneghetti [41] studied the effect of carbon black on styrene butadiene rubber-clay nanocomposites. It is reported that the synergistic effect of carbon black and organoclay brought similar property enhancements with carbon black alone, but at half filler loading.

In this part, NR filled with carbon black was prepared and compared with NR-clay nanocomposites. At the same time, the synergistic effect of carbon black and organoclay was investigated in NR samples, which contained both fillers at different concentration.

### 3.3.1 Cure characteristics

Cure characteristics of the vulcanisates obtained from Rubber process analyzer is given in table 3.5. The increase in maximum torque with increasing filler content indicates the enhancement of stiffness of the nanocomposite.

*Table 3.5 Cure characteristics of nanocomposites*

Sample code	Min Torque (dNm)	Max Torque (dNm)	T <sub>10</sub> (minutes)	T <sub>50</sub> (minutes)	T <sub>90</sub> (minutes)
CB <sub>30</sub>	0.104	3.426	2.59	4.98	9.85
CB <sub>30</sub> +15A <sub>1</sub>	0.108	4.537	1.87	3.91	8.72
CB <sub>30</sub> +15A <sub>3</sub>	0.127	4.916	1.43	3.27	7.71
CB <sub>30</sub> +15A <sub>5</sub>	0.202	5.207	0.93	2.58	6.78
CB <sub>20</sub> +15A <sub>10</sub>	0.157	4.874	0.76	2.30	6.92
CB <sub>40</sub>	0.163	4.413	1.95	3.84	8.33

Maximum torque value of the carbon black filled vulcanisates, which is a direct measure of the shear modulus, increases with the organoclay loading. Since the amine groups used for the modification of the nanoclay facilitates the vulcanisation reaction, a reduction in cure time is observed.

### 3.3.2 Mechanical properties

Stress strain properties for NR vulcanisate containing carbon black and/or organoclay are presented in figures 3.27 to 3.31. Mechanical properties like tensile strength, modulus at 100, 200 and 300% elongation, tear strength and hardness increases with

the increase in carbon black content from 30 phr to 40 phr. One of the reasons for such improvement is the reduction of the inter-aggregate distance within the fillers, which imposes greater resistance against crack propagation [36]. With the addition of 1 phr organoclay along with 30 phr carbon black, natural rubber nanocomposites exhibit higher tensile strength and modulus than NR vulcanisate with 40 phr carbon black alone. Heat build up of the samples is also decreased with the addition of nanoclay. When the nanoclay content is increased to 5 phr, tensile strength remains almost constant, but an increase in modulus is observed. Tear strength, abrasion resistance and hardness are also increased with the addition of nanoclay. The presence of the clay improves the elongation at break more than with the isotropic fillers. The longer clay particles provide more interfacial contact for the rubber molecules allowing for greater extensions.

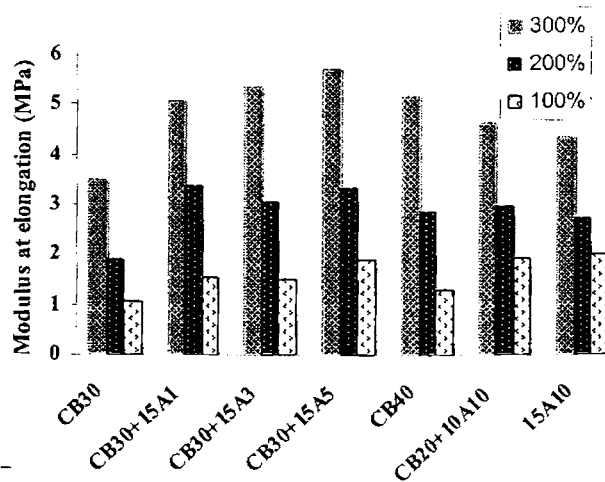


*Figure 3.27 Modulus at 100%, 200% & 300% elongation of vulcanisates*

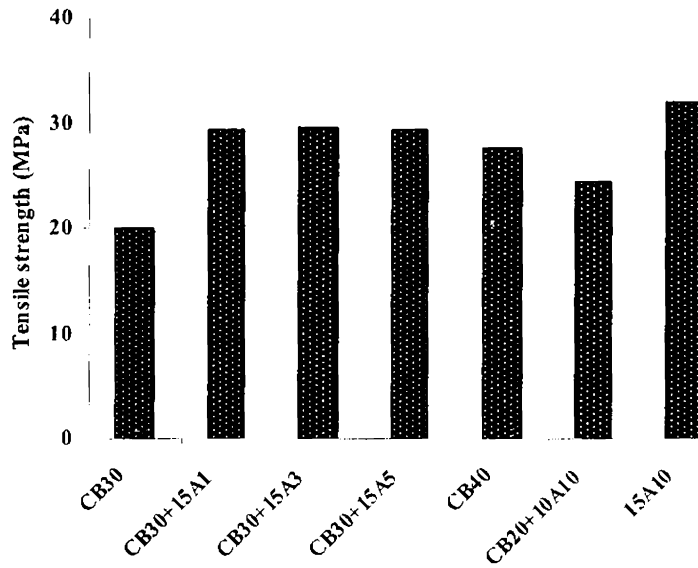


Figure 3. 28 Tensile strength of vulcanisates

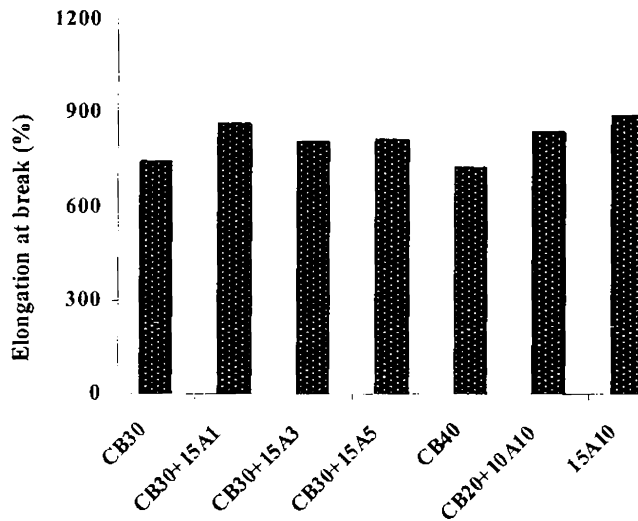


Figure 3.29 Elongation at break of vulcanisates



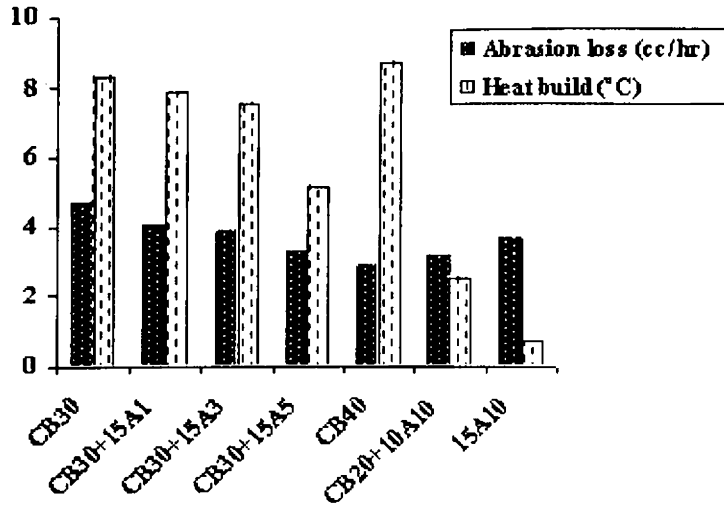


Figure 3.30 Abrasion loss and heat build up of vulcanisates

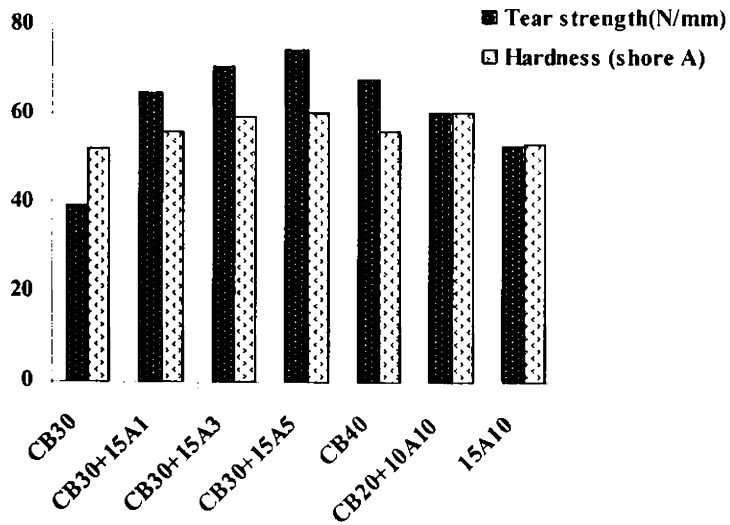


Figure 3.31 Tear strength and hardness of vulcanisates

When compared with 40 phr carbon black filled vulcanisate, nanocomposites having 10 phr of nanoclay alone have about 15% decrease in 300% modulus, but the tensile strength shows a 24% increase. Even though slightly lower tear strength (figure 3.31) is observed, a higher elongation at break is obtained for the nanocomposites. Heat build up of the nanocomposite with 10 phr nanoclay alone is 90% less than the carbon black filled vulcanisate (figure 3.30).

### **3.3.3 Assessment of rubber filler interactions by strain sweep studies**

#### **Strain sweep tests for uncured compounds**

Variation of complex modulus with strain for the uncured compounds is plotted in figure 3.32. It is seen that complex modulus at lower strain increase with carbon black content. With increasing carbon black content, the aggregates tend to associate into agglomerates or clusters, which are generally termed secondary structure or filler network. The formation of the filler network is responsible for such an improvement in modulus as the content of carbon black increases. The polymer chains adsorb over the filler surface, and reduce the mobility of the polymer segment. This results in a rubber shell with a high modulus near the surface of the filler, but as the polymer chains distance themselves from the surface, the modulus gradually decreases and finally reaches the same level as that of the polymer matrix [42]. When two or more aggregates are close enough, they form agglomerate via a joint rubber shell where the modulus of the occluded polymer is higher than that of the polymer matrix. The carbon black filler network, formed primarily by joint shell mechanism, is less rigid and begins to break down at a lower strain or temperature. However; the break down of the carbon black network proceeds less rapidly [43].

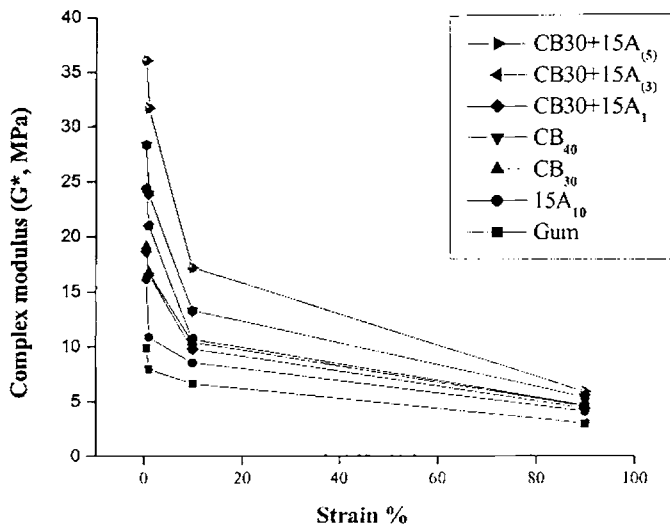


**Figure 3.32** Complex modulus versus strain for NR with carbon black and/or organoclays

When organoclays are mixed with carbon black, the effect on the complex modulus is superior compared to carbon black alone. A steep increase in the modulus is observed for the carbon black filled nanocomposites with increase in clay content. When both fillers are used simultaneously, three different types of filler networks are observed: carbon black network, organoclay network and organoclay-carbon black network. The organoclay-carbon black network is most likely to be stronger than for the carbon black network since the breakdown and reformation of the network begins at a higher strain than the organoclay system alone.

### 3.3.4 Swelling studies

Swelling studies of the vulcanisates were done in toluene and the sorption curves are plotted in figure 3.33. From the figure, it is seen that the maximum solvent uptake of the gum vulcanisate decrease with filler loading and the decrease is more significant for the nanoclay filled samples.

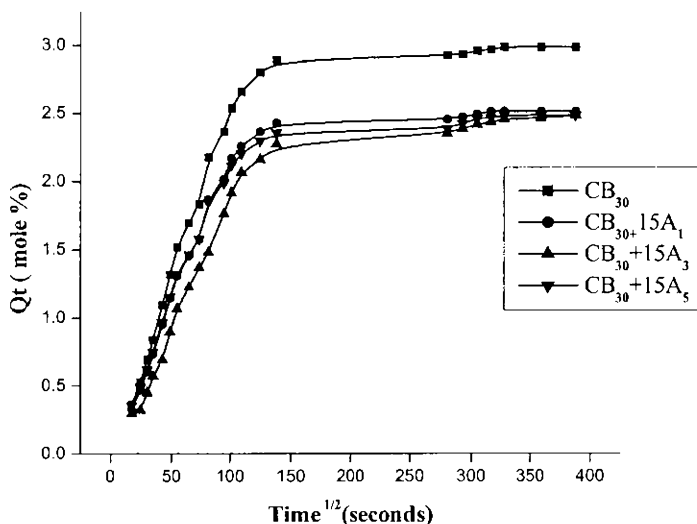


**Figure 3.33 Sorption curves of the carbon black filled vulcanisates**

Diffusion coefficient, Permeation coefficient and Sorption coefficient of the vulcanisates are calculated and given in table 3.6. It is seen that the effect of carbon black on the permeability of a rubbery vulcanisate is not as significant as the improvement in mechanical properties. About 35% reduction in diffusion coefficient is obtained with 30 phr of carbon black. The formation of filler network may contribute to the decrease in permeability. With the build up of the filler network, the rubber becomes trapped within the filler agglomerates leading to an increase in the effective filler volume fraction. By adding 5 phr nanoclay to the 30 phr carbon black filled vulcanisate the diffusion coefficient can be reduced to 64%. That is the swelling resistance gets almost doubled. This may be due to the presence of carbon black organoclay filler network as mentioned before. But the nanocomposite containing organoclay alone offers a higher swelling resistance. About 126% reduction in diffusion coefficient is obtained with 10 phr nanoclay. This is due to the tortuous path provided by the impermeable clay layers for the solvent molecule. With the addition of clay or carbon black, the permeation coefficient of the vulcanisate is also decreasing, but the decreasing value of the permeability of the carbon black filled

vulcanisates is dominated by the sorption whereas it is dominated by diffusion phenomenon in nanocomposites.

**Table 3.6** Variation of diffusion coefficient (*D*), sorption coefficient (*S*) and permeation coefficient (*P*) with loading of nanoclay

Sample code	Diffusion coefficient, $D \times 10^7$ (cm <sup>2</sup> s <sup>-1</sup> )	Sorption coefficient, <i>S</i>	Permeation coefficient, $P \times 10^6$ (cm <sup>2</sup> s <sup>-1</sup> )
Gum	9.98	3.96	3.95
15A <sub>10</sub>	4.41	2.94	1.3
CB <sub>30</sub>	7.36	2.73	2.01
CB <sub>30</sub> +15A <sub>1</sub>	6.14	2.54	1.55
CB <sub>30</sub> +15A <sub>3</sub>	6.65	2.27	1.51
CB <sub>30</sub> +15A <sub>5</sub>	6.06	2.29	1.39

### 3.4 Conclusion

Natural rubber-organoclay nanocomposites were prepared with two different types of nanoclay in varying clay loading and their influence on the cure characteristics, mechanical properties and transport properties on natural rubber were investigated. In presence of organoclays, both the cure time and scorch time are considerably reduced. This reduction in cure time is slightly boosted with the increase in interlayer distance of the clay. A dramatic increase in maximum torque value with increase in clay content is also observed for the nanocomposites prepared using the two different clays. It is seen that the nanocomposite with the clay having higher interlayer distance

shows better mechanical properties. Gas permeation resistance of the nanocomposites is evident from the results obtained. The presence of a tortuous path for the permeating molecules is confirmed by the Nielson's model. As the interlayer distance increases, polymer chains could penetrate more easily into the clay layers, which results in the formation of an intercalated structure. The increase in 'd' spacing for these layered clays evident from X-ray results and TEM photographs also confirmed the formation of an intercalated structure.

The compatibility of clay platelets with the rubber organic phase, in terms of wetting and dispersion, is substantially improved by the addition of organosilane coupling agents. The organoclay, treated with the silane coupling agent behaved as an effective reinforcement agent for NR and showed a stronger reinforcing character while retaining the elasticity of the rubber. The swelling of the material is strongly reduced in the presence of clay within the NR matrix. The presence of impermeable clay layers decreases the rate of transport by increasing the average diffusion path length in the specimen.

The synergistic effect of carbon black and organoclay in improving the mechanical properties of NR vulcanisates was also investigated. Incorporation of a small amount of nanoclay (1 phr) along with 30 phr carbon black in natural rubber results in the formation of composites with mechanical properties almost similar to composites with 40 phr carbon black without causing much decrease in elongation at break. Heat build up of the composites is also decreased with the addition of nanoclay. The organoclay-carbon black network is stronger than for the case of carbon black network since the breakdown and reformation of the network begins at a higher strain than the organoclay system alone. With the addition of both fillers, the permeation coefficient of the vulcanisate decreases but the decreasing value of the permeability of the carbon black filled vulcanisates is dominated by the sorption whereas it is dominated by diffusion phenomenon as in nanocomposites.

**References**

1. Kojima, Y., Kawasumi, M., Usuki, A., Okada, A., Fukushima, Y., Kurachi, T. and Kamigaito, O., *J. Mater. Res.*, 8 (5), 1185, 1993.
2. Fu, X. and Qutubuddin, S., *Polymer*, 42, 807, 2001.
3. Messersmith, P.B. and Giannelis, E.P., *Chem. Mater.*, 6, 1719, 1996.
4. Yano, K., Usuki, A., Okada, A., Kurauchi, T. and Kamigaito, O., *J. Polym. Sci. A: Polym. Chem.*, 31, 2493, 1993.
5. Ma, J., Yu, Z.Z., Zhang, Q.X., Xie, X. L., Mai, Y.W. and Luck, I., *Chem Mater.*, 16, 757, 2004.
6. Tyan, H.L., Liu, Y.C. and Wei, K.H., *Chem Mater.*, 11, 1942, 1999.
7. Ray, S.S. and Okamoto, M., *Prog Polym Sci.*, 28,1539, 2003.
8. Kormmann, X., Thomann, R., Mulhaupt, R., Finter, J. and Berglund, L., *J Appl Polym Sci.*, 86, 2643, 2002.
9. Alexandre, A. and Dubois, P., *Mater Sci Eng.*, 28, 1, 2000.
10. Kawasumi, M., Hasegawa, N., Kato, M., Usuki, A. and Okada, A., *Macromolecules*, 30, 6333, 1997.
11. Chow, W.S., Mohd Ishak, Z.A., Karger-Kocsis, J., Apostolov, A. A. and Ishiaku, U.S., *Polymer*, 44, 7427, 2003.
12. Zilg, C., Thomann, R., Finter, J. and Mulhaupt, R., *Macromol Mater Eng.*, 280/281, 41, 2000.
13. Fomes, T.D., Hunter, D.L. and Paul, D.R., *Macromolecules*, 37, 1793, 2004.
14. Fomes, T.D., Yoon, P.J., Keskkula, H. and Paul, D.R., *Polymer*, 42, 9929, 2001.

15. Zheng, H., Zhang, Y., Peng, Z. and Zhang, Y., *J. Appl Polym Sci.*, 92, 638, 2004.
16. Li, X. and Ha, C.S., *J Appl Polym Sci*, 87, 1901, 2003.
17. Maiti, P., Yamada, K., Okamoto, M., Ueda, K. and Okamoto, K., *Chem Mater.*, 14, 4654, 2002.
18. Lan, T., Kaviratna, D. and Pinnavaia, T. J., *Chem Mater.*, 7, 2144, 1995.
19. Theng, B. K. G., *Formation and Properties of Clay-Polymer Complexes*, Elsevier Scientific Publishing Company, New York, p 353. 1979
20. Wang, Z. and Pinnavaia, T. J., *Chem Mater.*, 10, 1820, 1998.
21. Lan, T., Pinnavaia, T. J., Chem, S. N. and Lopez, B. H., *J Appl Polym Sci.*, 44, 353, 1992.
22. Mousa, A. and Karger Kocsis, J., *Macromol. Mater. Eng.*, 286(4), 260, 2001.
23. Arroyo, M., Manchado, L. M. A. and Herrero, B., *Polymer*, 44, 2447, 2003.
24. Varghese, S., Karger Kocsis, J. and Gatos, K. G., *Polymer*, 44, 3977, 2003.
25. Lopez Manchado, M. A., Arroyo, M., Herrero, B. and Biagiotti, J., *J Appl Polym Sci.*, 89, 1, 2003.
26. Wolf, S., *Rubber Chem. and Technol.*, 69, 325, 1996
27. Nielsen, L. E. and Landel, R. F., *Mechanical Properties of Polymers and Composites*, 2nd ed., Marcel Dekker, Inc., p 545. 1994.
28. Kluppel, M., Schuster, H. R. and Heinrich, G., *Rubber Chem and Technol*, 70, 243, 1997
29. Jean, L. and Leblanc Marie cartault., *J. Appl, Polym. Sci.*, 80, 11, 2093, 2001.
30. Guth, E. and Gold, O., *Phys. Rev.*, 53, 322, 1938.



31. Smallwood, H.M., *J. Appl. Phys.*, 15, 758, 1944.
32. Stickney, P.B. and Falb, R.D., *Rub. Chem. Technol.*, 37, 1299, 1964.
33. Nielsen, L., *J. Macromol. Sci. Chem.A1*, 929, 1967.
34. Rotheron, R., Editor, *Particulate-Filled Polymer Composites*, Longman Scientific & Technical, New York, p 371, 1995.
35. Morton, M., Editor, *Rubber Technology*, 3 ed., Van Nostrand Reinhold Co., New York, p 631, 1987.
36. Donnet, J.B., Bansal, R. and Wang, M.J., (Eds.). *Carbon Black Science and Technology*, Marcel Dekker, Inc., New York, 1993.
37. Dick, J., Editor, *Rubber Technology Compounding and Testing Performance*, Hanser Gardner Publications, 2001.
38. Magaraphan, R., Thaijaroen, W. and Lim-Ochakun, R., *Rubber Chem. Technol.*, 76, 406, 2003.
39. Zhang, L., Wang, Y., Wang, Y., Sui, Y. and Yu, D., *J. Appl. Polym. Sci.*, 78, 1873, 2000.
40. Wang, Y., Zhang, L., Tang, C. and Yu, D., *J. Appl. Polym. Sci.*, 78, 1879, 2000.
41. Meneghetti, P. C., *Synthesis and properties of Rubber-clay nanocomposites*, PhD Thesis, Case Western Reserve University, p 114, 2005.
42. Wolff, S. and Wang, M. J., *Kautsch. Gummi Kunstst.*, 47, 17, 1994.
43. Wang, M.J., *Rubber Chem. Technol.*, 71, 520, 1998.

## *Chapter 4*

---

### *Natural Rubber Latex Clay Nanocomposites*

Natural rubber is an important material used in a wide assortment of engineering applications. Its use depends mainly on its inherent soft and highly deformable nature. Natural rubber latex basically consists of a dispersed phase of rubber particles (poly-cis-1, 4 - isoprene) and other non-rubber components in minor quantities, and the dispersing medium, water, which contains several organic substances and mineral salts. Rubber particles formed by the aggregation of molecules of rubber hydrocarbon are having spherical, oval, pear-like and various other constricted forms [1]. In NR latex, particle size of rubber range from 0.1 to 4 micron. These rubber particles are stabilized by the presence of adsorbed carboxylic anions from fatty acid soaps and protein molecules on their surfaces. The adsorbed anions cause the particle surface to have a net negative electrical charge, which produces inter-particle repulsive forces and hence ensures absence of aggregation and thereby stability of the latex.

The particle size of the chemicals used in compounding must be smaller than those of the rubber particles since the bigger particles get settled out. The addition of any filler usually reduces the strength of the rubber obtained from latex. But layered silicates can be used to overcome this disadvantage. A variety of clays have recently been used to obtain nanocomposites by exploiting the ability of clay silicate layers to be dispersed into polymers at the nanoscale level. Montmorillonite clay was used to prepare natural rubber latex nanocomposites. Montmorillonites are materials with fine-grained particle and high surface area. In addition, they are readily dispersed in water (latex) without the aid of dispersing agents and are easily incorporated as dry or as aqueous dispersion without risking the destabilization of the latex. The crystal structure of the clay itself is the most important parameter. The characteristic expansion of the interlayer structure exposes a large active surface area and permits

polymer molecules to enter into the intergalleries. This separation of clay platelets can occur under certain conditions giving very high aspect ratio filler, which dramatically improves composite properties. The water swelling capability of the natural clays depend upon the type of clay and its cation exchange capacity [2] and hence the mixing of the latex with the layered silicates, having high cation exchange capacity, followed by coprecipitation (coagulation) is a promising route for producing rubber nanocomposites [3]. Most of the rubbers are available in the form of latex, which is nothing but an aqueous dispersion of rubber particles in the sub micron–micron range, the particle size distribution vary depending on the type of rubber and manufacturing conditions. Several options are available to add and disperse the silicates in the latex, like dispersing the silicates directly in the latex, by using silicate slurry, restabilization of the layered silicate containing latex prior to appropriate comminution operations like ball milling.

The layered silicates are easily dispersed in water as water, acts as a swelling agent owing to the hydration of the intergallery cations, usually  $\text{Na}^+$ . US Patent 2003 0,144,401 refers to the preparation of clay-rubber nanocomposites by the latex route and such materials have been suggested for use in tyre components like tyre tread, sidewall and/or inner liner [4]. Another US Patent, US 2005 065,266 reports the preparation of nanocomposites comprised of water swellable clay particles in aqueous emulsions like anionic styrene butadiene rubber (SBR) or NR containing a novel amine for aiding in intercalation and partial exfoliation of the clay particles [5]. Applications of such rubber nanocomposites are contemplated, for example, as aircraft tyre tread where significant replacement of carbon black reinforcement is desired to reduce heat buildup for tyre durability and reduction in tyre weight for fuel economy. Wang et al. prepared natural rubber clay and chloroprene rubber clay nanocomposites by cocoagulating the rubber latex and the aqueous clay suspension [6]. The presence of more than 10 phr nanoclay inhibited the strain-induced crystallization of NR. Compared with the carbon black filled NR composites, NR-MMT nanocomposites exhibited high hardness, high modulus, high tear strength, and excellent antiaging and

gas barrier properties. The clay layers with large aspect ratio and planar orientation increased the diffusion distance by creating a more tortuous path for the diffusing gas and therefore exhibited better antiaging properties than the NR reinforced with the same loading of carbon black on prolonged aging. Similar to NR-MMT nanocomposites, CR-MMT nanocomposites also exhibited high hardness, high modulus, and high tear strength. Potential application areas suggested by Wang et al. for these nanocomposites were as inner tubes, inner liners, and dampers [6]. Zhang et al. prepared SBR-clay (natural clay fractionated from bentonite) nanocomposites by mixing the SBR latex with clay/water dispersion and coagulating the mixture [7]. Wang et al. compared the mechanical properties of SBR-clay (fractionated bentonite) nanocomposites prepared by the solution and latex blending techniques [8] and found that at equivalent clay loadings, the nanocomposites prepared by the latex route were better than those prepared by the solution blending technique. Zhang et al. investigated the flammability of SBR-MMT nanocomposites prepared by the technique of cocoagulating rubber latex and clay aqueous dispersion [9]. Jia et al. combined in-situ organic modification of MMT and the latex compounding method to prepare high performance SBR-MMT nanocomposites by improving the interfacial interaction between nanodispersed layered clay and SBR [10]. Wu et al. prepared carboxylated NBR (CNBR)-clay mixtures by cocoagulating rubber latex and clay aqueous suspension followed by traditional rubber compounding and vulcanization [11]. The aspect ratio of the clay platelets was reduced and silicate layers were aligned in a more orderly fashion during the compounding operation on a two roll mill. NBR-clay nanocomposites were prepared in a similar manner by Wu et al. [12]. The NBR-clay nanocomposites exhibited excellent mechanical and gas barrier properties, which was described by Nielsen's model [13]. Thus in literature, it is found that plenty of works has been used to develop rubber nanocomposites through latex route since better dispersion of the clay layers in the rubber matrix can be achieved. But the development of better reinforced latex nanocomposite is also considerably important while considering the application. Currently, about 50% of all latex concentrate is

consumed by the dipped goods industry. Dipped goods include products such as gloves (medical and household), balloons, catheters, teats and dummies. A sudden increase in the usage of dipped latex products occurred after the outbreak of the AIDS epidemic. About 63% of this is contributed by natural rubber latex. Other uses of latex are in carpet backing, thread and adhesives in rubber industries.

Varghese and Karger-Kocsis prepared NR based latex nanocomposites with 10 wt% natural (sodium bentonite) and synthetic (sodium fluorohectorite) layered silicates by the latex compounding method [14]. Commercial clay (inert material) was used as the reference material in their work. It was observed that the layered silicates outperformed the commercial clay in mechanical, thermal and swelling tests. Stephen et al. studied the impact of layered silicates such as sodium bentonite and sodium fluorohectorite on the rheological behavior of NR, carboxylated SBR lattices, and their blends with special reference to shear rate, temperature and filler loading [15]. They observed that the viscosity of the layered silicates increased with increasing filler concentration and also exhibited pronounced shear thinning behavior. A higher loading of clay resulted in processing difficulties due to viscosity build up. But application of a small amount of intercalated clay to the rubber matrix can provide considerable improvement in barrier performance of various rubbers [16]. According to the free volume concept, the chain mobility provides a driving force for diffusion of small molecules. In a nanocomposite the molecular mobility is severely reduced in the close vicinities of the clay platelets and this provide a tortuous path for the permeating molecules. Transport properties are of considerable importance for latex nanocomposites as their applications mainly involve barrier materials.

In this chapter, natural rubber latex nanocomposite was prepared using unmodified layered clay viz., cloisite Na<sup>+</sup> in low loadings and their transport properties were studied in detail. Latex nanocomposites developed were characterized using X-ray diffraction technique and Transmission electron microscopy. Mechanical properties of the nanocomposites were also determined.

#### 4.1 Preparation of NR latex-clay nanocomposites

Aqueous dispersion (2%) of layered clays was prepared by means of an ultrasonic stirrer (Oscar ultrasonics). Other compounding ingredients were prepared as water dispersions by ball milling. The compounding recipe is given in table 4.1. After compounding the latex is kept for five days for maturation. Slow speed stirring was continued during this period. The compounded latex after removing the coagulum of any coarse particles by filtering through 80 mesh sieve is then casted on raised glass plate having a dimension of 13 cm x 10 cm x 1mm. The casting was then allowed to dry in air till it becomes transparent and then vulcanized at 343 K for 4 hours in an air oven with provision for circulation of air.

*Table 4.1 Recipe for mixing*

Ingédients	Mix 1	Mix 2	Mix 3	Mix 4
	parts per hundred rubber (phr)			
NR latex (60% DRC)	100	100	100	100
Sulphur (50%)	1.5	1.5	1.5	1.5
Zinc Oxide (50%)	0.9	0.9	0.9	0.9
Potassium Oleate (10%)	0.8	0.8	0.8	0.8
ZDC (50%)	0.7	0.7	0.7	0.7
Wingstay L (50%)	0.5	0.5	0.5	0.5
Clay dispersion (2%)	0	1	2	3

## 4.2 Characterisation using X-ray diffraction technique

X-ray diffraction (XRD) patterns were obtained from Bruker, D8 Advance diffractometer at the wavelength  $\text{CuK}\alpha = 1.54\text{\AA}$ , a tube voltage of 40kV and tube current of 25mA. Bragg's law defined as  $n\lambda = 2d\sin\theta$ , was used to compute the crystallographic spacing ( $d$ ) for the clay [17]. The samples were scanned in step mode by  $1.0^\circ/\text{min}$ , scan rate in the range of 2 to  $12^\circ$ .

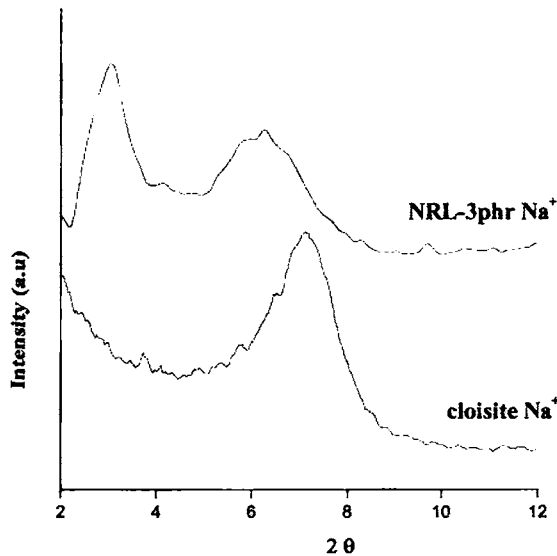


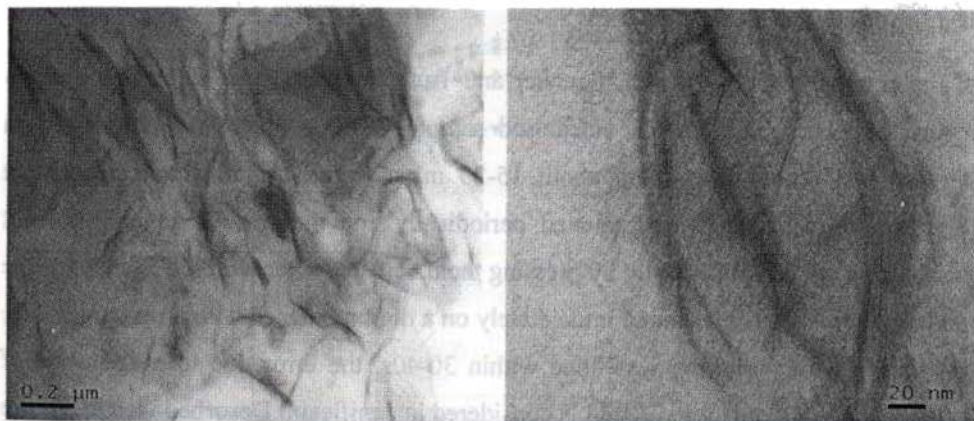
**Figure 4.1** X-ray diffraction spectrum of nanoclay (cloisite  $\text{Na}^+$ ) & nanocomposite with 3 phr nanoclay (NRL - 3phr  $\text{Na}^+$ )

X-ray diffraction pattern is widely used to characterise the structure of nanocomposite. If the crystalline order is manifested as a peak corresponding to the same basal spacing as in the pristine clay then we have a conventional composite. Appearance of peak at lower angle corresponding to higher basal spacing indicates the formation of intercalated nanocomposites. Figure 4.1 shows the X-ray diffraction pattern of (a) nanoclay (cloisite  $\text{Na}^+$ ) and (b) rubber – clay nanocomposite. The clay showed  $d_{001}$  peak at  $2\theta = 7.1^\circ$  which corresponds to  $d_{001}$  spacing  $12.35 \text{ \AA}$  and for the

nanocomposites a peak at  $2\theta = 3.07^\circ$  and a shoulder peak at  $2\theta = 5.88^\circ$  correspond to interlayer distance of  $28.74 \text{ \AA}$  and  $14.99 \text{ \AA}$  respectively. Both the peaks get shifted to a lower  $2\theta$  value/higher  $d_{001}$  spacing supporting the fact that rubber molecules in NR latex penetrate between the silicate layers. The more intense peak shows that the  $d_{001}$  spacing value increases by  $16.39 \text{ \AA}$ . This confirms the formation of intercalated nanocomposites.

#### **4.3 Transmission electron microscopy**

The transmission electron microscopy was performed using a JEOL JEM- 2010 (Japan) transmission electron microscope, operating at an accelerating voltage of 200 KV.



(a)

(b)

**Figure 4.2 TEM micrographs of nanocomposite with 3 phr nanoclay (a) at low magnification (b) at higher magnification**



The samples for TEM analysis were prepared by ultra-cryomicrotomy using a Leica Ultracut UCT. Freshly sharpened glass knives with cutting edge of 45° were used to get the cryosections of 50 - 70 nm thickness. Since these samples were elastomeric in nature, the temperature during ultra cryomicrotomy was kept at -50 °C. The cryosections were collected individually on sucrose solution and directly supported on a copper grid of 300 mesh size. TEM was used in order to visualize the morphology of the clay layers in the nanocomposites. TEM micrographs for sample with 3 phr of nanoclay shown in figure 4.2 reveals that the stacked silicate layers are partially peeled off and in between the peeled layers NR molecules could penetrate. There by the mobility of the rubber molecules becomes strongly hampered. Even though X-ray diffraction indicated only intercalated structures, exfoliated layers can also be observed in the TEM pictures.

#### **4.4 Swelling studies**

Circular specimens of 20 mm diameter and 1mm thickness were cut using a sharp edged circular disc from the vulcanised samples. The samples were immersed in airtight test bottles containing about 15-20 ml of toluene maintained at constant temperature. Samples were removed periodically and the surface adhered solvent drops were wiped off carefully by pressing them between filter wraps. The mass of the sorbed sample was determined immediately on a digital balance with an accuracy of ± 0.01mg. As the weighing was done within 30-40s, the error due to evaporation of other than surface adsorbed liquid is considered insignificant. Desorbed weights of the samples were also taken after complete removal of the solvent.

The mole percent uptake of the sample is calculated from the diffusion data. The  $Q_t$  values were determined as

$$Q_t = \frac{(\text{Wt. of the solvent sorbed at a given time})/(\text{Mol. wt. of the solvent})}{(\text{Initial wt of the rubber specimen} \times 100)}$$

At equilibrium swelling,  $Q_t$  becomes  $Q_x$ . Sorption curves of the vulcanisates which are obtained by plotting  $Q_t$ , mole% uptake per 100 g of the solvent, against time are shown in figure 4.3. For all compositions, the uptake is rapid in the initial zone. After this, the sorption rate decreases leading to a plateau corresponding to equilibrium swelling. Note that the gum has maximum toluene uptake at equilibrium swelling. The swelling of the material is strongly reduced in the presence of clay within the NR matrix. The presence of impermeable clay layers decreases the rate of transport by increasing the average diffusion path length in the specimen. In order to determine how the clay content affects the permeability, we measured the transport properties of the samples.

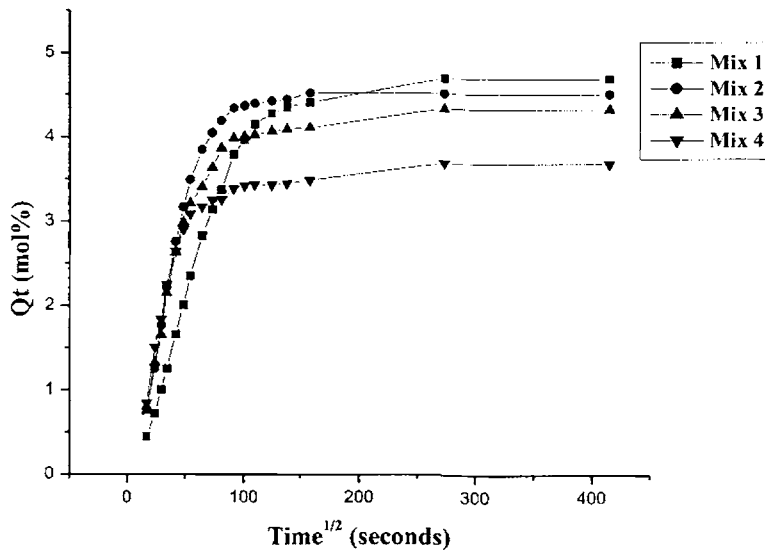


**Figure 4.3 Swelling behavior of the NR latex samples in toluene at 303 K**

The mechanism of diffusion was investigated using the equation [18, 19, 20]

$$\log Q_t/Q_\infty = \log k + n \log t$$

The value of  $k$  depends on the structural features of polymer, whereas the value of  $n$  determines diffusion mechanism. For the Fickian mode, the value of  $n$  equal to 0.5 and the rate of diffusion of penetrant molecules is much less than the relaxation rate of the polymer chains. For non-Fickian transport, where the value of  $n$  equal to 1, the diffusion is rapid when compared with the simultaneous relaxation process. However, in the case of anomalous transport, where the value of  $n$  is in between 0.5 and 1, both solvent diffusion and polymer relaxation rate are comparable. The values of  $n$  and  $k$  are given in table 4.2. In this study, it is seen that with increase in clay content anomalous mechanism shifts to the Fickian mode.

**Table 4.2 Variation in  $n$  and  $k$  values with loading of nanoclay**

Samples	$n$	$k$
Mix 1	0.6679	-1.4621
Mix 2	0.6647	-1.2099
Mix 3	0.5038	-1.1144
Mix 4	0.4792	-0.9262

The swelling of polymer is also affected by solvent transport. As swelling increases, free volume increases due to chain mobility, which facilitates transport process. The diffusion coefficient,  $D$  can be determined using the relation [21, 22]

$$D = \pi \left[ \frac{h\theta}{4Q_{\infty}} \right]^2$$

where  $h$  is the initial thickness of rubber sample,  $\theta$  the slope of the linear portion of the sorption curve and  $Q_{\infty}$  is obtained from the  $Q_t$  versus  $t^{1/2}$  graph (figure 4.3). The values of  $D$  are given in the table 4.3. The variation of  $D$  depends on the solvent uptake, which is maximum for the gum vulcanisate. Adding clay within the NR matrix results in a progressive decrease of  $D$  value and a substantial decrease with increase in clay content. This may be due to the reduced availability of space for solvent molecules in the intercalated structure of the nanocomposites. This also shows the strong interaction between the filler and the matrix, which limits the toluene diffusivity within the entangled polymer matrix.

The permeation of a solvent into a polymer membrane will also depend on the sorptivity of the penetrant in the membrane. Hence sorption coefficient,  $S$  has been calculated using the relation [23]

$$S = \frac{W_s}{W}$$

where  $W_s$  is the weight of the solvent at equilibrium swelling and  $W$ , the initial weight of the polymer sample. The numerical values of sorption coefficient are also given in table 3. The values are slightly higher in the gum than in the nanocomposites because of the higher contribution of the layered silicates.

Since the permeability depends on both diffusivity and sorptivity, the permeation coefficient has been determined using the relation [23]

$$P = D \times S$$

The permeation coefficient, the net effect of sorption and diffusion process is also found to be decreased. The values obtained for  $P$  are given in table 4.3. It is seen that the decreasing value of the permeability of the nanocomposites is largely dominated by the diffusion phenomenon, as shown by the respective values of sorption and diffusion reported in the table 4.3.

**Table 4.3** Variation of diffusion coefficient (*D*), sorption coefficient (*S*) and permeation coefficient (*P*) with loading of nanoclay

Samples	$D \times 10^7$ ( $\text{cm}^2 \text{s}^{-1}$ )	S	$P \times 10^6$ ( $\text{cm}^2 \text{s}^{-1}$ )
Mix 1	7.12	4.31	3.08
Mix 2	6.22	4.15	2.58
Mix 3	4.22	3.33	1.43
Mix 4	4.20	3.39	1.40

As diffusion is influenced by polymer morphology, the molar mass between cross links  $M_c$  from the sorption data is also determined. The rubber solvent interaction parameter, which is needed for the estimation, has been calculated using the equation [23]

$$\chi = \beta + \frac{V_s}{RT} (\delta_s - \delta_p)^2$$

where  $V_s$  is the molar volume of the solvent,  $\delta_s$  and  $\delta_p$  are the solubility parameters of solvent and polymer taken from the polymer handbook. R is the universal gas constant and T the absolute temperature and  $\beta$  is the lattice constant which is 0.38 in this calculation.

Using  $\chi$  values the molar mass between crosslinks ( $M_c$ ) of the polymer was estimated from the Flory Rehner equation [24, 25]

$$M_c = \frac{-\rho_p V_s (V_r)^{1/3} \chi}{\ln(1 - V_r) + (V_r) + \chi(V_r)^2}$$

where  $\rho_p$ , density of the polymer,  $V_r$ , volume fraction of swollen polymer.  $V_s$ , molar volume of the solvent and  $\chi$ , the interaction parameter.

The volume fraction of the polymer is calculated using the equation [26]

$$V_r = \frac{(d - fw)\rho_p^{-1}}{(d - fw)\rho_p^{-1} + A_o\rho_s^{-1}}$$

where  $d$  is the desorbed weight of the polymer,  $f$ , the weight percent of filler,  $w$ , the initial weight of the polymer,  $\rho_p$  and  $\rho_s$ , the density of polymer and the solvent respectively and  $A_o$ , the net solvent uptake of the polymer. The monomeric molecular weight of NR being  $68 \text{ g mol}^{-1}$ , the average number of monomeric units between crosslinks can be calculated. A decrease in the value is observed. Using the  $M_c$  values crosslink density can be calculated using the equation  $\nu = 1/2M_c$  and is given in the table 4.4

**Table 4.4 Variation in crosslink density and molar mass between cross links with loading of nanoclay**

Samples	Crosslink density, $\nu$ $\times 10^5$ (moles $\text{gm}^{-1}$ )	Molar mass between crosslinks, $M_c$ ( $\text{g mol}^{-1}$ )
Mix 1	4.25	11764.71
Mix 2	4.46	11210.76
Mix 3	5.83	8576.329
Mix 4	7.61	6570.302

Thermodynamic effects occurring during swelling of the elastomer chains were also analysed. The thermodynamic approach is of great importance for understanding the rubber filler interaction in the nanocomposites. Swelling of a vulcanised rubber depends on the crosslink density and the solvent used. The expansion of the rubber in the presence of a solvent will significantly modify the conformational entropy ( $\Delta S$ ) and the elastic Gibbs free energy ( $\Delta G$ ). The elastic Gibbs free energy can be determined from the Flory- Huggins equation [27]

$$\Delta G = RT \left[ \ln(1 - V_r) + (V_r) + \chi(V_r)^2 \right]$$

**Table 4.5 Thermodynamical parameters  $\Delta G$  and  $\Delta S$  of the compounds**

Samples	$\Delta G$ (J mol <sup>-1</sup> )	$\Delta S \times 10^2$ (J mol <sup>-1</sup> )
Mix 1	-10.61	3.50
Mix 2	-11.17	3.68
Mix 3	-15.21	5.00
Mix 4	-20.66	6.82

And from the statistical theory of rubber elasticity,  $\Delta S$  can be obtained from the relation  $\Delta G = -T\Delta S$ , which assumes that no change in internal energy of the network occurs upon stretching. Both thermodynamical parameters,  $\Delta S$  and  $\Delta G$  of the studied material are reported in table 4.5. It should be noted that  $\Delta G$  increases in the presence of clay. It is assumed that  $\Delta G$  is closely related to the elastic behavior of the material. i.e., the nanocomposites shows a better elasticity than the gum compound and it increases with increase in clay content. These results can be attributed to better compatibility between the silicate and rubber, the rubber molecules can penetrate into the galleries more easily giving rise to a process of exfoliation of the silicate layer. This exfoliation is responsible for the noticeable increase of entropy as compared with gum.

#### **4.5 Gas permeability testing**

The air permeability of the latex layered silicate membranes were measured using Lyssy Manometric Gas Permeability Tester L100-2402. The test gas used was oxygen



at a rate of 500ml/minute. The oxygen permeability of the nanoclay filled and gum vulcanisate having 1mm thickness are depicted in figure 4.4. It is clearly seen that the oxygen permeability decreases substantially (66%) by incorporation of 1 phr of layered silicate. As the silicate loading is increased to 3 phr, only a slight improvement in permeation resistance was observed.

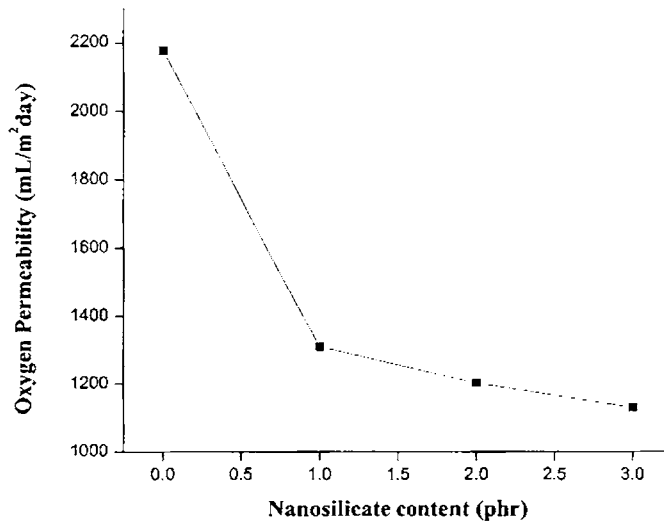


*Figure 4.4 Oxygen permeability of the NR latex films having 1mm thickness*

Gas barrier in plate like particle filled polymer nanocomposites was traditionally explained in terms of Nielson model, originally adopted to describe the tortousity effect of plate like particulates on gas permeability of polymer composite structures [28]. This model system consists of uniform platelets homogeneously dispersed in the polymer matrix and oriented parallel to the polymer film surface. The model can be applied using the equation,

$$\frac{P}{P_0} = \frac{1 - \phi_f}{1 + \frac{L}{2W} \phi_f}$$

to obtain the clay aspect ratio from the permeability data of these nanocomposites. In the equation,  $P$  is the permeability of the nanocomposite,  $P_0$  is the permeability of the gum vulcanisate and  $\phi_f$  is the volume fraction of the clay.  $L$  and  $W$  are length and width of the clay sheets, respectively, its ratio  $L/W$ , defines the aspect ratio  $\alpha$ , of the fillers. The model assumes that the fillers are impermeable to the diffusing gas or liquid molecule, and are oriented perpendicularly to the diffusion direction. Thus, the presence of the filler particles creates tortuous path for the permeant to travel through the composites. The denominator on the right hand side of the equation is also referred to as the tortuosity factor,  $\tau$ , defined as the distance a molecule must travel to get through the film divided by the thickness of the film. From table 4.6, it can be seen that with the increase in clay content the aspect ratio is decreasing (table 4.6) and thus the tortuosity factor increases. Permeability data (figure 4.4) of the nanocomposites also suggests the same and thus the permeation of oxygen molecules through the nanocomposites fits with Nielsen model. Sample with lower clay content presents the higher aspect ratio due to the better dispersion of clay in the rubber matrix, thus only a slight decrease in the permeability is observed with the increase in clay content.

Bharadwaj [29] modified Nielsen model to incorporate an orientation parameter  $S$ , in which, a range of relative orientations of the clay sheets with respect to each other represented by  $\theta$  (the angle between the direction of preferred orientation and the sheet normal) could be applied.

$$\frac{P}{P_0} = \frac{1 - \phi_f}{1 + \frac{L}{2W} \phi_f \left( \frac{2}{3} \right) \left( S + \frac{1}{2} \right)}$$

Bharadwaj's expression is shown in the equation accompanied by the orientation parameter equation

$$S = \frac{1}{2}(3 \cos^2 \theta - 1)$$

In the case of random platelet orientation ( $S = 0$ ), the tortuosity decreases with orientation and diffusion is facilitated as opposed to parallel orientation ( $S = 1$  or Nielson model). This model predicts higher aspect ratios for the nanocomposites than the Nielson's model. Moreover, in the case of latex nanocomposites prepared by the solution casting method, majority of the clay layers orient in the same direction rather than randomly oriented due to the small restriction for the mobility of clay layers in the latex. Thus the Bharadwaj model cannot be applied to the latex nanocomposite.

Another model used to describe gas behavior through a membrane was developed by Cussler et al. [30] with focus on the diffusion of a small gas molecule through a matrix partly filled with impermeable flakes. The flakes are oriented perpendicular to the direction of diffusion and have one very long dimension so that the diffusion is essentially two dimensional. The diffusion is mainly related to three factors: the tortuous wiggles to get around the flakes, the tight slits between the flakes and the resistance of going from the wiggle to the slit. The model assumes that the diffusion depends on the aspect ratio and volume fraction of the impermeable filler.

$$\frac{D}{D_0} = \frac{1}{1 + \frac{(L/2W)^2 \phi_f^2}{(1-\phi_f)}}$$

Where  $D$  is the diffusion coefficient of the composites and  $D_0$  is the diffusion coefficient of the pure polymer.

A permeability model can be obtained by multiplying the diffusion by the appropriate solubility. Since the model assumes linear relationship between solubility of filled composites and volume fraction,  $S = S_0 (1-\phi_f)$ , where  $S$  is the solubility of the filled

composites and  $S_0$  is the solubility of pure polymer. The permeability expression is the following.

$$\frac{P}{P_0} = \frac{(1 - \phi_f)^2}{1 - \phi_f + (L/2W)^2 \phi_f^2}$$

*Table 4.6 Aspect ratio of clay from permeability studies*

Samples	Aspect ratio		
	Nielsen's model	Bharadwaj's Model	Cussler's model
Mix 2	129.04	387.12	159.84
Mix 3	77.34	232.02	87.06
Mix 4	57.80	122.38	61.14

The aspect ratio calculated using the Cussler model is much higher than that calculated from the Nielsen model. For the nanocomposites with very low clay loading, a better homogeneous dispersion is achieved and thus this model cannot be applicable for latex nanocomposite.

#### **4.6 Mechanical properties**

Stress strain properties of the latex based nanocomposites are given in table 4.7. It is observed that silicate reinforced systems prepared by mixing nanoclay in natural rubber latex show a superior modulus and strength relative to ordinary rubber. This highest enhancement in property improvement can only be realized when the nanoparticles are dispersed uniformly (exfoliated) in the polymer matrix.

**Table 4.7 Mechanical properties of the vulcanisates**

Sample code	Tensile strength (MPa)	Modulus at 100% elongation (MPa)	Modulus at 200% elongation (MPa)	Modulus at 300% elongation (MPa)	Elongation at break (%)
Mix 1	20.04	0.63	0.76	1.19	1262
Mix 2	26.78	1.12	1.45	1.91	1319
Mix 3	29.65	1.19	1.67	2.11	1284
Mix 4	32.97	1.23	1.84	2.38	1273

The nanometric dispersion of silicate in NR matrix and exfoliated structure results in an effective reinforcement. The reinforcement of rubbers with fillers combines the elastic behavior of rubber with the strength and stiffness of the reinforcing phase. It is obvious that even with the addition of such a low loading of montmorillonite (1 phr-3 phr), the tensile modulus and tensile strength increases considerably (table 4.7). For example, compared to unfilled rubber, 3 phr clay composite has 100% higher modulus at 300% elongation and 65% higher tensile strength. Generally, rigid fillers cause a dramatic decrease in elongation at break [31], whereas elongation at break is higher for the nanocomposites than the gum vulcanisate, but it decreases slightly with increase in clay content.

#### **4.7. Thermal decomposition**

The thermal decomposition behavior of NR latex clay nanocomposites is given in table 4.8. At 400°C, the percentage of weight retained is higher for the nanocomposites. This increase in thermal stability of the hybrid may result from the dispersion of the clay and from a strong interaction between the clay platelets and rubber molecules. The stability increases with increase in clay content. This is a hint

for the dispersion state of the layered silicates in the rubber. It has been reported that hybrids with a good dispersion of organoclay are thermally more stable [32, 33]. A characteristic feature of the nanocomposites is that the thermal property improvement occurs at very low filler content, often making the obtained material cheaper, lighter and easier to process than conventional composites.

**Table 4.8 TGA analysis of the NR-based composites**

Sample code	Onset point (°C)	300 °C	400 °C	500 °C
Mix 1	304.99	95.53	28.91	1.85
Mix 2	305.33	96.72	37.63	4.19
Mix 3	309.40	96.98	39.56	4.95
Mix 4	315.51	96.05	45.67	5.20

#### **4.8 Conclusion**

Natural rubber latex - clay nanocomposites were prepared with low-level of clay loading using conventional compounding technique. The increase in d spacing value as evident by X-ray analysis and the TEM pictures suggests the formation of an intercalated structure. Transport properties of the nanocomposites were studied in detail. The sorption, diffusion and permeation coefficients were measured using toluene at 303K. Due to the tortuous path available for the solvent molecule in the intercalated nanocomposites, a considerable decrease in diffusion, permeation and sorption coefficients are observed. It is observed that the decreasing value of the permeability of the nanocomposites is largely dominated by the diffusion phenomenon. The permeation resistance of the nanocomposite is confirmed by the gas permeability testing and it fits with the Nielson's model, which describes the tortousity effect of plate like particulates on gas permeability of polymer composite structures. Oxygen permeability of the natural rubber latex film is decreased by 66%

with 1 phr of nanoclay loading. Better reinforcement of clay layers in the rubber matrix is evident from the mechanical property improvement also. The thermodynamical parameters  $\Delta S$  and  $\Delta G$  directs the formation of a better elastic and exfoliated nanocomposite. As the barrier properties of latex films have a prominent role in dipped goods, it has high potential for commercialization.

## References

1. Eirich, F. R. Editor, Science and Technology of Rubber, Academic Press, New York, p 633, 1978.
2. Theng, B.K.G. Formation and Properties of Clay-Polymer Complexes, Elsevier Scientific, Amsterdam 1979.
3. Karger-Kocsis, J. and Wu, C.M., Polym. Eng. Sci., 44, 1083, 2004.
4. Ajbani, M. J., Geiser, F. and Parker, D.K., U.S. Patent, 014, 440,1A1, 2003.
5. Yang, X., Cohen, M.P., Senyck, M. L., Parker, D.K., Cronin, S.W., Lukich, L.T., Francik, W.P. and Gurer, C., U.S. Patent, 006,526,6A1, 2005.
6. Wang, Y., Zhang, H., Wu, Y., Yang, J. and Zhang, L., J. Appl. Polym. Sci., 96, 318, 2005.
7. Zhang, L., Wang, Y., Wang, Y., Sui, Y. and Yu, D., J. Appl. Polym. Sci., 78, 1873, 2000.
8. Wang, Y., Zhang, L., Tang, C. and Yu, D., J. Appl. Polym. Sci., 78, 1879, 2000.
9. Zhang, H., Wang, Y., Wu, Y., Zhang, L. and Yang, J., J. Appl. Polym. Sci., 97, 844, 2005.
10. Jia, Q.X., Wu, Y.P., Xu, Y.L., Mao, H.H. and Zhang, L.Q., Macromol. Mater. Eng., 291, 218, 2006.
11. Wu, Y.P., Zhang, L.Q., Wang, Y.Q., Liang, Y. and Yu, D.S., J. Appl. Polym. Sci., 82, 2842, 2001.
12. Wu, Y.P., Jia, Q.X., Yu, D.S. and Zhang, L.Q., J. Appl. Polym. Sci., 89, 3855 2003.
13. Nielsen, L.E., J. Macromol. Sci. Chem., 1, 929, 1967.
14. Varghese, S. and Karger-Kocsis, J., Polymer, 44, 4921, 2003.



15. Stephen, R., Alex, R., Cherian, T., Varghese, S., Joseph, K. and Thomas, S., J. Appl. Polym. Sci., 101, 2355, 2006.
16. Hanser. In Engineering with Rubber: How to Design Rubber Components Gent A N Ed.; Chap. 1 and 8, 1992.
17. L H Sperling. Introduction to Physical Polymer Science, 2<sup>nd</sup> Ed.; Wiley, US, 204, 2001.
18. Aithal, U. S., Aminabhavi, T .M. and Cassidy, P. E., J Memb. Sci., 50, 22, 1990.
19. Franson, N. M. and Peppas, N. A., J Appl Polym Sci., 28, 1299, 1983.
20. Chiou, J. S. and Paul, D. R., Polym Eng Sci., 26, 1228, 1986.
21. Crank, J. In: The mathematics of diffusion. 2<sup>nd</sup> Ed. Oxford: Clarendon Press, p 244, 1975.
22. Britton, L. N., Ashman, R .B., Aminabhavi, T. M. and Cassidy, P. E., J. Chem Edn., 65, 368, 1988.
23. Aprem, A. S., Joseph, K., Mathew, A. P. and Thomas, S., J Appl Polym Sci., 78, 941, 2000.
24. Khinnava, R. S. and Aminabhavi, T. M., J Appl Polym Sci., 42, 2321, 1991.
25. Flory, P.J. and Rehner, Jr., J Chem Phys., 11, 521, 1943.
26. Cassidy, P.E., Aminabhavi, T.M. and Thompson, C.M., Rubber Chem. Tech., 56, 594, 1983.
27. Kojima, Y., Usuki, A., Kawasumi, M., Okada, A., Fukushima, Y., Kurauchi, T. and Kamigaito, O., J Mater Res., 8, 1174, 1993.
28. Nielsen, L., J. Macromol. Sci Chem., A1, 929, 1967.
29. Bharadwaj, R., Macromolecules, 34, 9189, 2001.

30. Cussler, E., Hughes, S., Ward III, W., Aris, R., J. Memb. Sci, 38,161, 1998.
31. Nielsen, L. E. and Landel, R. F., Mechanical Properties of Polymers and Composites, 2<sup>nd</sup> ed. Marcel Dekker, Inc., 545 p 1994.
32. Usuki, A., Tukigase, A. and Kato, M., Polymer, 43, 2185, 2002.
33. Ganter, M., Gronski, W., Semke, H., Zilg, T., Thomann, C. and Mulhaupt R., Kautschuk Gummi Kunststoffe, 54, 166, 2001.

## ***Chapter 5***

---

### ***Modification of Nanoclay with Cationic Surfactants and Preparation of Natural Rubber Latex Clay Nanocomposites with Antimicrobial Properties***

The interest in rubber clay nanocomposites is mainly due to the reinforcement anisotropy and barrier properties that can be achieved by exfoliated silicate layers having nanoscale thickness. As long as the layered silicate layers fully delaminate (exfoliate), dispersing less than 10% of them in the rubber matrix, they may replace a three to four times greater amount of traditional fillers without the mechanical properties being sacrificed [1-4]. These improvements are the result of a complex interplay between the properties of the individual constituent phases: the polymer, the filler, and the interfacial region. One of the drawbacks of clays is the incompatibility between hydrophilic clay and hydrophobic polymer, which often causes agglomeration of clay mineral in the polymer matrix. Therefore, surface modification of clay minerals is the most important step to achieve polymer nanocomposites [5]. Upon organic treatment, clays become hydrophobic and hence become compatible with the specific polymers such as thermoplastics, thermosets or elastomers. Such modified clays are commonly referred to as organoclays. The surface modification process is similar to the treatment of fiberglass with silane coupling agents to ensure a perfect compatibility or chemical bonding with polymers. Because of the weak interactions between the nanolayers, the cations can be easily exchanged with alkylammonium cations, or phosphonium salts thus making the layered silicate compatible with the rubber matrix. These bulky cations also increase the interlayer distance to an extent that is easily measurable. If energetically favourable interactions exist between the modified silicate and the polymer, then the polymer chains can be inserted between the silicate layers, further increasing the interlayer spacing and

leading to an ordered multilayer with a repeat distance of a few nanometers. If the polymer and the silicate are not compatible, agglomerates of layered silicate surrounded by polymer are formed.

During the process of mixing organoclay into rubber matrix, natural rubber (NR) molecules with the lower molecular weight intercalate into the galleries with greater ease. We would expect that the interaction between silicates and polymer chains occurs via entropy loss. This is because, as the size of the polymer molecules is almost close to the distance between the silicate platelets, the penetration of the polymer into the interlayer distance is associated with some “ordering” and thus entropy loss is expected. i.e., polymer chains, which are initially in an unconstrained environment, are entering the constrained environment of the narrow silicate interlayer [6]. But the entropy change per interlayer volume is comprised of two factors: an entropy decrease per interlayer volume associated with confinement of the polymer upon intercalation and an entropy increase per interlayer volume associated with conformational freedom of the aliphatic chains upon layer separation. In earlier works [7], it has been reported that the organic chains gain configurational freedom as the interlayer distance increases and this may compensate for the entropic penalty of the polymer confinement. Polar interaction between polymer and organoclay can promote the formation of nanocomposites [8]. The intergallery environment of organoclay is still polar, although the polarity of clay is reduced by organophilic intercalant. The polarity of polymer is closely related to chemical structure of polymer chain. As far as the molecular chemical structure is concerned, the backbone of NR contains a larger number of unsaturated double bonds. Moreover the interaction between the organic modifiers and the molecules of the polymer matrix will favour the intercalation process of polymer molecules into the interlayer of silicates. It was also reported that morphology and properties of nanocomposites are often greatly influenced by the properties of the modifying group. The length of the alkyl ammonium cations (modifying groups) [9] and the presence of double bonds [10] are crucial factors for the preparation of exfoliated polymer clay nanocomposites.

Arroyo et al. [11] showed that the blending of 10 phr octadecyl amine modified montmorillonite with natural rubber is enough to obtain the same mechanical behaviour as the compound with 40 phr carbon black. Vu et al. [12] found that organic modification of clay facilitated the intercalation of the synthetic cis-1, 4 polyisoprene and epoxidized natural rubber (ENR) into the clay gallery thus increasing the tensile and modulus properties of the compound cured by sulfur. Sadhu and Bhowmick studied the preparation and properties of different nanoclays based on sodium montmorillonite, bentonite, potassium montmorillonite and organic amines of varying chain lengths in the styrene butadiene (SBR) matrix [13]. Mechanical properties such as tensile strength, elongation at break, modulus and energy required to break improved on incorporation of nanoclay in SBR. The tensile strength increased with increasing chain length of the amine. Joly et al. observed that organically modified galleries of montmorillonite (MMT) were easily penetrated by natural rubber chains and led to intercalated structures along with partial exfoliation [14]. Modulus increase comparable to that achieved by high loadings of conventional micrometer sized fillers was observed at only 10 wt% modified MMT loading demonstrating the advantages of high-surface-area filler. Magaraphan et al. showed that MMT clays modified with long primary amines showed much more improved mechanical properties than the quaternary amines (having the same carbon numbers) in NR matrix [15]. The length of the hydrocarbon in the alkylamines had no effect on the cure time whereas the nanocomposites prepared with long quaternary amine showed comparatively faster cure rate.

In this chapter, three different quaternary ammonium surfactants are used for the organophilic modification of the clays. The different surfactants used contain different functional groups viz., an aliphatic, an aromatic and a heterocyclic group. An effort is made to find which surfactant-clay system provided the best performance of the nanocomposite in NR matrix, both in latex stage and dry rubber.

## 5.1 Modification of nanoclay

### 5.1.1 Organophilic modification

Montmorillonite clays used in this study were provided by Southern clay Products Inc., USA. Montmorillonite clay (cloisite Na<sup>+</sup>), has an ion exchange capacity of 92.6meq/100g clay and an interlayer distance of 11.7Å°. Three quarternary ammonium groups; cetyltrimethyl ammonium bromide (CTAB), cetylpyridinium chloride (CPC) and benzalkonium chloride (BAC) were used for the organophilic modification. Their chemical formulae are shown in figures 5.1 (a), 5.1 (b) and 5.1 (c), respectively. Benzalkonium chloride is a mixture of alkylbenzyl dimethylammonium chlorides of various alkyl chain lengths.

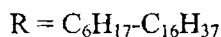
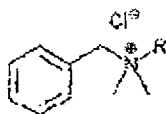


Figure 5.1 (a) Benzalkonium chloride (alkyl dimethyl benzyl ammonium chloride)

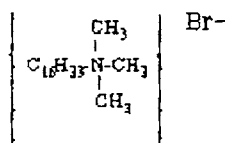


Figure 5.1 (b) Cetyltrimethylammonium bromide (Hexadecyltrimethylammonium bromide)

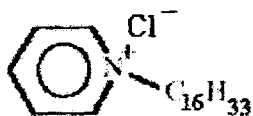


Figure 5.1 (c) Cetylpyridinium chloride (Hexadecylpyridinium chloride)

### 5.1.2 Preparation of organically modified nanoclay

Organophilic clays were prepared by ion exchange of  $\text{Na}^+$  with the quaternary ammonium salts: Cetyl trimethyl ammonium bromide (CTAB), Cetyl pyridinium chloride (CPC) and Benzalkonium chloride (BAC). 10 g of MMT was suspended in 1 litre of distilled water and stirred for 30 minutes. An aqueous solution of 12 millimoles of the surfactant was added to the clay suspension with continuous stirring for 3 hours. The solution was left idle overnight. The product was then filtered, washed several times with hot distilled water until no chloride was detected with 0.1M  $\text{AgNO}_3$  solution and vacuum dried. The cation exchanged MMT was ground using a mortar and pestle.

### 5.1.3 Characterisation of the modified clays

#### 5.1.3.1 X-ray diffraction

X-ray diffraction (XRD) is a common technique used in examining cationic group intercalation and expansion of MMT. As MMT interlayer spacing can expand or contract, the  $d_{001}$  reflection of XRD will shift proportionally.

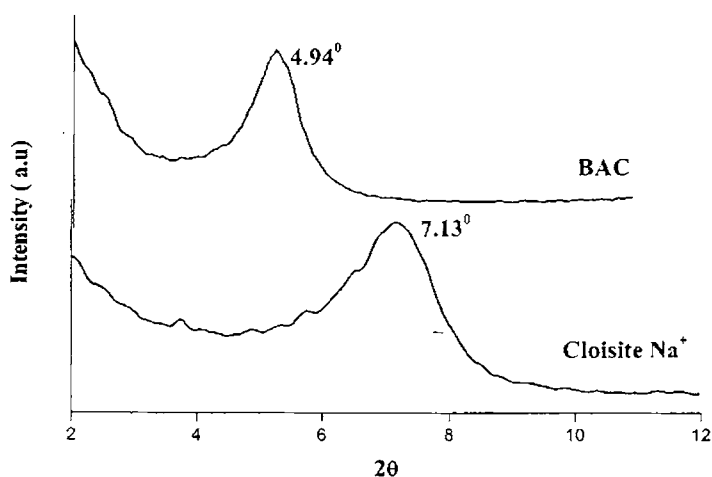


*Figure 5.2 XRD spectrum of unmodified clay and BAC modified clay*

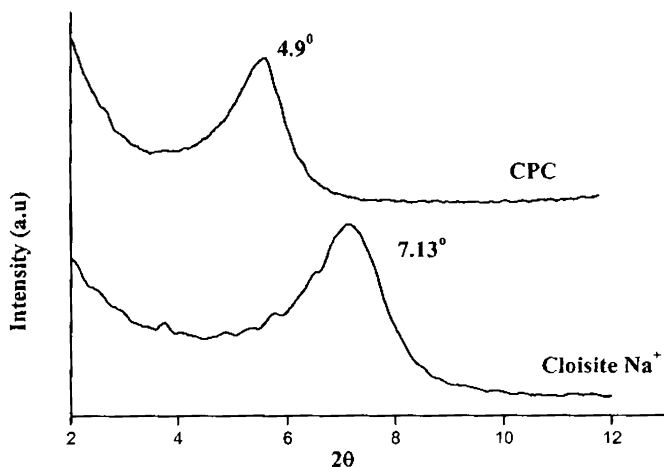


Figure 5.3 XRD spectrum of unmodified clay and CPC modified clay

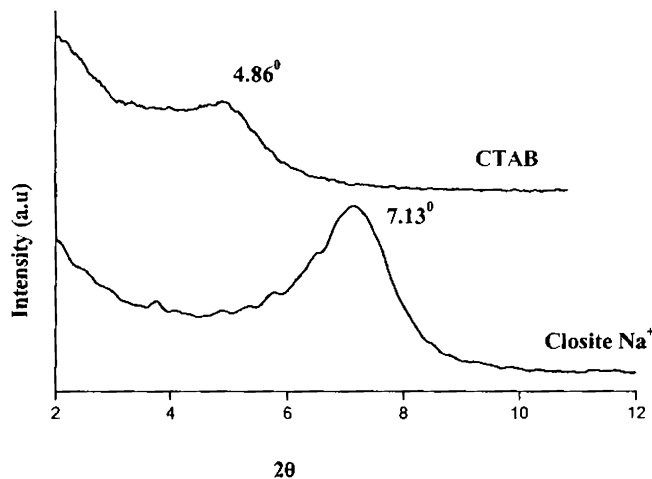


Figure 5.4 XRD spectrum of unmodified clay and CTAB modified nanoclay

The  $d_{001}$  spacing was calculated from the XRD peak position using Bragg's law,  $d = n\lambda / (2\sin\theta)$  where  $d$  is the  $d_{001}$  spacing,  $\lambda$  is the wave length of X-ray equal to 1.54Å, and  $\theta$  is the angle of incidence of X-ray.



Figures 5.2, 5.3 and 5.4 show the XRD patterns of untreated MMT (cloisite Na<sup>+</sup>) and modified clays. The unmodified clay has a diffraction peak at  $2\theta = 7.13^\circ$  which is assigned to an interlayer spacing of 12.39 Å. In the case of modified clays, the organic cations penetrate into the interlayer space, replacing the sodium cations and peak position shifts to a lower angle. The interlayer distance of modified clays gets increased to 18.20 Å, 18.03 Å and 17.90 Å for CTAB, CPC and BAC respectively. An increase of about 6 Å in the interlayer distance is registered for the modified clays.

### 5.1.3.2 Thermogravimetric analysis (TGA)

For further evidence of intercalation, TGA measurements were performed on the unmodified clays, organoclays and the different organic modifiers which are used for modification. The resultant thermograms are presented in figure 5.5.

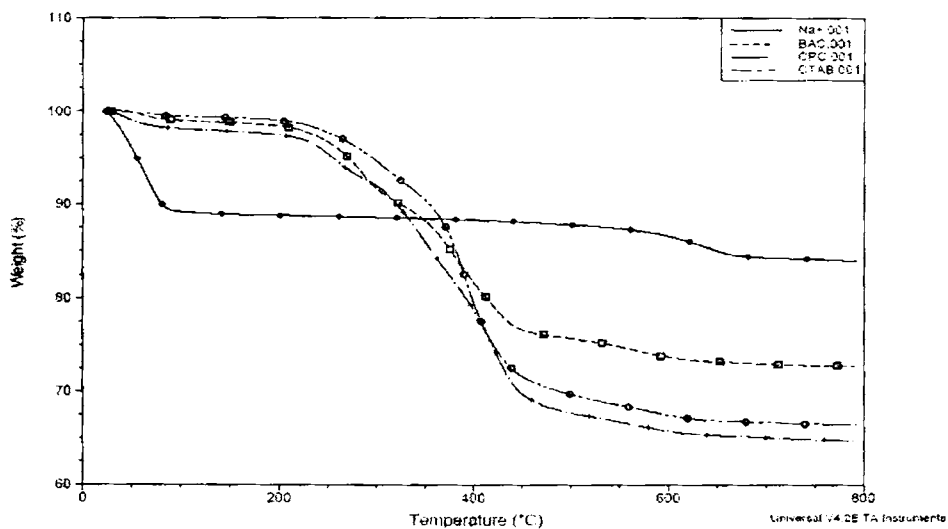


*Figure 5.5 TGA curves of unmodified and modified clays*

TGA curves of unmodified clay ( $\text{Na}^+$ ) display two degradations at 97 °C & 644 °C corresponding to the loss of hydrated water of the interlayer cations and structural hydroxyls respectively. Unmodified clay is stable in the temperature range of 200-500°C. TGA curves of modified clays display several degradations around 285 °C, 255 °C, 379 °C, 391 °C, 423 °C, 572 °C and 583 °C. The degradations at 285 °C and 255 °C corresponds to the evaporation of physically adsorbed organic groups since the TGA curves of the organic modifiers show this degradation peaks. The degradations at 379 °C, 391 °C and 423 °C are attributed to the decomposition of the intercalated cations within the clay interlayer. The weight loss at 450 °C to 590 °C is related to the oxidation of the residual organic group present in the organoclays.

### 5.1.3.3 Fourier Transform Infrared (FTIR) spectroscopy

Figures 5.6, 5.7 and 5.8 show the FTIR spectrum of unmodified and organically modified clays. The infrared spectrum of the unmodified clay presents two peaks, which corresponds to the Si-O stretching ( $1012\text{cm}^{-1}$ ) and -OH groups ( $3624\text{cm}^{-1}$ ). All the three modified clays present extra peaks in the FTIR spectrum.

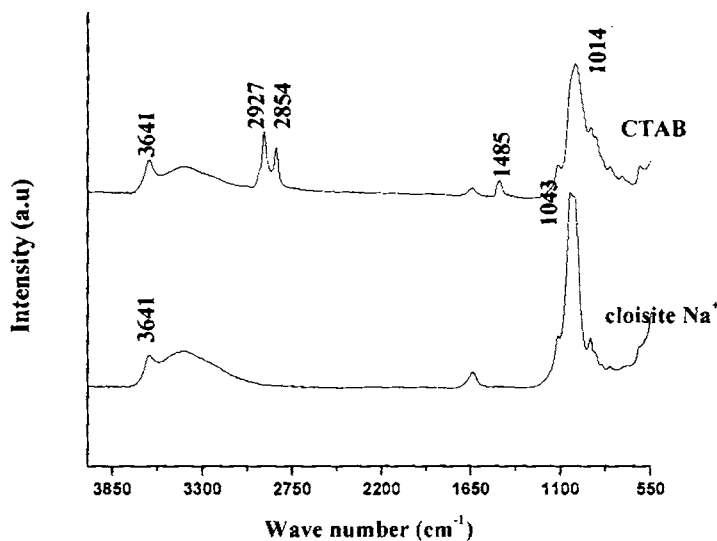
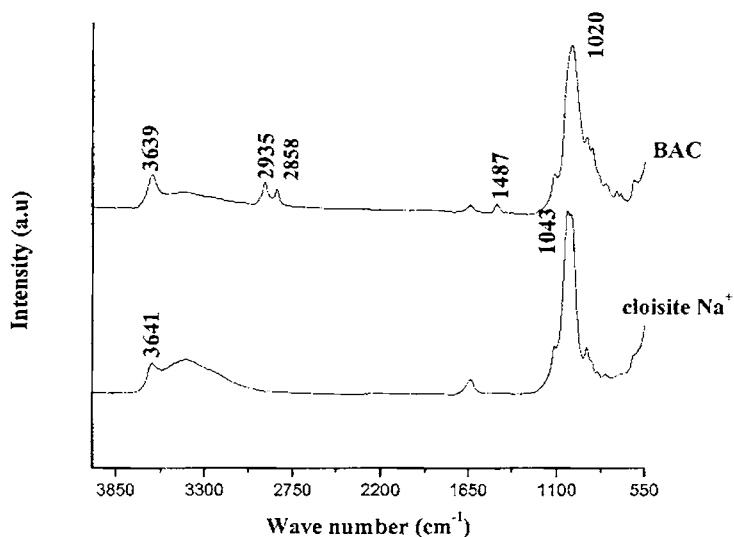
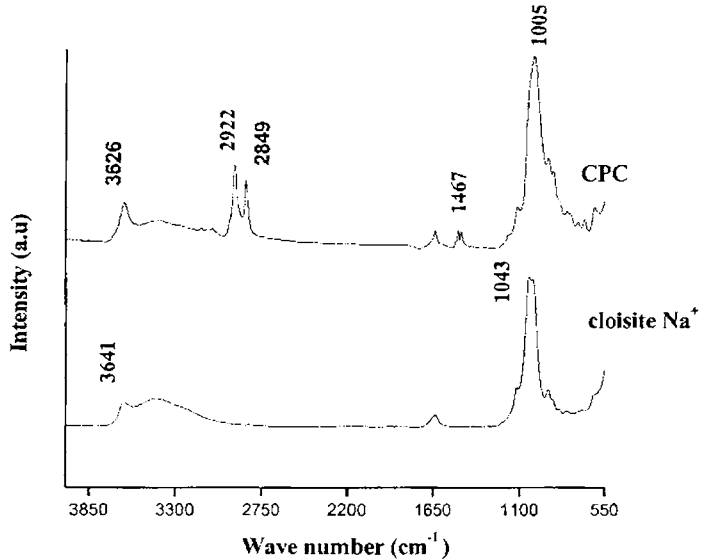


Figure 5.6 FTIR spectrum of cloisite  $\text{Na}^+$  & CTAB modified clay

Bands at 2922 and 2850  $\text{cm}^{-1}$  are attributed to the C-H asymmetric and symmetric stretching vibrations of the modifying groups, respectively. The band at 1470  $\text{cm}^{-1}$  for the modified clays is assigned to the ammonium salt.



**Figure 5.7** FTIR spectrum of cloisite  $\text{Na}^+$  & BAC modified clay



**Figure 5.8** FTIR spectrum of cloisite  $\text{Na}^+$  & CPC modified clay

## 5.2 Modification of natural rubber latex

### 5.2.1 Modification of natural rubber latex by methyl methacrylate (MMA) grafting

Methyl methacrylate (MMA) was made inhibitor free by washing with 10% aqueous sodium hydroxide and then with water. This was emulsified in water containing cumene hydroperoxide (0.35 % on DRC) with ammonium oleate emulsifier. The required quantity of NR latex was charged into the reaction vessel and diluted with an equal volume of water. The MMA emulsion was then added to the latex with vigorous stirring and stirring continued for further 30 minutes at 50 - 60 rpm speed. A 10 % aqueous solution of tetraethylene pentamine was added to the latex as an activator (0.3% on DRC) and stirring continued for a few more minutes. When the contents are thoroughly mixed, stirring was stopped and the reaction was allowed to continue overnight.

### 5.2.2 Characterisation of MMA grafted latex using FTIR Spectroscopy

An FTIR spectrum of natural rubber and MMA grafted natural rubber obtained from the insoluble portions after extraction with acetone is shown in figure 5.9.

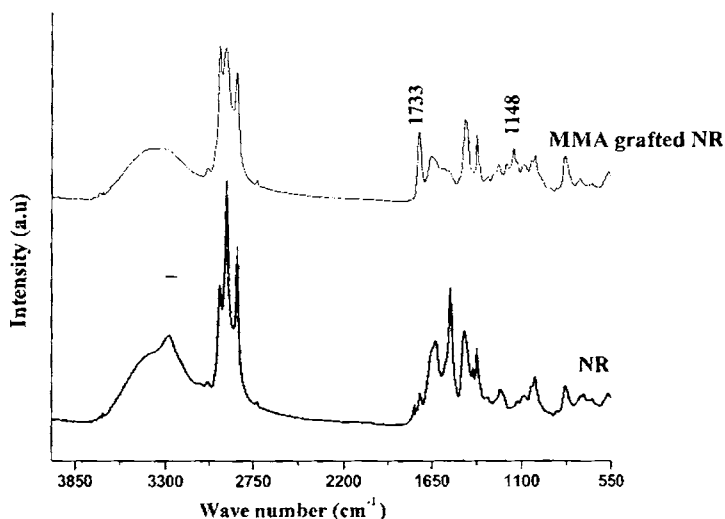


Figure 5.9 FTIR spectrum of NR and MMA grafted NR

The spectrum obtained compares favorably to those in literature. The presence of grafted MMA in the natural rubber molecules was confirmed using FTIR. Intense absorption peaks at  $1733\text{ cm}^{-1}$  ( $\text{-C=O}$  stretch) and  $1148\text{ cm}^{-1}$  ( $\text{-C-O}$  stretch) were observed.

### 5.2.3 Preparation of methyl methacrylate grafted NR latex - clay nanocomposite

Methacrylated latex nanocomposite with 1, 2 and 3 phr of unmodified clay (cloisite  $\text{Na}^+$ ) were prepared as per the formulation given in table 5.1 using the same procedure described in section 4.1. Mechanical properties and swelling characteristics of the vulcanisates were determined.

*Table 5.1 Recipe for mixing*

Ingredients	Mix 1	Mix 2	Mix 3	Mix 4
	parts per hundred rubber (phr)			
MMA grafted NR latex (60% DRC)	100	100	100	100
Sulphur (50%)	1.5	1.5	1.5	1.5
Zinc Oxide (50%)	0.9	0.9	0.9	0.9
Potassium Oleate (10%)	0.8	0.8	0.8	0.8
ZDC (50%)	0.7	0.7	0.7	0.7
Wingstay L (50%)	0.5	0.5	0.5	0.5
Clay dispersion (2%)	0	1	2	3

### 5.2.4 Mechanical properties NR latex clay nanocomposites

Mechanical properties of the vulcanised nanocomposites prepared with MMA grafted NR latex are given in table 5.2. The enhanced mechanical properties of the nanocomposites compared to the gum vulcanisate are due to the high polymer-filler interactions. The polar nature of the methacrylate ester containing a –CO-O functional unit improves its dispersion with the polar surfaces of the silicates making them more amenable to penetration into the clay galleries. As a result, about a two fold increase in mechanical properties are observed with 3 phr nanoclay. The enhanced modulus and tensile strength observed reflect a direct result of the better polymer-clay adhesion. Physical Van der Waals attraction between rubber segments and clay surfaces may play a vital part in the overall adhesion process.

*Table 5.2 Mechanical properties of the vulcanisates*

Sample	Tensile strength (MPa)	Elongation at break (%)	Modulus at 100% elongation (MPa)	Modulus at 200% elongation (MPa)	Modulus at 300% elongation (MPa)
gum	24.82	1160	0.88	1.17	1.47
1phr	37.08	1190	1.18	1.43	1.70
2 phr	42.25	1210	1.2	1.52	1.75
3 phr	44.59	1248	1.28	1.64	1.83

### 5.2.5 Swelling studies

Swelling studies of the methyl methacrylate grafted NR latex- clay nanocomposites in toluene are done and the sorption curves are shown in figure 5.10. It is observed that

gum vulcanisate has the maximum absorption of solvent at the equilibrium swelling. Swelling resistance increases with increase in clay content. Composites with 1 phr and 2 phr nanoclay show almost similar sorption curve.

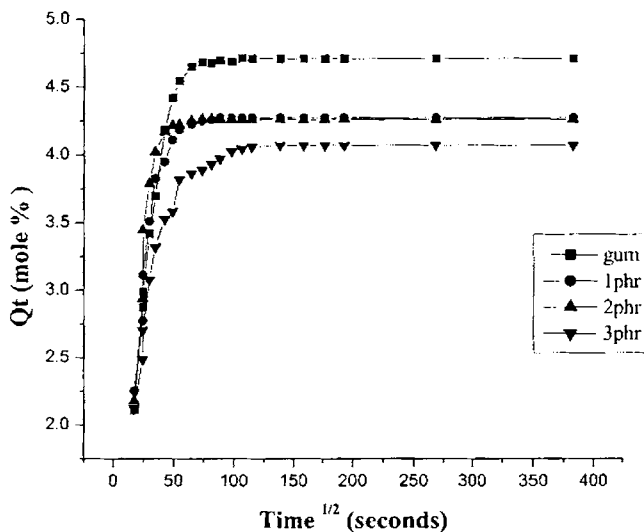


*Figure 5.10 Sorption curves of the vulcanisates in toluene at 303K*

### 5.3 NR latex (NRL) - organomodified clay nanocomposites as a microbial barrier

Composites prepared from natural rubber latex with layered silicates as the reinforcing filler was studied in chapter 4. Application of a small amount of intercalated clay to the rubber matrix provides considerable improvement in barrier performance.

As discussed, the compatibility of clay platelets with the rubber organic phase, in terms of wetting and dispersion, may be substantially improved by, for instance, the covalent addition of some organic modifiers to the reactive surface of the clay. Usually, quaternary ammonium salts and phosphonium salts are used for the organophilic modification. It is reported that quaternary ammonium salts and phosphonium salts are able to kill microorganisms such as bacteria, algae and fungi [16] when one substituent is an alkyl chain with at least eight carbon atoms [17]. The

present part of the work, investigates whether the quaternary ammonium groups used for the organophilic modification of clays can impart antibacterial property to the natural rubber nanocomposite.

The ability of microorganisms to adhere to polymeric surfaces inside the body and subsequently proliferate on that surface is the most crucial factor for the long term utility of *in vivo* biomedical devices [18]. A serious clinical complication associated with the use of disposable medical devices such as endotracheal tubes, urinary catheters etc. are the incidence of infection [19]. Up to 45% of hospital infections are connected with implants or medical devices and mortality rates of 50-60% have been reported [20, 21]. Thus any design of the device and/or modification of its polymeric surface that would minimize bacterial adhesion are exceedingly desirable and clinically important. Although several types of polymer-layered silicate nanocomposite products with different shapes and applications including food packaging films and containers, engine parts, dental materials, etc. are now available in markets [22], polymer-layered silicate nanocomposites with antimicrobial activity, which will be very much favourable to the nanocomposites applications are rarely seen. It is reported that acrylic fibers that contain antimicrobial agents such as quaternary ammonium salts has numerous applications including incontinence and sanitary products, mattress covers, wound dressing, hospital drapes and gowns. Since polymer nanocomposites possess active positive cations, it can efficiently sterilize bacteria. Chitosan layered silicate with antibacterial effect against Gram positive bacteria is reported [23].

Although the compatibility of clay platelets with the rubber organic phase, in terms of wetting and dispersion, may be substantially improved by using organically modified clays, this procedure does not work for natural rubber latex systems since the organically modified clay surface is typically more hydrophobic to make it more compatible with the typically non-polar polymer. This problem can be avoided by using MMA - grafted natural rubber latex. They are made by polymerizing methyl



methacrylate monomer in the presence of natural rubber latex whereby methylmethacrylate (MMA) chains are grafted to the rubber molecules. The polar character of the methacrylate ester containing a  $-\text{CO}-\text{O}$  functional unit was expected to have improved its dispersion with positively charged cationically modified clays. Therefore the antimicrobial clay-ammonium complex reinforced natural rubber latex may exhibit not only high mechanical strength but also antimicrobial activity.

The aim of the present part of the work is to prepare natural rubber latex organoclay nanocomposites with the modified clays having three different modifiers viz., BAC, CPC, CTAB and evaluation of the physical properties, swelling resistance and antibacterial properties of these composites.

### **5.3.1 Preparation of poly methyl methacrylate grafted NR latex-organoclay nanocomposite**

Methyl methacrylate grafted NR latex was stabilized using a nonionic stabilizer and latex nanocomposites were prepared as per the procedure described in section 4.1. Nanocomposites with three different clays in varying concentration of 0.25, 0.5 and 1 phr were prepared. Organoclay dispersions (5%) were made by using an ultrasonic stirrer. Because of the larger surface area of the nanoclay up to 15 parts of dispersing agent (Dispersol F) was added for hundred parts of clay while preparing the dispersion.

### **5.3.2 Characterisation of NR latex organoclay nanocomposite**

#### **5.3.2.1 X- ray diffraction studies**

The structure of the dispersed silicate layer in the composites was studied with X- ray diffraction studies and transmission electron microscopy. XRD patterns were obtained using Bruker, D8 advance diffractometer at the wavelength  $\text{CuK}_\alpha = 1.54\text{\AA}$ , a tube voltage of 40Kv and tube current of 25mA.

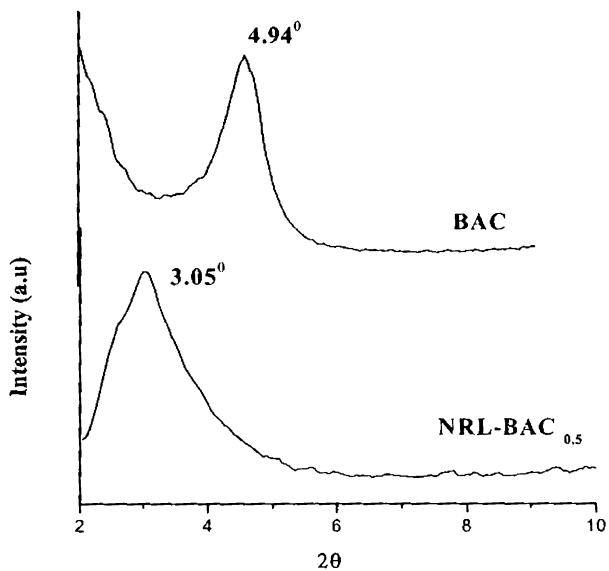


Figure 5.11 XRD spectrum of BAC modified clay and NRL – BAC (0.5 phr) nanocomposite

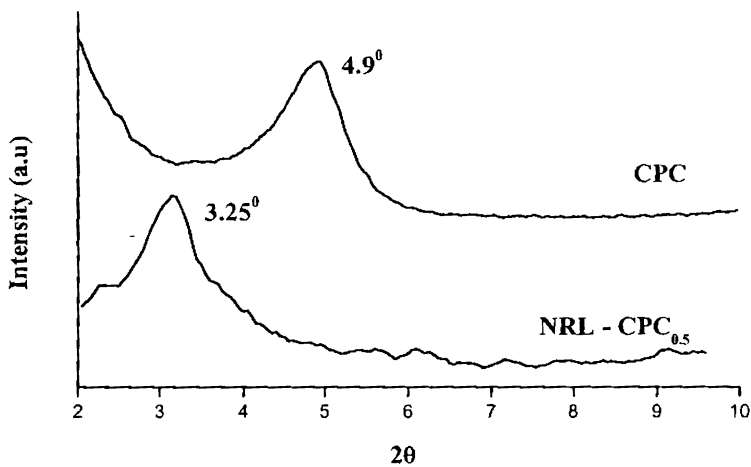
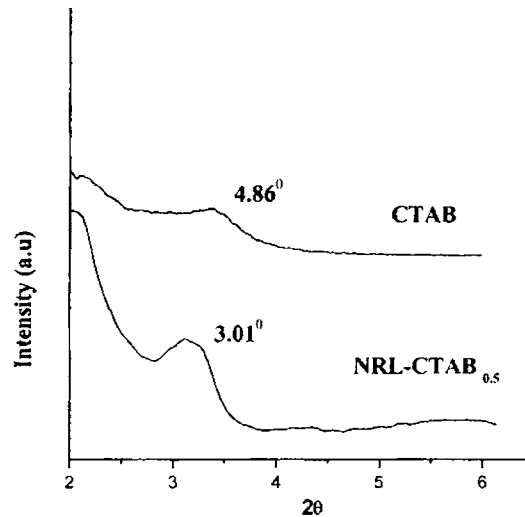


Figure 5.12 XRD spectrum of CPC modified clay and NRL – CPC (0.5 phr) nanocomposite



**Figure 5.13 XRD spectrum of CTAB modified clay and NRL – CTAB (0.5 phr) nanocomposite**

XRD spectra of the modified clays are compared with their natural rubber latex (NRL) nanocomposites in figures 5.11, 5.12 and 5.13. In all the XRD patterns, it can be observed that the X ray diffraction peak shifts to lower  $2\theta$  value which corresponds to an increase in interlayer distance. An interlayer distance of  $28.94 \text{ \AA}$ ,  $27.15 \text{ \AA}$  and  $29.38 \text{ \AA}$  were obtained for 0.5 phr of BAC, CPC and CTAB modified clay filled composites, respectively. In all the X-ray diffraction diagrams d spacing has increased to about  $10 \text{ \AA}$ . This increase in d spacing suggests the intercalation of the polymer chains between the clay layers.

### 5.3.2.2 Transmission electron microscopy

The transmission electron microscopy was performed using a JEOL JEM- 2010 (Japan) transmission electron microscope, operating at an accelerating voltage of 200 KV. Figure 5.14 shows a TEM micrograph of the natural rubber latex nanocomposite with 0.5 phr of BAC modified clay. The dark lines in the photo correspond to the intersections of the silicate layer. The clay is dispersed to one or several layers in the rubber matrix which suggests the formation of an intercalated nanocomposite.

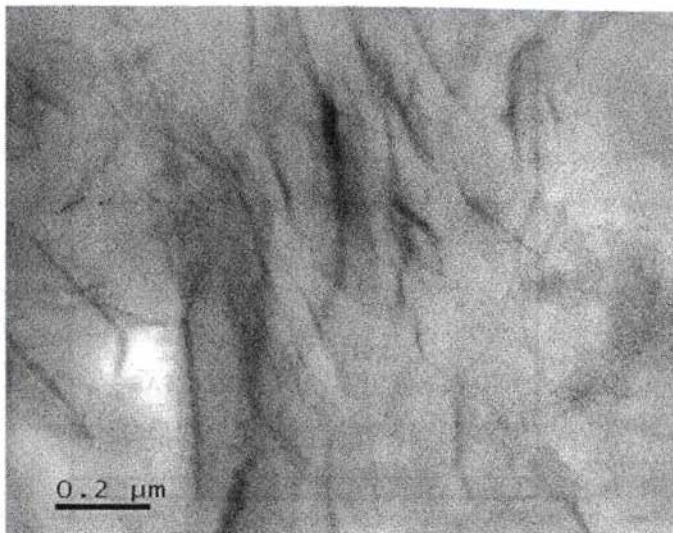


***Figure 5.14 TEM micrograph of NRL nanocomposite with 0.5phr BAC modified clay***

### **5.3.3 Mechanical properties**

The mechanical properties of NR latex-clay nanocomposites showed significant improvements in stress-strain properties as presented in figures 5.15 to 5.18. It is seen that NR latex - organoclay nanocomposites demonstrated greatest increase in tensile strength and modulus at 100%, 200%, and 300% elongation as a function of clay content when compared with other organoclay systems. An increased modulus presumably occurs as a direct result of attachment of rubber to the clay filler, which has the effect of reducing polymer mobility. The increase in mechanical properties is only upto 0.5 phr of clay content and is decreased slightly with 1 phr organoclay. This decrease in properties may be due to the lack of better dispersion of the modified clay in the latex at higher concentrations. On comparing the property improvement for the three different clays, it is seen that NR latex BAC modified clay nanocomposites is superior. This may be due to the better interaction between the rubber molecules and the surfactant used for the clay modification. The presence of the aromatic group may be responsible for the better improvement in properties since the three different clays

used do not differ much in their interlayer distance. NR latex-CPC clay nanocomposites also show moderate mechanical properties. This may be due to the presence of heterocyclic group in the modifying surfactant molecules.

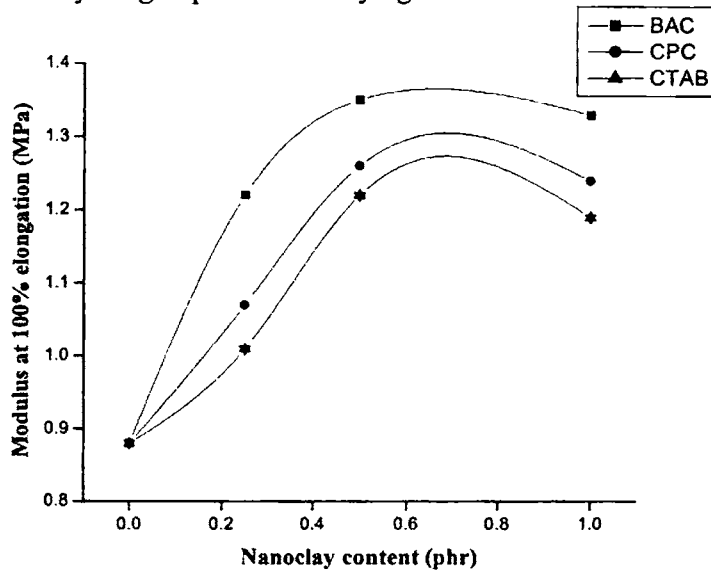


**Figure 5.15** Modulus at 100% elongation of the organoclay nanocomposites

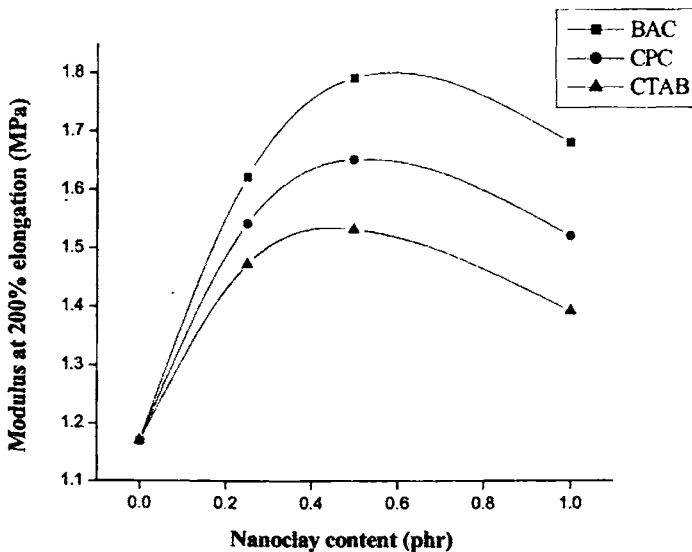


**Figure 5.16** Modulus at 200% elongation of the organoclay nanocomposites

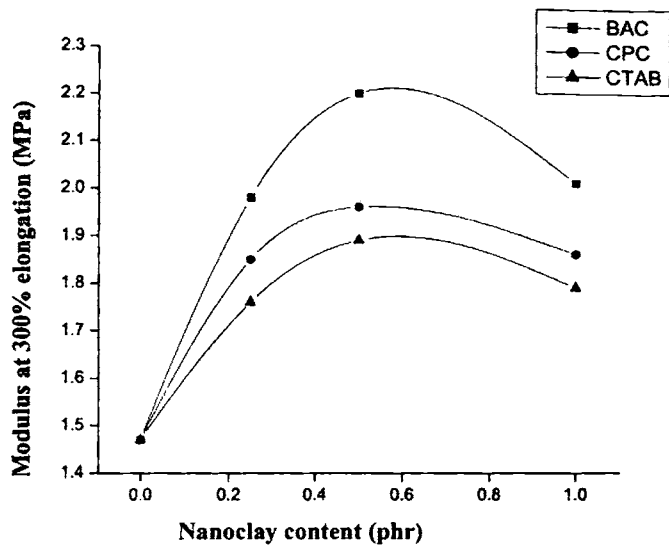


Figure 5.17 Modulus at 300% elongations of the organoclay nanocomposites

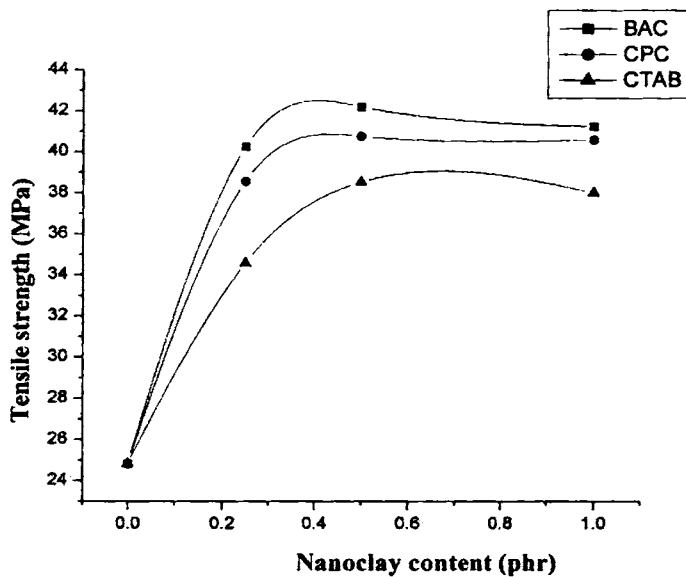
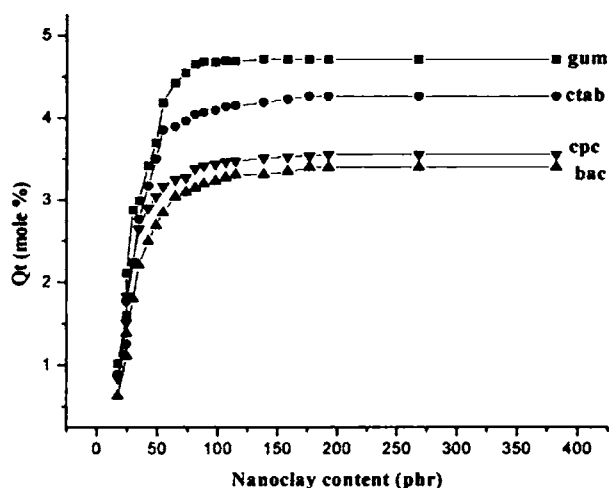


Figure 5.18 Tensile strength of the organoclay nanocomposites

### 5.3.4 Swelling studies

Sorption curves of the gum vulcanisate and nanocomposite with 0.5 phr modified clay are shown in figure 5.19. The solvent uptake of the sample decreases in the presence of layered silicates, which is associated with the tortuous path. The best performance of nanocomposites containing BAC modified clay is attributed to the presence of the aromatic group in the surfactant which provides higher compatibility with NR and greater dispersion of the organoclay, increasing the tortuous path for gas diffusion through the rubber.



**Figure 5.19** Sorption curves of the nanocomposites in toluene at 303K

The diffusion coefficient, Sorption coefficient and Permeation coefficient are presented in table 5.3. It is seen that swelling resistance is higher for the nanocomposites than the gum vulcanisate. According to the permeation data, natural rubber latex nanocomposite with BAC modified clay demonstrated the highest decrease in permeability. It gets reduced from 22.5 to 5.3  $\text{cm}^2\text{s}^{-1}$ . A considerable reduction in diffusion coefficient is also observed. The reactivity of BAC modified clay contributes to the clay nano-dispersion and the enhancement in the barrier properties. The CPC modified clay nanocomposite has a lower diffusion coefficient than the CTAB modified clay samples. The presence of reactive heterocyclic group in

the CPC modified clay nanocomposite may be responsible for the better dispersion. The solubility also decreases for the nanocomposites and the most decrease is for BAC modified clay nanocomposite because of the nano-dispersion.

**Table 5.3 Variation of diffusion coefficient (D), sorption coefficient (S) and permeation coefficient (P) with modified clays**

Sample code	Diffusion Coefficient $\times 10^7$ ( $\text{cm}^2 \text{s}^{-1}$ )	Sorption Coefficient	Permeation Coefficient $\times 10^7$ ( $\text{cm}^2 \text{s}^{-1}$ )
GUM	5.2	4.33	22.5
CTAB	2.31	4.15	9.59
CPC	1.70	3.27	5.58
BAC	1.69	3.13	5.30

### 5.3.5 Antibacterial properties

Antibacterial activity of the three different organoclays-NR latex nanocomposites was determined against Gram positive bacteria, *Bacillus cereus* and Gram negative bacteria, *E.coli*. It was assayed by so-called halo method as follows [24]. A melted beef agar medium was poured into a Petri dish and solidified. Then, the medium containing bacteria ( $1 \times 10^6$  cells of *E.coli*, *Bacillus cereus* per ml) was layered over it. The samples were poured into a well cut on the surface. Samples were added in four different amounts viz., 5, 10, 15, 20 microlitres into each well and then incubated for 1 day at 37 °C. Antibacterial activity was evaluated by the transparent halo circle around the specimen after incubation. That is to say, when an agent has antibacterial activity, a halo circle is formed along the periphery of the specimen. When materials have an excellent antibacterial activity, the halo ring formed will be very wide. All glassware used in this study was sterilized in the autoclave at 120 °C for 30 min before each experiment to exclude any possible microbial disturbance. Similarly, the antibacterial



properties of the vulcanised samples were also determined. Circular specimens punched from the vulcanised sheets were used for the purpose.

All the three organoclay nanocomposites possess antibacterial property against both Gram positive and Gram negative bacteria in all the four different concentrations. Although the mode of action of cations against bacteria is not known, it was suggested that an adsorption of cations onto the negatively charged cell surface by electrostatic interaction takes place [25-27]. Then the long lipophilic chains diffuse through the cell wall, which leads to a weakening of the cytoplasmic constituents and the death of the cell. Cell walls of the bacteria are usually negatively charged due to functional groups such as carboxylates present in lipoproteins at the surface. The presence of the intercalated cations in the organoclay nanocomposite increases the electrostatic force between the organoclays and bacteria, and immobilizes the bacteria on the surface of the organoclays. Since organophilic modification improves the hydrophobicity of the clays, the affinity towards the negatively charged cell wall of the bacteria increases. Greatest antibacterial property is shown against Gram positive bacteria. This may be related to the cell structure of the bacteria: Gram-positive bacteria have thick cell wall and no outer membrane, whereas Gram-negative bacteria have thin cell wall and its layers have outer membranes [28]. Hence, organoclays may have different action mechanisms against Gram-negative bacteria and Gram-positive bacteria [29-31]. Halo ring with highest diameter was obtained for BAC modified clay nanocomposites as seen in table 5.4. Since organophilic modification of the clays with bulky group improves the hydrophobicity more, more will be the affinity towards the negatively charged cell wall of the bacteria and thus the antibacterial property. The increase in bactericidal activity with the increase in chain length for the quaternary ammonium groups is reported [32, 33].

Halo ring having a diameter greater than 13 mm were obtained for all the three type of nanocomposites in all the four different concentrations against *Bacillus cereus* and halo ring having diameter greater than 9 mm were obtained against *E.coli*.

Photographs of the experimental result of BAC modified clay nanocomposites against *E.coli* and *Bacillus cereus* bacteria are given in figure 5.20 and figure 5.21 respectively. Antibacterial activity of the nanocomposite against *Bacillus cereus* is compared with the gum compound in figure 5.22. Figure 5.23 shows the antibacterial assessment of the vulcanised sample.

**Table 5.4 Halo ring diameter obtained from antibacterial assessment**

Samples	<i>Bacillus cereus</i> (mm)	<i>E.coli</i> (mm)
CTAB	15	10
CPC	17	11
BAC	20	13

20 micro litre of the 0.5 phr clay added samples were poured into the well for testing

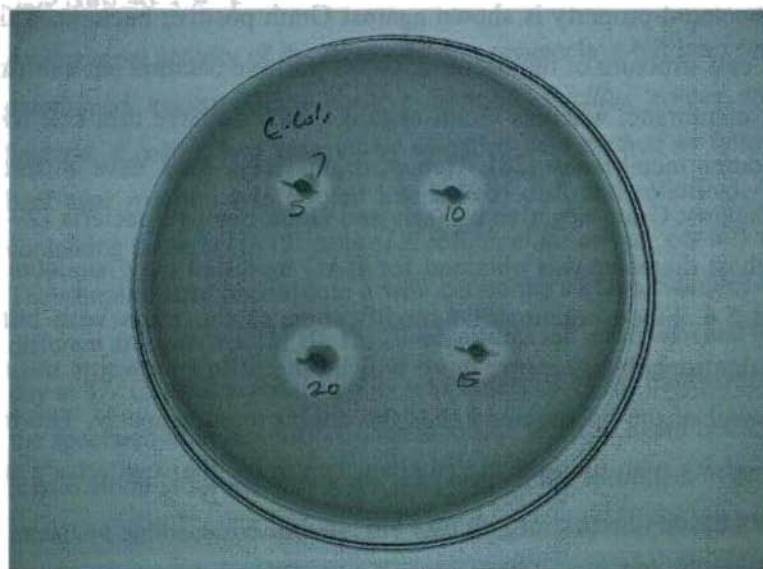


**Figure 5.20 Well plate during the antibacterial assessment of latex nanocomposite with 0.5 phr BAC modified clay against *E.coli***

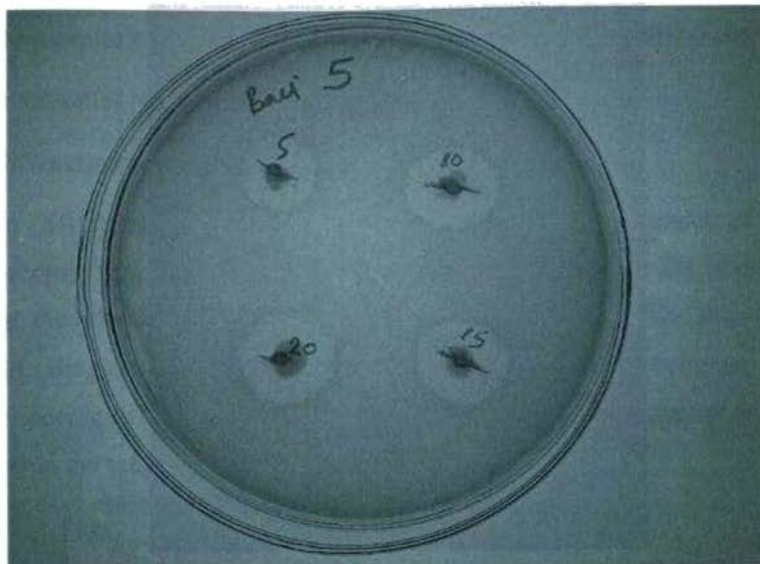


*Figure 5.21 Well plate during the antibacterial assessment of latex nanocomposite with 0.5 phr BAC modified clay against Bacillus cereus*

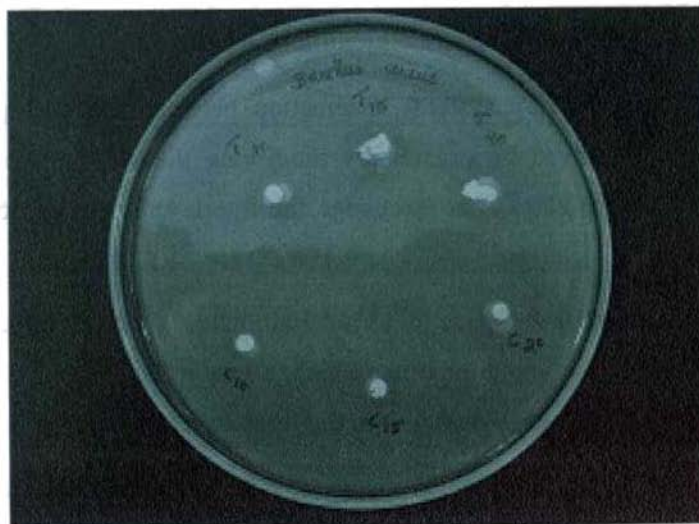


*Figure 5.22. Well plate during the antibacterial assessment of latex nanocomposite with 0.5 phr BAC modified clay against Bacillus cereus on comparison with control*

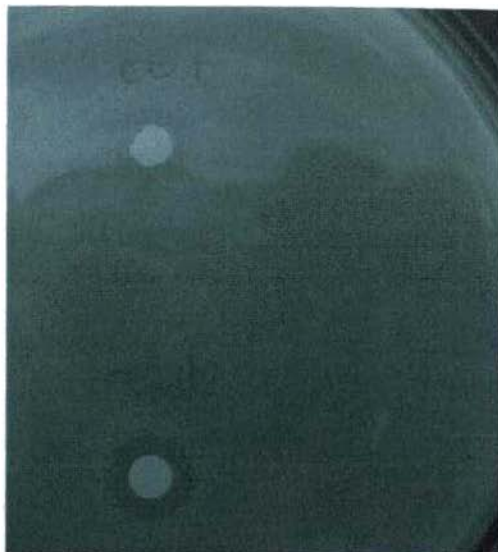


***Figure 5.23 Well plate during the antibacterial assessment of vulcanised latex nanocomposite sheet with 0.5 phr BAC modified clay against *Bacillus cereus* on comparison with control***

#### **5.4 Studies on natural rubber organoclay nanocomposites**

In a number of polymer-clay systems, interaction between the clay platelets and polymer chains is improved by organically modifying the clay surface. The most popular modification for clays is to exchange the interlayer inorganic cations (e.g.,  $\text{Na}^+$ ,  $\text{Ca}^+$ ) with organic ammonium cations. Organophilic modification also results in the swelling of the interlayer space up to a certain extent (normally over 20 Å) and hence reduce the layer-layer attraction, which allow a favourable diffusion and accommodation of polymer or precursor into the interlayer space.

This part of the work describes the synthesis of NR-clay nanocomposites via shear mixing of dry form of NR with four different types of nanoclays. The effects of using different surfactant with varying chain lengths and different functional groups to modify montmorillonite for NR nanocomposites are investigated. Mechanical and

barrier properties of these nanocomposites showed significant improvements compared to NR vulcanisate and NR nanocomposite prepared with unmodified clay.

#### 5.4.1 Characterisation of NR -Clay nanocomposites

##### 5.4.1.1 X- ray diffraction technique

X-ray diffraction (XRD) was used to study the nature and extent of dispersion of the clay in the nanocomposite. XRD patterns were obtained using Bruker, D8 advance diffractometer at the wavelength  $\text{CuK}\alpha = 1.54\text{\AA}$ , a tube voltage of 40Kv and tube current of 25mA. Bragg's law defined as  $n\lambda = 2d\sin\theta$ , was used to compute the crystallographic spacing (d) for the clay. The samples were scanned in step mode by  $1.0^\circ/\text{min}$  scan rate in the range of  $2$  to  $10^\circ$ .

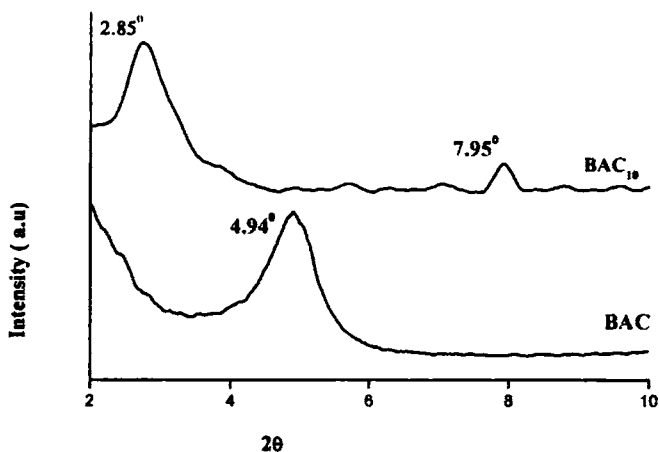


**Figure 5.24 XRD patterns of BAC modified clay and nanocomposite with 10 phr of BAC modified clay in NR**

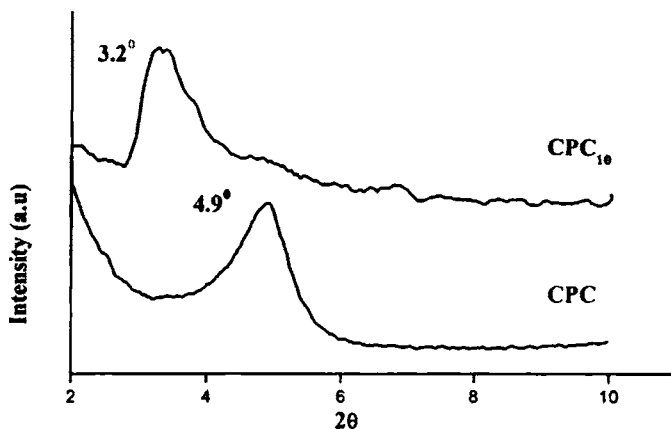


**Figure 5.25 XRD patterns of CPC modified clay and nanocomposite with 10 phr of CPC modified clay in NR**

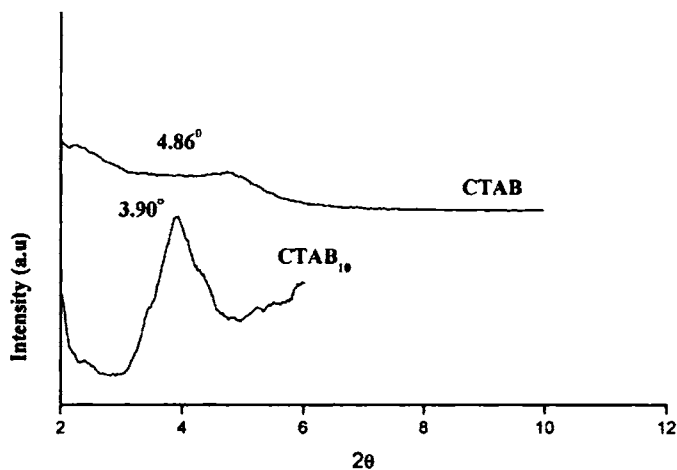


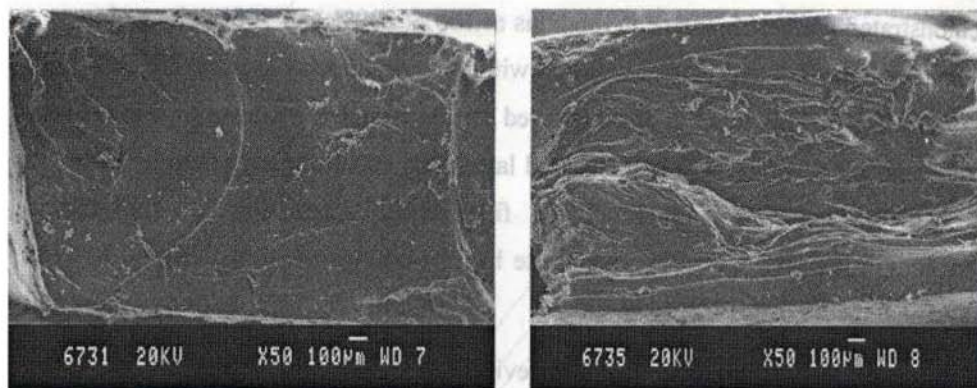
**Figure 5.26 XRD patterns of CTAB modified clay and nanocomposite with 10 phr of CTAB modified clay in NR**

The XRD spectra of organoclays, and their NR based nanocomposites with 10 phr of modified clay are shown in figures 5.24, 5.25 and 5.26. In figure 5.24 the BAC modified organoclay shows ( $d_{001}$ ) diffraction peak at  $2\theta = 4.94^\circ$ , corresponding to an interlayer distance of  $17.90\text{\AA}$ . The obvious shift of ( $d_{001}$ ) diffraction peak of NR - BAC<sub>10</sub> nanocomposite towards lower angle indicates the effective expansion of the

interlayer distance of the clay. The interlayer distance of clay expanded to  $30.96 \text{ \AA}$  due to the formation of nanocomposite. A small peak at  $2\theta = 7.95^\circ$  indicating collapsed clay layers ( $11.07 \text{ \AA}$ ) is also observed. The expansion of gallery height should be attributed to the intercalation of the NR chains into the galleries of the organoclay. Similarly the interlayer distance of CPC modified organoclay increases from  $18.03 \text{ \AA}$  to  $27.59 \text{ \AA}$  when NR- CPC<sub>10</sub> nanocomposite is formed (figure 5.25). For NR-CTAB<sub>10</sub> nanocomposite, a sharp peak was observed at  $2\theta = 3.90^\circ$  which corresponds to the interlayer distance of  $22.64 \text{ \AA}$  indicating rubber intercalation since the CTAB modified organoclay has the diffraction peak at  $2\theta = 4.86^\circ$ .

#### **5.4.1.2 Scanning electron microscopy (SEM)**

The morphological characterisation of the gum vulcanisate and nanocomposites were carried out using scanning electron microscope (model - Philips Scanning Electron Microscope, ESEM-FEG XL30).



**(a)**

**(b)**

**Figure 5.27 Scanning electron microscopy photographs of (a) gum vulcanisate and (b) nanocomposites with 10 phr BAC modified clay**

SEM photographs of the fractured surface of the nanoclay reinforced NR composite and the gum vulcanisate are given in figure 5.27. In the case of nanocomposite, sliding surfaces of the polymer can be clearly observed; since the nanoclays restrict the

mobility of the NR matrix such flow imperfections are not noticed. This is due to the better interfacial adhesion between the rubber and clay. In the case gum vulcanisate of NR, such flow imperfections are not noticed. It seems that the rougher the fracture surface, better the mechanical properties of the related nanocomposite. A smooth fracture surface usually indicates low compatibility accompanied with premature, rather brittle type fracture [34]. The appearance of a rough surface is due to the fact that failure starts on in homogeneities located away from that of the major fracture plane.

#### **5.4.2 Mechanical properties**

NR-clay nanocomposites showed significant improvements in stress-strain properties as presented in figures 5.28 to 5.33. This was attributed to a good dispersion of the clay (i.e. pronounced intercalation without agglomeration) accompanied with strong interfacial adhesion between matrix and filler. NR-BAC modified clay composites demonstrated greatest increase in modulus at 100%, 200% and 300% elongation as a function of clay content when compared with other organoclay systems (figures 5.28, 5.29 and 5.30). This trend is also observed for the complex modulus of these rubber nanocomposites, which will be discussed later. This enhancement has to be traced to the filler dispersion and beneficial filler-rubber interaction in the related nanocomposites. NR-CPC nanocomposite has the second position followed by NR-CTAB nanocomposite.

Highest increase in modulus is more evident at higher elongation for the entire nanocomposite. Increments of 82, 148, & 153% on the modulus are observed at 100, 200 and 300% elongations for 10phr BAC filled nanocomposite compared to gum vulcanisate. The difference in moduli for different silicate filled NR nanocomposite is prominent at low elongations (100 and 200%). This is because the filler – polymer interactions play a critical role at low elongations just as at high elongations the strain-induced crystallization of NR dominates. This is similar to the observation obtained by Varghese et al. [35]. NR containing untreated  $\text{Na}^+$  also showed modulus enhancement



as a function of clay, but less compared to modified clay. As the unmodified clay was added, the rubber chains intercalated into the gallery gap of the clay and exfoliated it. However, the unmodified clay was an inorganic substance incompatible with the organic rubber matrix. Therefore, because of intercalation and subsequent exfoliation, there were slight increases in the strength, elongation at break, and modulus. The increase in the modulus could also be attributed to the addition of inorganic particles to the rubber matrix and to the increasing number of particles due to the exfoliation of the clay. Ultimate tensile strength is enhanced tremendously for NR-modified clay nanocomposites in comparison to the NR gum vulcanisate and NR-untreated clay nanocomposite, as shown in figure 5.31. In particular, NR-BAC nanocomposite systems show highest tensile strength followed by NR-CPC and NR-CTAB. A tensile strength of 35 MPa for 10 phr organoclay treated NR nanocomposites is obtained with bulky chain surfactant.

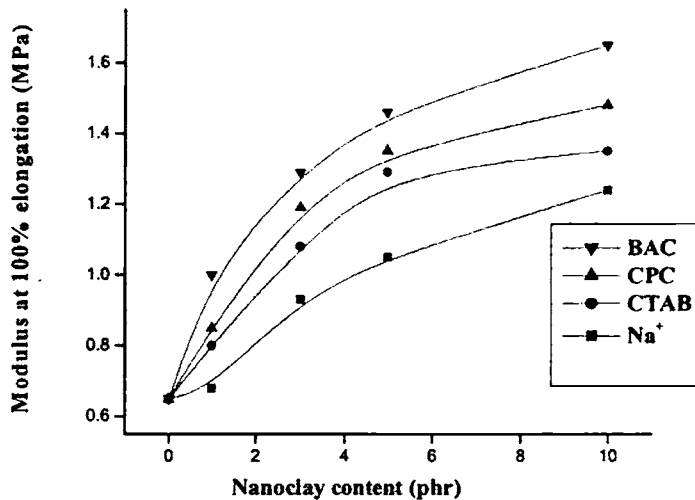


*Figure 5.28 Modulus at 100% elongation of organoclay nanocomposites*

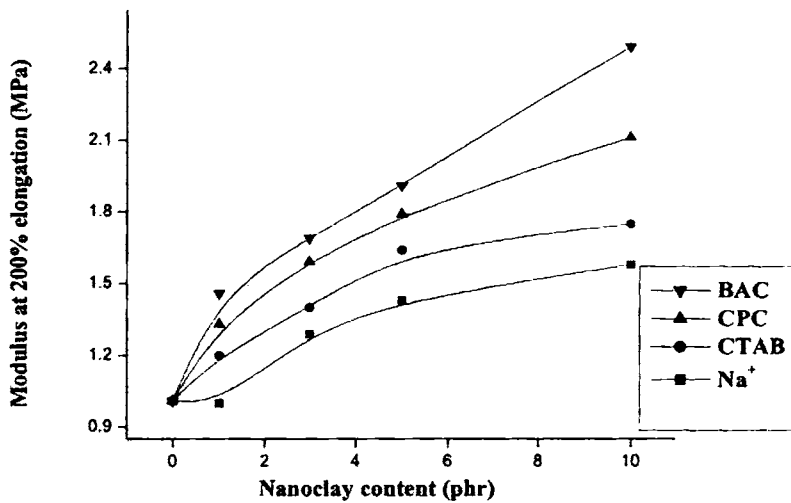


Figure 5.29 Modulus at 200% elongation of organoclay nanocomposites

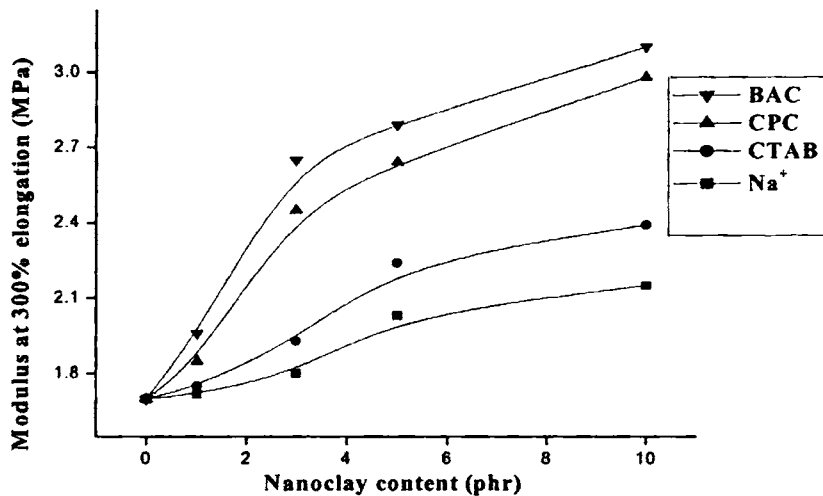


Figure 5.30 Modulus at 300% elongation of organoclay nanocomposites

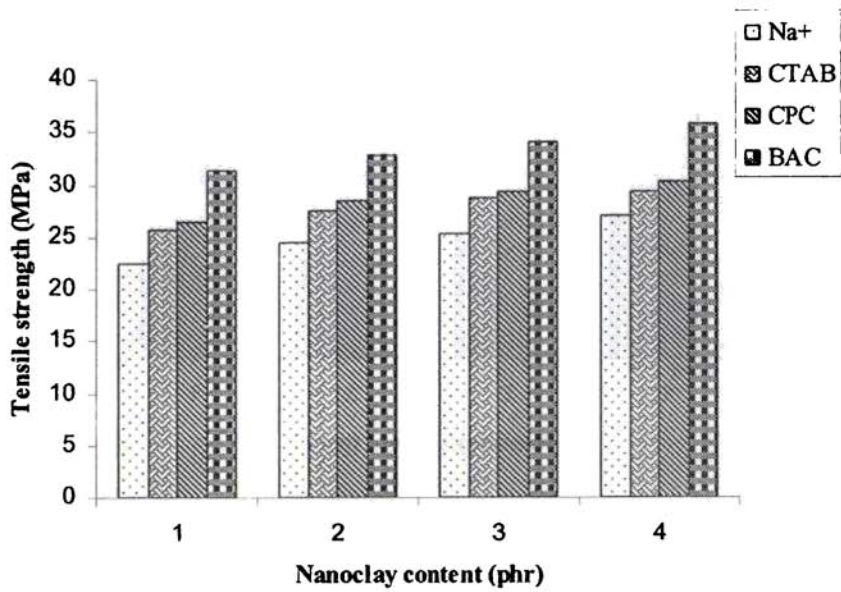


Figure 5.31 Tensile strength of nanocomposites

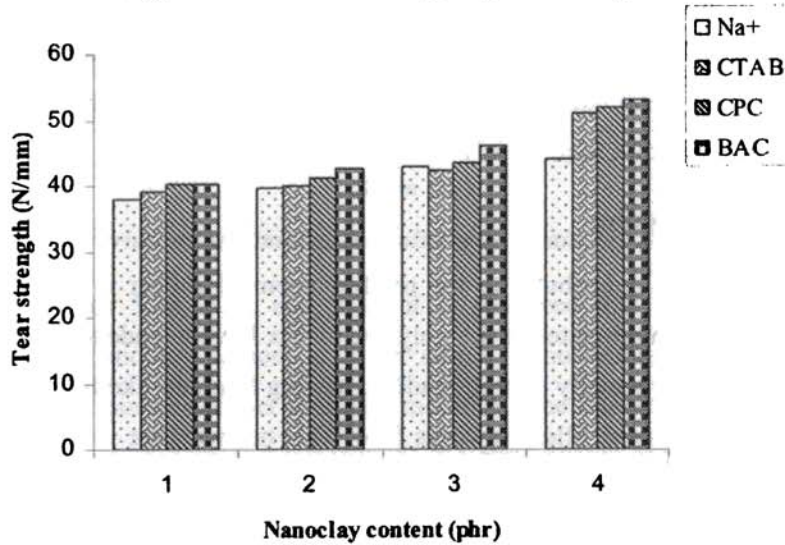
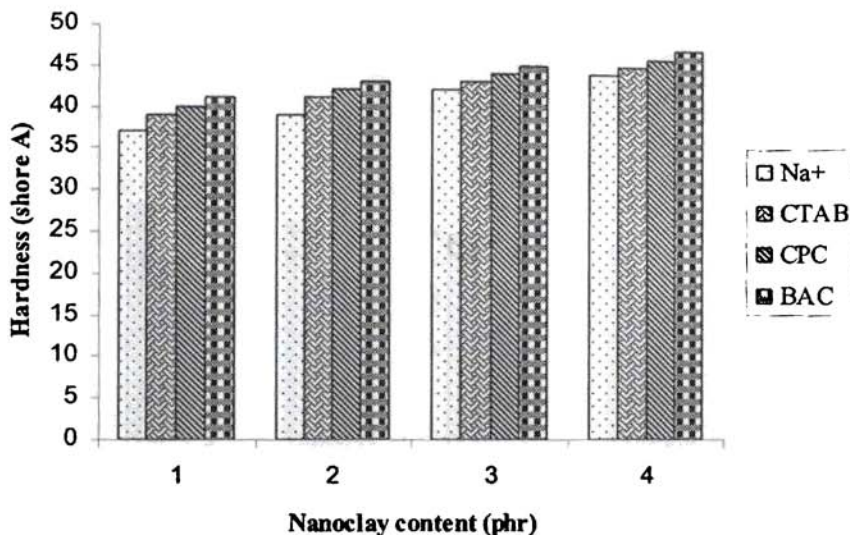


Figure 5.32 Tear strength of nanocomposites



**Figure 5.33 Hardness of nanocomposites**

Tear strength, which is also a measure of reinforcement shows the same trend as observed in figure 5.32. The hardness of NR-clay nanocomposites is much higher compared to the NR gum vulcanisate and NR-untreated clay as shown in figure 5.33. At 10 phr clay loading, NR-BAC presents highest hardness, followed by nanocomposites with CPC and CTAB.

#### **5.4.3 Strain sweep studies**

Another factor which contributes to the reinforcement of rubber is the formation of filler network. Filler aggregates in the polymer matrix have a tendency to associate to form agglomerates, especially at high loading, leading to chain-like filler structures or clusters which are termed filler networks [36]. This net working is formed by filler-filler interactions in the case of highly polar fillers such as silica, or via immobilized layers of rubber on the filler surface in the case of strong interactions between filler and rubber. In clay composites, besides the confinement of polymer chains between the silicate layers, there could also be interactions of polymer chains with the long alkyl groups of the organically modified clays. Destruction of this networking occurs by the application of strain with a reduction in complex modulus but the values at low

strain increases with filler concentration. As the complex modulus ( $G^*$ ) values at low strains (<15 %) are a measure of the filler polymer interaction, the high values of  $G^*$  is only due to filler networks, either filler-filler or filler polymer. Studies on the mechanical properties of the nanocomposites show that the networks are formed mainly between polymer and filler.

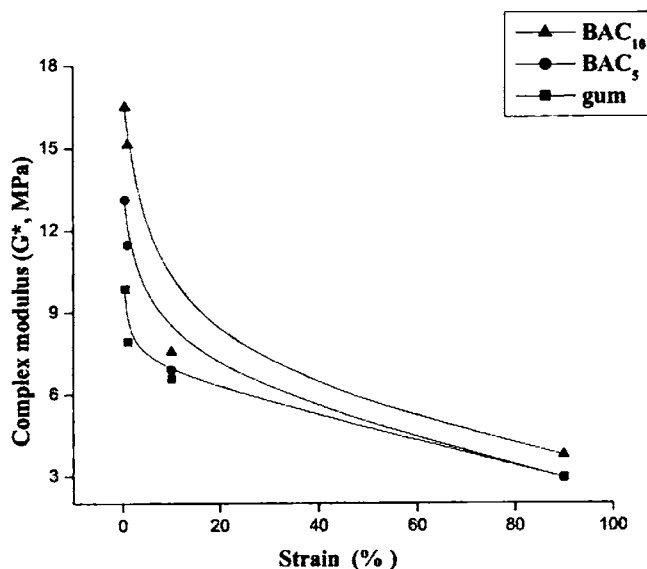


**Figure 5.34** Variation of complex modulus with strain for BAC nanocomposites

From the figures 5.34, 5.35 and 5.36, it is observed that the complex modulus increases with nanoclay content at lower strain. Nanocomposites with clay having bulky surfactant possess higher complex modulus. The interaction between clay and natural rubber can predominantly occur via the alkyl chains of the ammonium cation and could arise from van der Waals forces or through entanglements. Organically modified galleries of montmorillonites are easily penetrated by natural rubber chains and lead to intercalated structures and partial exfoliation.

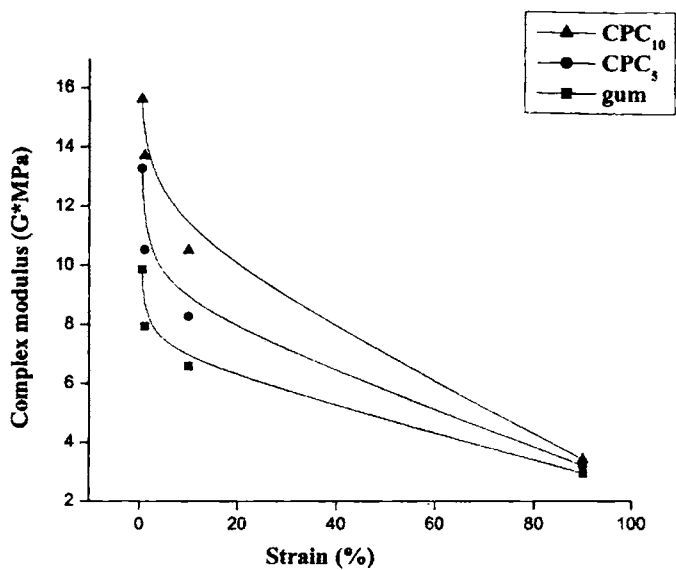


Figure 5.35 Variation of complex modulus with strain for CPC nanocomposites

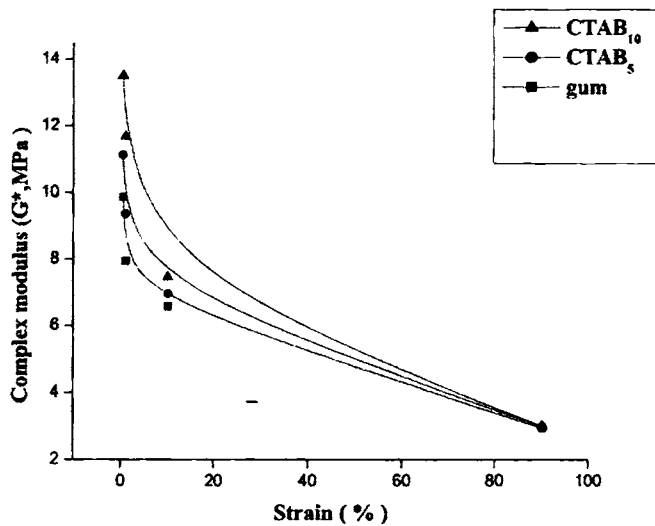
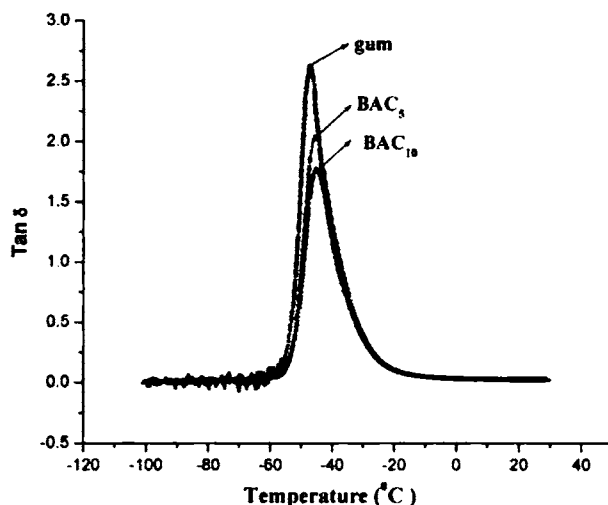


Figure 5.36 Variation of complex modulus with strain for CTAB nanocomposites

#### 5.4.4 Dynamic Mechanical Analysis

Dynamic mechanical thermal analysis (DMTA) spectra were recorded on rectangular specimens (length  $\times$  width  $\times$  thickness = 5  $\times$  4  $\times$  2.11 cm) in the tensile mode at a frequency of 1 Hz with a TRITEC2000B DMA 1L dewar (Triton-technology, U K). DMTA spectra [i.e., the storage modulus and mechanical loss factor ( $\tan \delta$ )] were measured from -120 to 30 °C at a heating rate of 1°C/min.



**Figure 5.37** *Tan delta measured with DMTA for NR and NR-clay nanocomposites*

The tan delta values obtained from DMTA measurements are plotted in figure 5.37 for gum vulcanisates and BAC modified clay filled nanocomposites. Tan delta is the ratio of the storage modulus over the loss modulus. From the curves, it can be seen that the intensity of tan delta peak at the glass transition temperature ( $T_g$ ) decreases with clay loading. The position of the tan delta peak corresponding to the  $T_g$  of the nanocomposites does not shift significantly from NR gum vulcanisate. According to Schon and coworkers [37, 38], the decrease in intensity of the tan delta peak can be used as an indication of higher degree of intercalation/exfoliation. When a greater

amount of polymer is in between the clay layers, the amount of polymer in the amorphous matrix is reduced. Nanocomposite with 10 phr BAC modified clay shows greatest decrease in tan delta value.

### 5.4.5 Swelling studies

Enhancement of the permeation-barrier properties of NR was obtained by incorporating impermeable plate like particles because the permeant molecules have to wiggle around them in a random walk, thus diffusing through a tortuous pathway [39-41]. Plate like nanoparticles are ideal for this purpose because of their geometrical shape and high aspect ratio, and effective improvements can be obtained at low volume fraction.

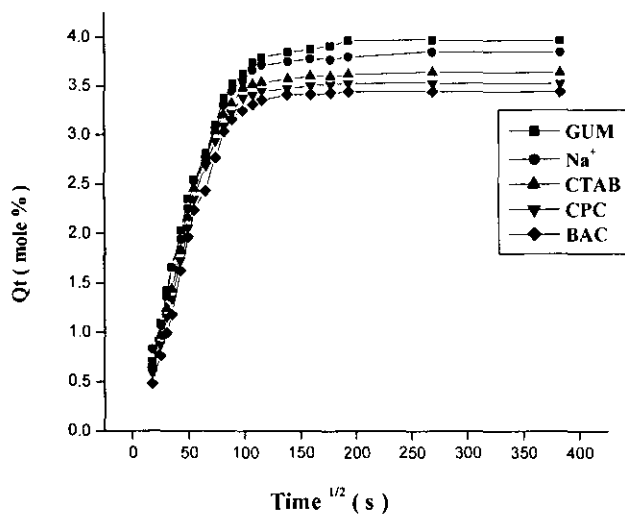
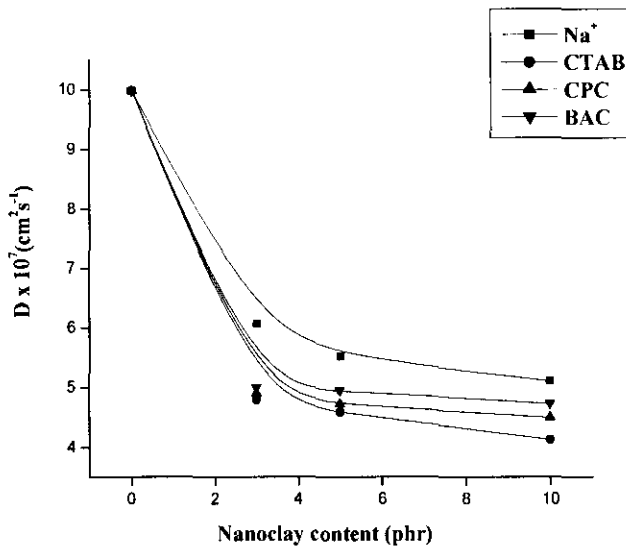


Figure 5.38 Sorption curves of the vulcanisates at 303K

The presence of highly dispersed clay layers in the NR-BAC modified clay nanocomposites increases the tortuosity, which decreases the diffusion of solvent molecules. Thus, BAC modified clay nanocomposite have the smallest diffusion



coefficient among all the samples. The solubility typically decreases proportionally to the filler content in the case of nanocomposites as shown in figure 5.38. The solubility decrease the most for BAC modified clay nanocomposite because of the nano-dispersion. These samples showed highest amount of intercalation/exfoliation corresponding to a greater amount of polymer in between the clay layers and a reduced amount of polymer in the amorphous matrix. This reduction of the rubber in the amorphous phase leads to the steep decrease in the solubility. From figures 5.39 to 5.41 it can be observed that the diffusion coefficient, permeation coefficient and sorption coefficient decreases with increase in nanoclay loading.



*Figure 5.39 Variation of Diffusion Coefficient with clay content in NR vulcanisates*

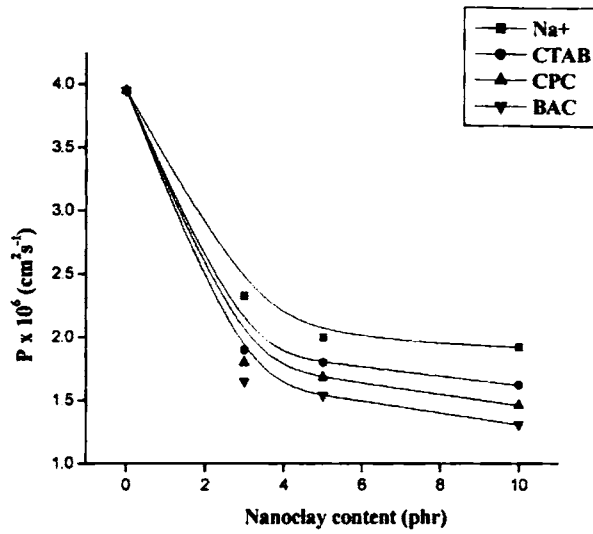


**Figure 5.40** Variation of Permeation Coefficient with clay content in NR vulcanisates

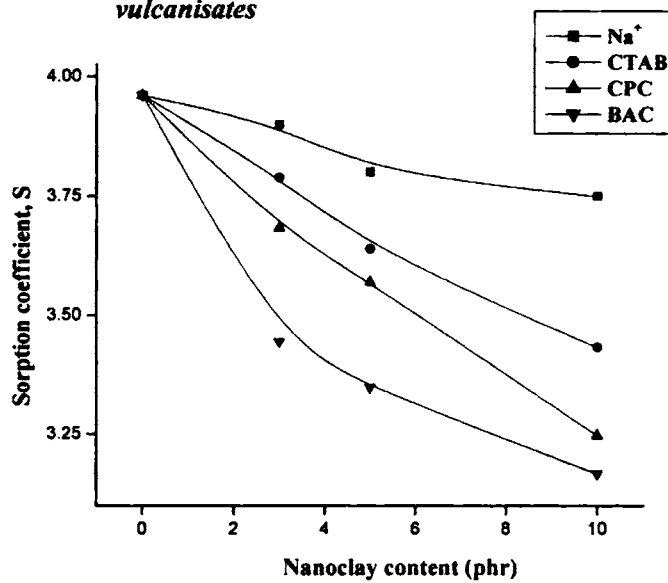


**Figure 5.41** Variation of Sorption Coefficient with clay content in NR vulcanisates

## **5.5 Conclusion**

Organophilic modification of nanoclay is done using three different quarternary ammonium surfactants viz., BAC, CPC and CTAB. The incorporation of the ammonium groups in between the clay layers are confirmed by X-ray diffraction technique, IR spectroscopy and Thermogravimetric analysis. These modified clays are successfully incorporated in methacrylated natural rubber latex. The formation of the intercalated natural rubber latex organoclay nanocomposite is confirmed using XRD and Transmission electron spectroscopy. The mechanical properties of NR latex - clay nanocomposites show significant improvement. The stress-strain properties and other mechanical properties show considerable improvement even at 0.5 phr of clay loading. On comparing the property improvement for the three different clays, it is seen that NR latex - BAC clay nanocomposites is superior. This is due to the better interaction between the rubber molecules and the surfactant used for the clay modification. Higher swelling resistance is also offered by the nanocomposites due to the presence of tortuous path for solvent diffusion through the rubber.

Antibacterial property is shown by the latex nanocomposite against a Gram positive and Gram negative bacteria when examined using halo ring test and halo ring with highest diameter is obtained for BAC samples. Greatest antibacterial property is shown against Gram positive bacteria. Therefore, organoclay reinforced natural rubber latex based composites with high mechanical strength, swelling resistance and antibacterial property was prepared by utilizing this study.

The effect of the three surfactants used for the organophilic modification of the clay in natural rubber in the dry stage is also investigated. Analysis of the stress-strain properties, dynamical mechanical properties and swelling behaviour shows a considerable enhancement in the polymer filler interactions.

**References**

1. Usuki, A., Kawasumi, M., Kojima, Y., Okada, A., Fukushima, Y., Kurachi, T. and Kamigaito, O. *J. Mater. Res.*, 8, 5, 1179, 1993.
2. Lan, T. and Pinnavaia, T.J., *Chem. Mater.*, 6, 2216, 1994.
3. Qutubuddin, S. and Fu, X., In: *Nano-Surface Chemistry*, Editor, Rosoff, M., Marcel Dekker, p 653, 2001.
4. Ray, S. and Okamoto, M. *Polym. Sci.*, 28, 1539, 2003.
5. Alexandre, M. and Dubois, P., *Mater. Sci. Eng.*, 28, 1, 2000.
6. Ko, M. B. *Polym. Bull.* 45, 183, 2000.
7. Vaia, R. and Giannelis, E. *Macromolecules*, 30, 7990, 1997.
8. Sherman, L. M. *Plast Technol.*, June, 52, 1999.
9. Vaia, R. A. *Polymer melt intercalation in mica-type layered silicates*. PhD Thesis. USA: Cornell University, 1995.
10. Zhang, W. A., Chem, D. Z., Xu, H. Y., Shen, X. F. and Fang, Y. E., *European Polymer Journal*, 39, 2323, 2003.
11. Arroyo, M., Lopez-Manchado, M. A., and Herrero, B., *Polymer*, 44, 2447, 2003.
12. Vu, Y.T., Mark, J.E., Pham, L.H., and Engelhardt, M., *J. Appl. Polym. Sci.*, 82, 1391, 2001.
13. Sadhu, S. and Bhowmick, A.K., *Rubber. Chem. Technol.*, 76, 860, 2003.
14. Joly, S., Garnaud, G., Ollitrault, R. and Bokobza, L., *Chem. Mater.*, 14, 4202, 2002.
15. Magaraphan, R., Thaijaroen, W. and Lim-Ochakun, R., *Rubber Chem. Technol.*, 76, 406, 2003.

16. Rahn, O., Van Eseltine, W., *Ann. Rev. Microbiol.*, 1, 173, 1947.
17. Domagk, J. G., *Deut. Med. Wochs.*, 61, 829, 1935.
18. Vigo, L.T., *Advances in Antimicrobial Polymers And Materials.*, In; *Biotechnology and Bioactive Polymers*, Gebelein, C. G; Charles, E., Carraher, Jr.(eds), Plenum Press, New York, p 225, 1994.
19. Danker, J., Hoght, A. H. and Feijen, J., *Biomedical Polymers: Bacterial Adheshion Colonization and Infection*, C R C Crit Rev, Biocomp. 2, CRC Press, Boca Raton, p 219, 1986.
20. Collins, C. H., *Lab Acquired Infections-History, Incidence, Causes, and Prevention*, Butterworths, London, 1983.
21. Gristina, A. G., Hobgood, C. D. and Barth, E., *Pathogenesis and Clinical Significances of Coagulase- negative Staphylococci*. Pulverer, P. G., Quie, Peters, G (eds) Fischer Veriag, Stuttgart, p.143, 1987.
22. Pinnavaia, T.J. and Beal, G.W., *Polymer clay nanocomposites*. 1st ed. England: Wiley, 2001.
23. Wang, X., Du, Y., Yang, J., Wang, X., Shi, X. and Hu, Y., *Polymer*, 47, 6738, 2006.
24. Oya, A., Banse, T., Ohashi, F. and Otani, S., *Appl. Clay Sci.*, 6, 135, 1991.
25. Russel, A., *Prog. Med. Chem.*, 6, 135, 1969.
26. Franklin T.J. and Snow, G. A., *Biochemistry of Antimicrobial Action*, Chap.3, Chapman and Hall Ltd., London, 1981.
27. Ikeda, T. and Tazuke, T., *Macromol.Chem.*, 185, 869, 1984.
28. Liu, H., Du, Y.M., Yang, J.H. and Zhu, H.Y., *Carbohydr Polym.*, 55, 291, 2004.
29. Rabea, E.I., Badawy, M.E.T., Stevens, C.V., Smaghe, G. and Steurbaut, W., *Biomacromolecules*, 4, 1457, 2003.

30. Huang, R.H., Du, Y.M., Zheng, L.S., Liu, H. and Fan, L.H., *React Funct Polym.*, 59, 41, 2004.
31. Tokura, S.K., Ueno, S., Miyazaki, S. and Nishi, N., *Macromol Symp.*, 120, 1, 1997.
32. Hoogerheide, J. C., *J. Bact.*, 49, 277, 1945.
33. Shelton, R. S., Van Campen, M. G., Tilford, C. H., Lang, H. C., Nisonger, L., Bandelin, F. J. and Rubenkoenig, H. L., *J Am. Chem. Soc.*, 68, 753, 1946.
34. Mousa A, Ishiaku U. S. and Mohd Ishak Z.A. *J Appl Polym Sci.*, 69, 1357, 1998.
35. Varghese, S. and Karger Kocsis, J., *Polymer*, 44, 4921, 2003.
36. Joly, S., Garnaud, G., Ollitrault, R., Bokobza, L. and Mark, J. E., *Chem. Mater*, 14, 4202, 2002.
37. Schon, F., Thomann, R. and Gronski, W., *Macromol. Symp.*, 189, 105, 2002.
38. Schon, F. and Gronski, W. *Kautschuk Gummi Kunststoffe*, 56, 166, 2003.
39. Eitzman, D. M., Melkote, R. R., and Cussler, E. L., *AIChE J*, 42, 2, 1996.
40. Fredrickson, G. H. and Bicerano, J., *J. Chem. Phys.*, 110, 2181, 1999.
41. Gusev, A. A., and Lusti, H. R., *Adv. Mater.*, 13, 1641, 2001.

### *Nitrile Rubber Clay Nanocomposites*

Synthetic rubbers are more uniform in quality and compounds prepared from them are more consistent in processing and product properties [1]. Natural rubber crystallizes on stretching giving high tensile strength to the gum vulcanisate; on the other hand gum vulcanisate of synthetic rubbers like styrene butadiene rubber, nitrile rubber etc are generally weak and requires the incorporation of reinforcing fillers to produce products having high strength. Acrylonitrile butadiene rubber, known as nitrile rubber (NBR) shows no self reinforcing effect, as it cannot undergo stress induced crystallization on stretching. Since the gum vulcanisates have very low tensile strength, NBR is used in combination with reinforcing fillers to obtain vulcanisates having excellent mechanical properties. Rubber-clay nanocomposite technology has been extended to synthetic rubbers besides natural rubber. The polarity of the polymer chains and the basal spacing of the clay are important for the structure of the polymer-clay nanocomposites. In general, higher the polarity of the polymer chains and the wider the basal spacing of the clay, the more easily the polymer/clay nanocomposites with intercalated or exfoliated structure are formed [2]. NBR is a polar rubber and is generally considered as a special purpose rubber being used for applications requiring oil and solvent resistance. Presence of acrylonitrile (ACN) makes it polar and provides special features to the polymers.

Toyota group synthesized intercalated NBR-clay nanocomposites with 4 percentage of clay by volume which had hydrogen and water vapor permeability 30% lower than pure gum vulcanisate [3]. Similar barrier properties were also observed by Wu et al. [4] with 10% clay by volume, nitrogen permeability decreased by almost 50%. Nanocomposites also showed enhanced tensile strength and modulus [5].

## **6.1. Nitrile rubber clay nanocomposites**

### **6.1.1 Preparation of nitrile rubber clay nanocomposites**

Nitrile Rubber (N-03868) with an acrylonitrile content of 40 weight percentage supplied by Gujarat Apar Polymers Ltd., India was used for the study. In the first part of the work two different types of nanoclay differing in the interlayer distance and in modifying groups were used. They were obtained from Southern Clay Products, USA. The interlayer distance of the clays used were 18.3Å and 30.6Å for cloisite 10A [2MBHT: dimethyl, benzyl, hydrogenated tallow, quaternary ammonium], and cloisite 15A [2M2HT: dimethyl, dihydrogenated tallow, quaternary ammonium] respectively. Other chemicals used were of commercial grade. Compounds were prepared in a two roll mill with various filler loading from 1 to 10 parts per hundred rubber (phr) with the two clays according to the recipe given in table 6.1. In the second part of the study, the clays were modified adopting the procedure mentioned in section 5.1.2 and they are used instead of cloisite 10A and 15A.

The mixed compounds were matured for a period of 24 hours and the cure characteristics like cure time, scorch time, maximum and minimum torque were determined using rubber process analyzer at a temperature of 150 °C. From the respective cure curves, the optimum cure time for the vulcanisation were determined. Sheet for preparing the test specimens were moulded to a thickness of 2 mm using an electrically heated hydraulic press at 150 °C and 200 kgcm<sup>-2</sup> up to their respective cure times.



**Table 6.1 Compounding recipe**

Ingredients	Gum	10A	15A
Nitrile Rubber	100	100	100
ZnO	4	4	4
Stearic acid	1.5	1.5	1.5
Sulphur	1.5	1.5	1.5
CBS	1.25	1.25	1.25
Antioxidant-HS	1	1	1
Cloisite 10A	-	X	-
Cloisite 15A	-	-	Y

X = 1, 3, 5, and 10 phr of cloisite 10A

Y = 1, 3, 5 and 10 phr of cloisite 15A

### **6.1.2 Characterisation using X-Ray diffraction technique**

XRD curves of cloisite 15A nanoclay and 10 phr clay filled nanocomposite is shown in figure 6.1. For the nanocomposite the peaks are displaced from the original  $2\theta$  value of cloisite 15A,  $2.88^\circ$  to  $2.36^\circ$ . The interlayer distance between the clay layers increased from  $30.6 \text{ \AA}$  to  $38.50 \text{ \AA}$ . This increase in d spacing suggests the intercalation of the polymer chains between the clay layers.

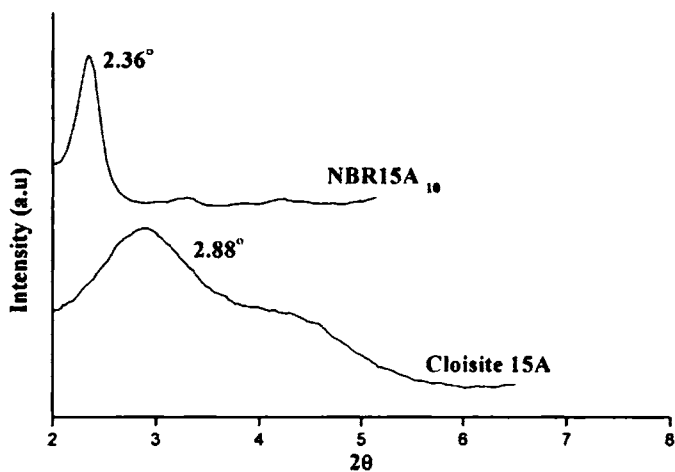


**Figure 6.1** X-ray diffraction curves for cloisite 15A nanoclay and NBR-clay nanocomposites

Figure 6.2 shows the X-ray diffraction curves for cloisite 10A nanoclay and an NBR based nanocomposite with 5 and 10 phr of cloisite 10A. For cloisite 10A clay a diffraction peak at  $2\theta = 4.80$  which corresponds to an interlayer spacing of  $18.39 \text{ \AA}$  is obtained. For the nanocomposites, with 5 phr nanoclay this peak exhibited two shoulders at  $2\theta = 2.18$  and  $3.12^\circ$  corresponding to an interlayer spacing of  $40.52$  and  $28.51 \text{ \AA}$  respectively, which reflect the formation of an intercalated nanocomposite. For 10 phr clay filled nanocomposites also the X-ray diffraction peaks are obtained at almost similar  $2\theta$  values which represent the diffraction of the (001) crystal surface of layered silicates in the nanocomposites, corresponding to d-spacing of  $39.48$  and  $27.59 \text{ \AA}$ . For nanocomposites at higher organoclay concentration, the dispersed silicates have slightly lower d-spacing. Steric hindrance of the silicates at high concentration may decrease the expansion of the layers.

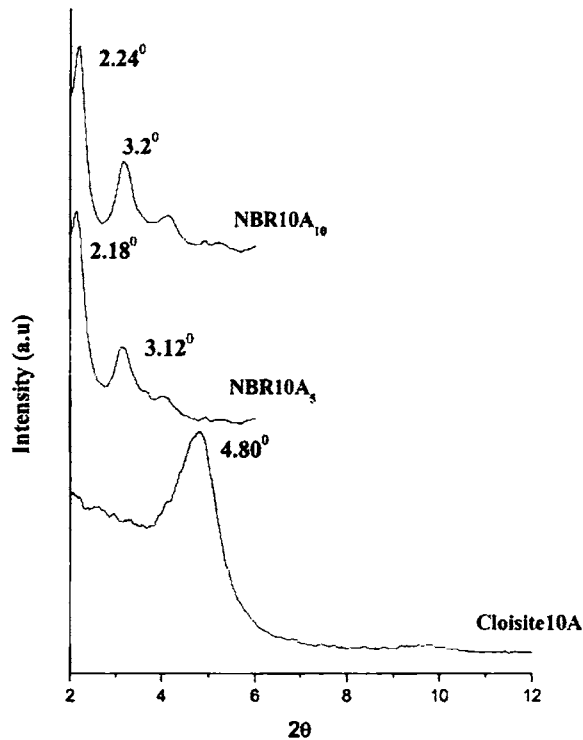
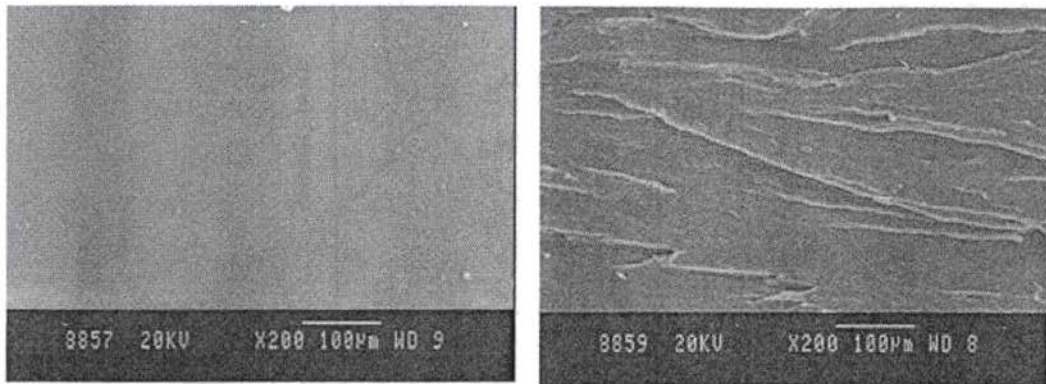


*Figure 6.2 X-ray diffraction curves for cloisite 10A nanoclay and NBR-clay nanocomposites*

### 6.1.3 Scanning Electron Microscopy

The SEM photographs of the fractured surface of the gum vulcanizate and the layered clay filled nanocomposites are shown in figure 6. 3. The morphology of the fractured surface of the nanoclay reinforced NBR composite can be studied using the SEM photographs. It can be observed that the NBR matrix is stretched by shear forces, the opposite surfaces move from one side to the other. Material displacement occurred in the direction of applied stresses, channels and raised parts are produced. Sliding surfaces of the polymer can be clearly observed in the case of fractured surfaces of the nanocomposites, since the nanoclays restrict the mobility of the NBR matrix. This is

due to the better interfacial adhesion between the rubber and clay. In the case gum vulcanisate of NBR, such flow imperfections are not noticed.



(a)

(b)

***Figure 6.3 Scanning electron microscopy photographs of (a) gum vulcanisate and (b) layered clay filled nanocomposites with 10 phr cloisite 15A***

#### **6.1.4 Cure characteristics**

Cure characteristics of the NBR based nanocomposites with two different types of nanoclay differing in the interlayer distance at varying filler loading and that of the gum compound are given in table 6.2. As expected, the addition of organoclay results a significant increase in the maximum torque. Maximum torque can be regarded as a measure of the shear modulus which is increased due to improved clay-rubber interactions, including intercalation and exfoliation. The organoclay behaves as a vulcanisation accelerator for NBR, thus decreasing the scorch time and cure time. This effect is essentially attributed to the quaternary ammonium salt present in the nanosilicate structure which comes from the organic modification of the clay. The quaternary ammonium salt involves itself in the cure reaction by forming a complex with zinc salt and sulfur [6].

**Table 6.2 Cure characteristics of compounds**

Sample code	Min. Torque (dNm)	Max. Torque (dNm)	T <sub>10</sub> (minutes)	T <sub>50</sub> (minutes)	T <sub>90</sub> (minutes)
Gum	0.065	3.308	9.77	11.83	20.31
10A <sub>1</sub>	0.197	3.423	5.99	7.72	14.05
10A <sub>3</sub>	0.192	3.987	4.16	5.42	11.43
10A <sub>5</sub>	0.196	4.095	3.47	4.75	10.39
10A <sub>10</sub>	0.241	4.707	2.12	3.26	8.30
15A <sub>1</sub>	0.167	3.364	7.34	8.88	14.46
15A <sub>3</sub>	0.212	3.435	5.82	7.15	13.10
15A <sub>5</sub>	0.251	3.801	4.79	6.06	12.01
15A <sub>10</sub>	0.320	4.818	2.92	4.19	10.37

### 6.1.5 Mechanical Properties

From figures 6.4 to 6.8 it can be understood that intercalation of rubber chains in between the silicate layers provided rubber-clay nanocomposites with outstanding mechanical properties. The tensile strength increases by more than 440% for 10 phr of cloisite 15A clay filled NBR vulcanisate compared to the gum vulcanisate with a slight variation in the elongation at break. The tear properties of these NBR-silicate nanocomposites display the similar trend to that of the tensile properties. About 165% increase in the tear strength is obtained with the addition of 10 phr of nanoclay. This effect can be assigned to the silicate surface area, the extent of dispersion of the silicate in the NBR matrix and the increase in the crosslink density. The same trends

are recorded in the case of the modulus at 300% elongation and hardness which are also indicators of the stiffness of the rubber vulcanisate.

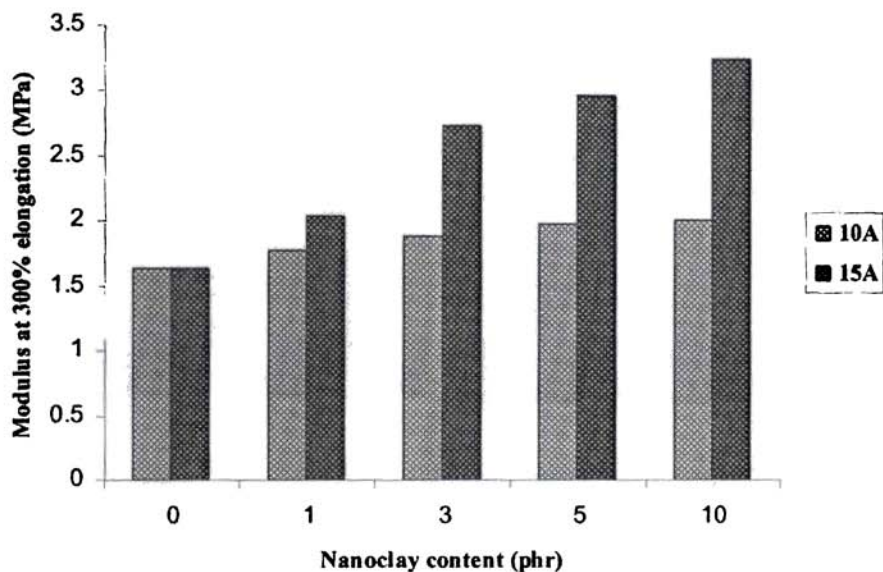


Figure 6.4 Variation of tensile modulus with clay content

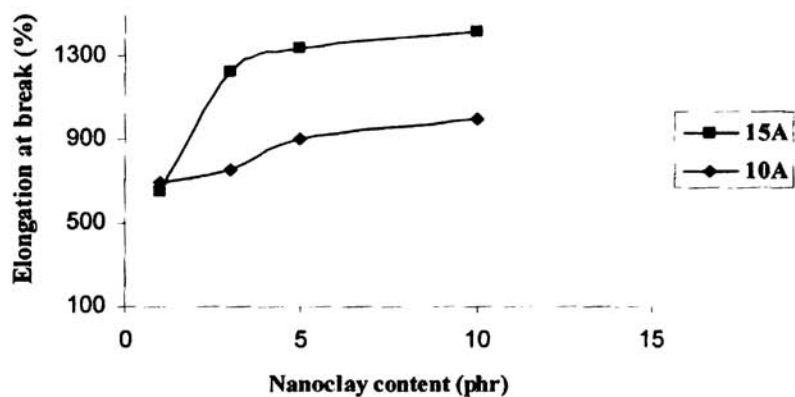


Figure 6.5 Variation of elongation at break with clay content

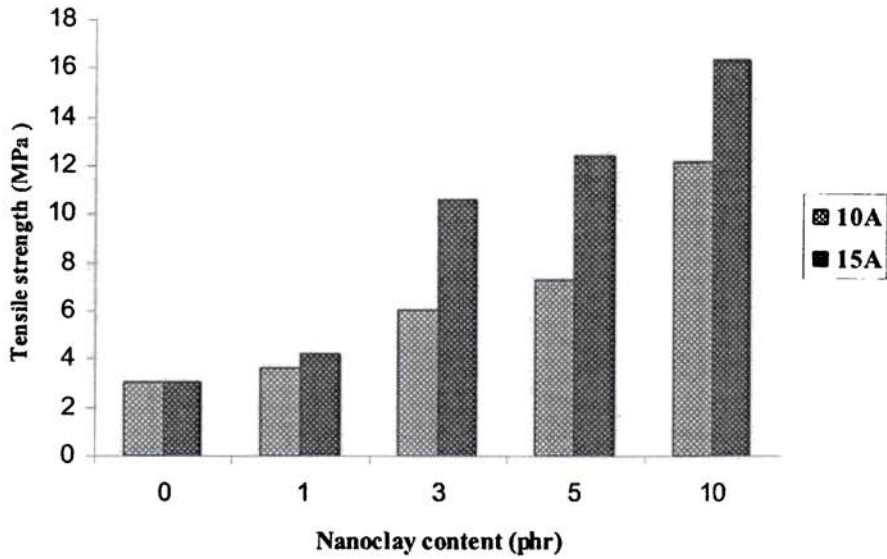


Figure 6.6 Variation of tensile strength with clay content

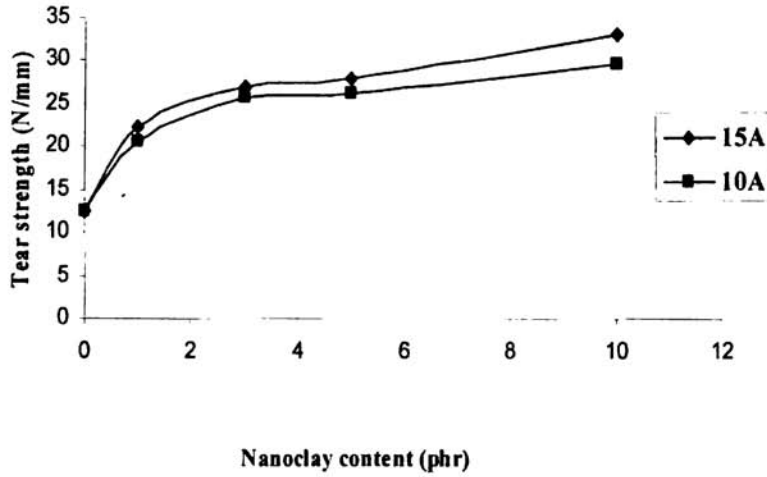
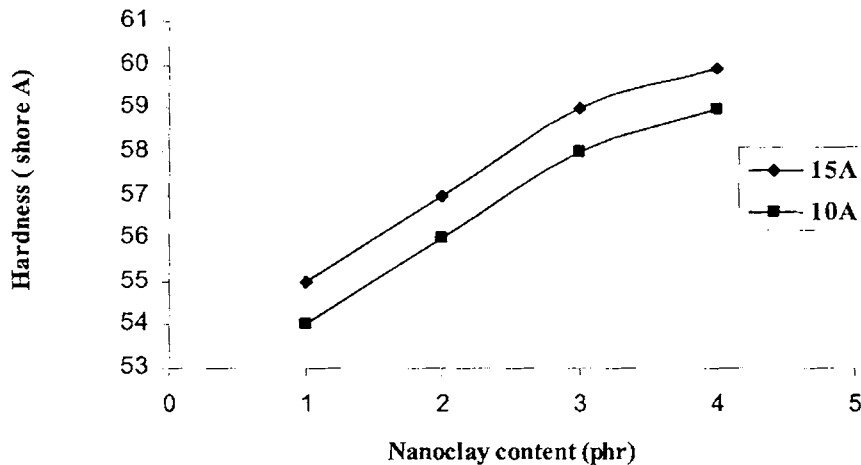


Figure 6.7 Variation of tear strength with clay content



**Figure 6.8** Variation of hardness with clay content

The reinforcement of rubbers with fillers combines the elastic behaviour of rubber with the strength and stiffness of the reinforcing phase. Further, the elongation at break (EB) has been improved with increasing nanosilicate content. These results suggest that the nano-scale dispersion controls the tensile strength of the material; the stress applied in the exfoliated nanocomposite can be distributed to each individual layer and the layers may align themselves for maximum elongation. As in the case of natural rubber better physical properties are obtained for NBR based nanocomposite prepared with clay having higher interlayer distance.

#### 6.1.6 Strain sweep studies

The storage modulus values at low strain (<15%) are a measure of the filler polymer interactions. So the variation of storage modulus with strain was studied for the uncured compounds with the two types of clays at 1 to 10 phr loading. The values obtained were plotted and shown in figures 6.9 and 6.10.



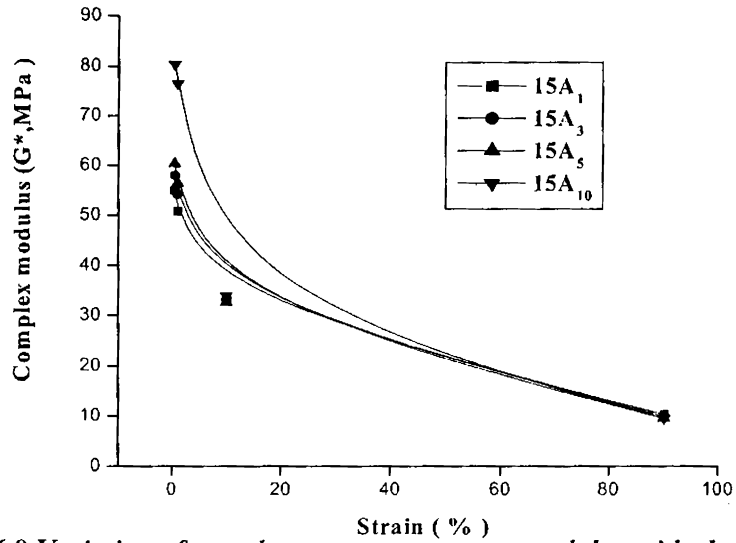


Figure 6.9 Variation of complex modulus with clay content of 15A nanocomposites

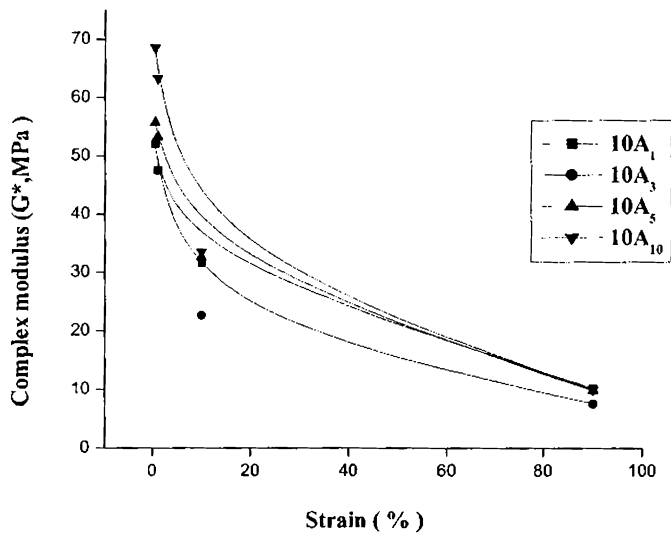


Figure 6.10 Variation of complex modulus with clay content of 10A nanocomposites

From the figures, it is clear that the complex modulus values is increasing with the clay content and is higher for the compound with clay having higher interlayer distance, indicating better rubber filler interactions. The increase in modulus is due to the inclusion of rigid filler particles in the soft rubber matrix, hydrodynamic effect and additional contribution arise from the molecular interaction between the rubber and the filler leading to the additional crosslinks into the polymer network structure. The additional cross-links can be confirmed by equilibrium swelling studies.

### 6.1.7 Swelling studies

Nano level dispersion of the layered silicate in the polymer matrix results in a greater enhancement in solvent barrier property compared to conventional phase separated composites [7-12]. The presence of the silicate layers may cause a decrease in permeability because of a more tortuous path for the diffusing molecules that must bypass impenetrable platelets. Therefore, to determine how the content of layered silicates in a hybrid composite affects the permeability, we measured the transport properties for all the samples with methyl ethyl ketone as the solvent.

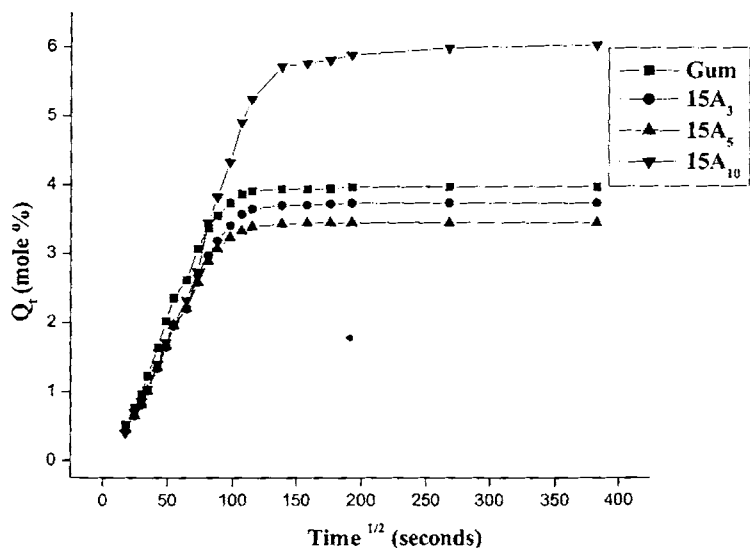
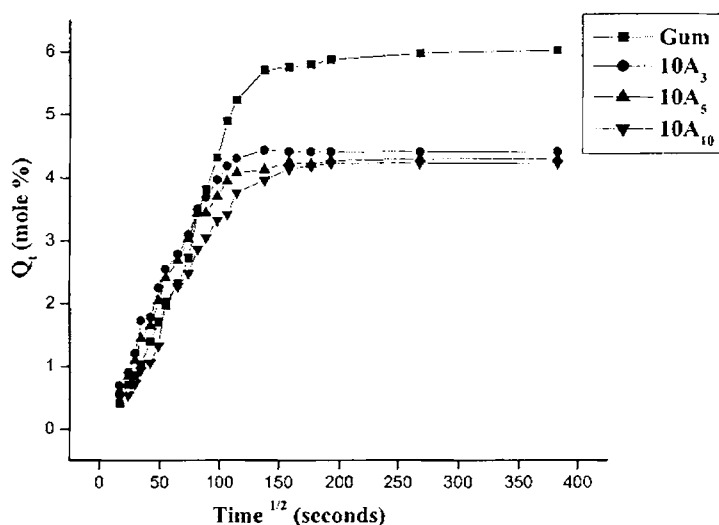


Figure 6.11 Swelling behaviour of NBR samples with cloisite 15A in MEK at 303 K



**Figure 6.12 Swelling behaviour of NBR samples with cloisite 10A in MEK at 303 K**

The samples with filler loading from 0 up to 10 phr of the two types of clays were immersed in the solvent and the solvent uptake was determined in each case. It was observed that all the samples swelled upon immersion in toluene. In figure 6.11 and figure 6.12, the toluene uptake up to equilibrium swelling is plotted against time. It can be seen that for all compositions the uptake is rapid in the initial zone. After this the sorption rate decreases leading to a plateau, corresponding to equilibrium swelling. It is noted that the gum vulcanisate has the maximum uptake at equilibrium swelling. The diffusion coefficient,  $D$  for the nanocomposites are given in table 6.3. The unfilled matrix presents the maximum diffusion coefficient of around  $7.12 \times 10^{-7} \text{ cm}^2\text{s}^{-1}$ . Adding nanoclay within the NBR matrix results in a progressive decrease of  $D$  value. Diffusion coefficient decreased to half for nanocomposite with 10 phr of cloisite 15A clay.

**Table 6.3 Variation of Diffusion, Sorption and Permeation Coefficient with nanoclay loading**

Sample code	gum	10A <sub>3</sub>	10A <sub>5</sub>	10A <sub>10</sub>	15A <sub>3</sub>	15A <sub>5</sub>	15A <sub>10</sub>
Diffusion Coefficient $\times 10^7$ (cm <sup>2</sup> s <sup>-1</sup> )	7.12	5.27	5.06	4.55	4.05	3.79	3.39
Sorption Coefficient	4.31	2.83	2.66	2.47	3.09	3.06	3.046
Permeation coefficient $\times 10^6$ (cm <sup>2</sup> s <sup>-1</sup> )	3.08	1.49	1.35	1.13	1.25	1.16	1.03

The permeation coefficient, the net effect of sorption and diffusion process is also found to be decreased. With an increasing clay loading up to 10 phr, regardless of the type of organoclay, the permeability decreased linearly. This was due to an increase in the lengths of the tortuous paths followed by the solvent molecules and the interaction between the solvent molecules and the alkyl moiety in the organoclays. The intercalated system with highest d-spacing shows the highest tortuosity leading to the lowest permeability. It is seen that the decreasing value of the permeability of the nanocomposites is largely dominated by the diffusion phenomenon, as shown by the respective values of sorption and diffusion coefficient reported in table 6.3.

Contribution of fillers to the reinforcement effect arises from molecular interaction between the rubber and filler. This interaction leads to an increase in the effective increase in crosslink density. The increase in crosslink density can be evaluated by the equilibrium swelling method. From table 6.4 it can be observed that the crosslink density of the nanocomposites is higher than the gum compound. The increased crosslink density of the nanocomposites indicates a better adhesion between the rubber and the clay.

**Table 6.4 Variation of cross link density,  $\Delta G$  and  $\Delta S$  with loading of nanoclay**

Sample code	gum	10A <sub>3</sub>	10A <sub>5</sub>	10A <sub>10</sub>	15A <sub>3</sub>	15A <sub>5</sub>	15A <sub>10</sub>
Crosslink density ( $\nu$ ) $\times 10^4$ (moles gm <sup>-1</sup> )	1.37	1.69	1.77	1.85	2.07	2.23	2.26
$\Delta G$ (J mol <sup>-1</sup> )	-27.84	-35.64	-37.77	-39.76	-45.37	-49.43	-50.24
$\Delta S$ $\times 10^2$ (J mol <sup>-1</sup> )	0.91	1.17	1.24	1.31	1.49	1.63	1.65

Table 6.4 demonstrates the influence of the nanoclay loading on the Gibbs free energy,  $\Delta G$ , and entropy of mixing,  $\Delta S$ , of the NBR-clay nanocomposites swollen in methyl ethyl ketone. As  $\Delta G$  represents the elastic behaviour, the increase in  $\Delta G$  for the nanocomposites suggests the increased number of possible rearrangements in the NBR-clay nanocomposites at high overall degree of cross linking. This may imply that a peculiar, heterogeneous network structure was formed in the nanocomposites. This is in accordance with the conclusion obtained by J. Karger-Kocsis et al for SBR silicate nanocomposites [13]. The formation of an exfoliated nanocomposite is responsible for the noticeable increase of entropy as compared with gum compound.

## 6.2 Modified clay based NBR nanocomposites

In this study, NBR-clay nanocomposites were prepared via melt processing. Three surfactants having different ammonium cations, as mentioned in chapter 5, were used

and their influence on the morphology and mechanical properties of the NBR/clay nanocomposites were investigated.

### 6.2.1 Characterisation using X-ray diffraction technique

The variation of the (001) d-spacing of the clay interlayer of the nanocomposites, which was calculated from the observed peaks by using the Bragg formula is shown in figure 6.13 – 6.15.

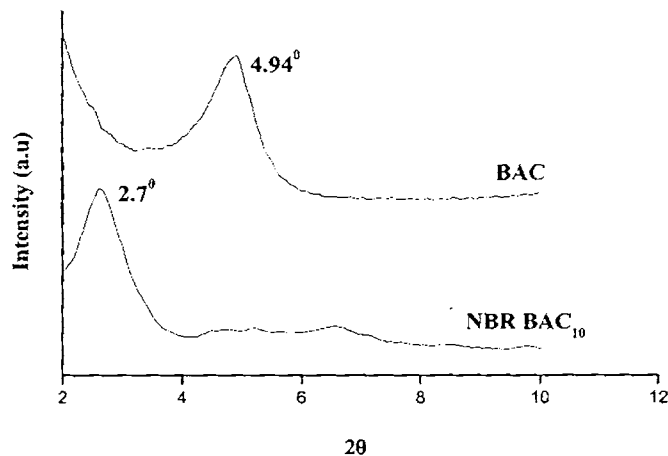


Figure 6.13 XRD patterns of BAC- modified clay and 10phr BAC -NBR nanocomposite

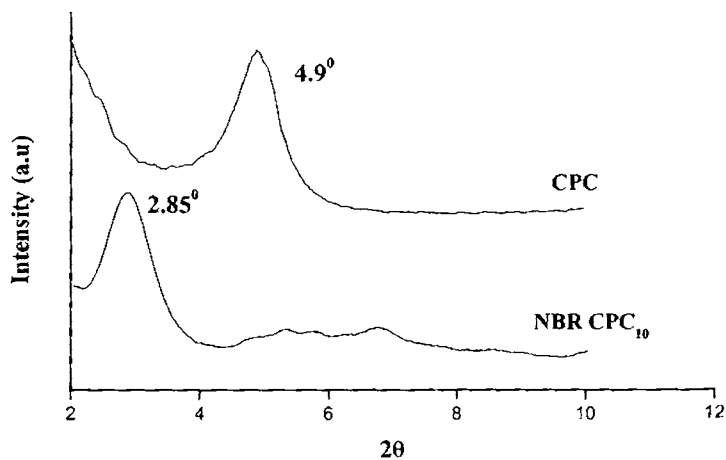
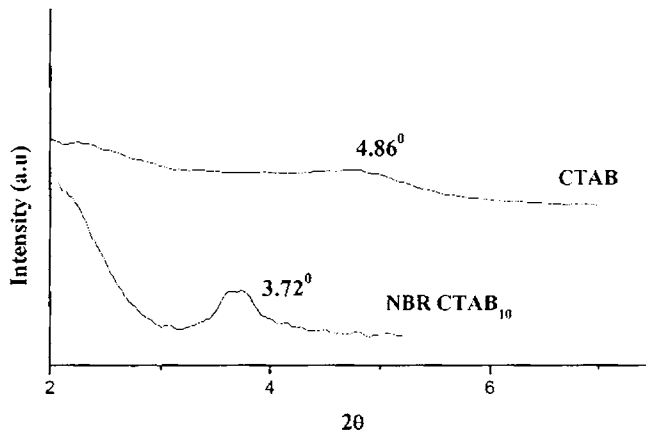


Figure 6.14 XRD patterns of CPC - modified clay and 10phr CPC -NBR nanocomposite

A shift in d-spacing for the modified clay-nanocomposites to a lower diffraction angles in comparison to that of the modified clay is obtained for the nanocomposites. Increase in d-spacing follows the order NBR - BAC > NBR - CPC > NBR - CTAB. The higher extent of intercalation corresponding to the largest interlayer distance of  $32.76 \text{ \AA}$  in NBR- BAC nanocomposite compared with  $23.69 \text{ \AA}$  for NBR-CTAB which has a relatively bulkier cation than the other two surfactants.



*Figure 6.15 XRD patterns of CTAB-modified clay and 10phr CTAB-NBR nanocomposite*

### 6.2.2 Cure Characteristics

When filler is incorporated into a rubber compound, the increase in maximum cure torque during vulcanization is directly proportional to the filler loading. Figure 6.16 depicts the relation between  $D_{\max} - D_{\min}$  ( $\Delta$  torque) and nanoclay loading. Where  $D_{\max} - D_{\min}$  is the change in maximum torque during vulcanisation. The increase in  $\Delta$  torque with filler loading indicates that the incorporation of nanoclay enhances the crosslinking between the polymer chains. Nanocomposite with BAC modified clay possess higher torque value which is confirmed by the swelling studies

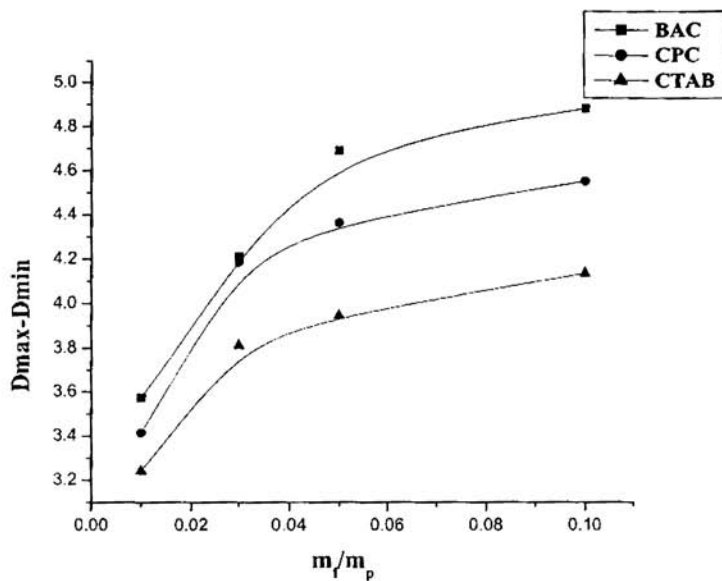


Figure 6.16 Variation of  $\Delta$  torque against filler loading

### 6.2.3 Mechanical Properties

The stress-strain properties of the vulcanisates prepared from rubber compounds having different nanoclay loading (0 to 10 phr) are given in the figures 6.17 to 6.20.

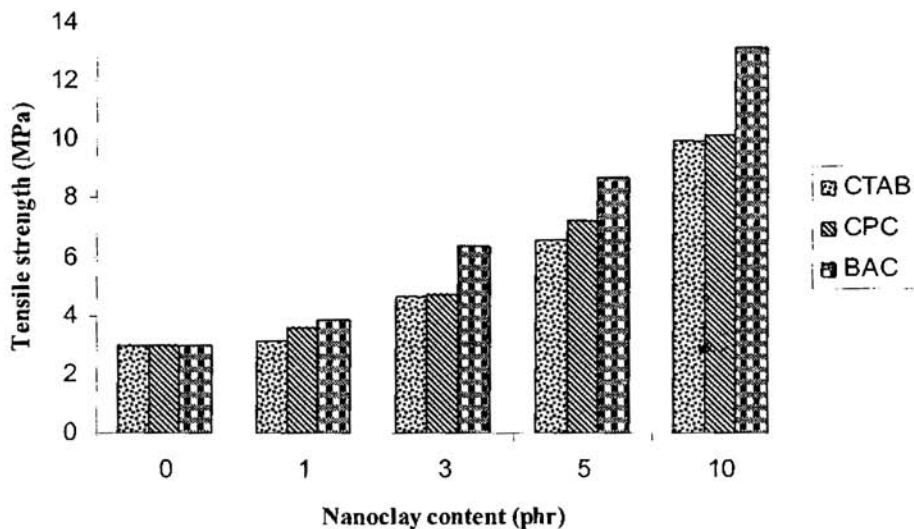
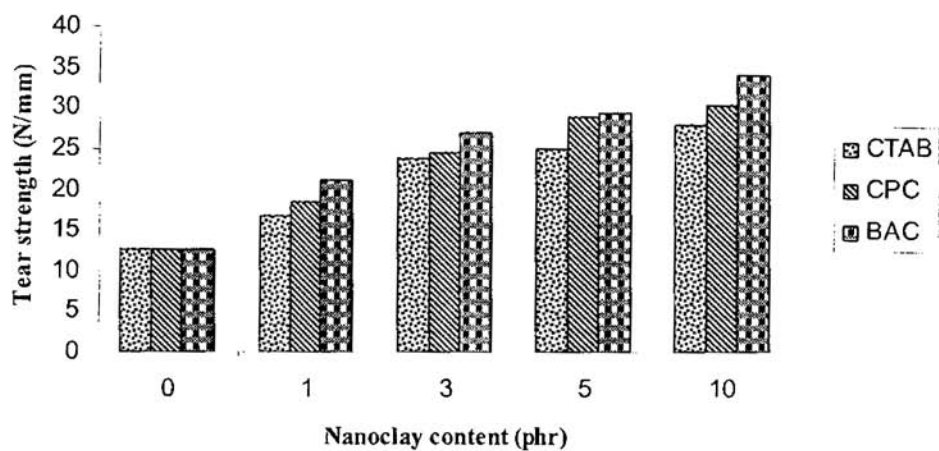
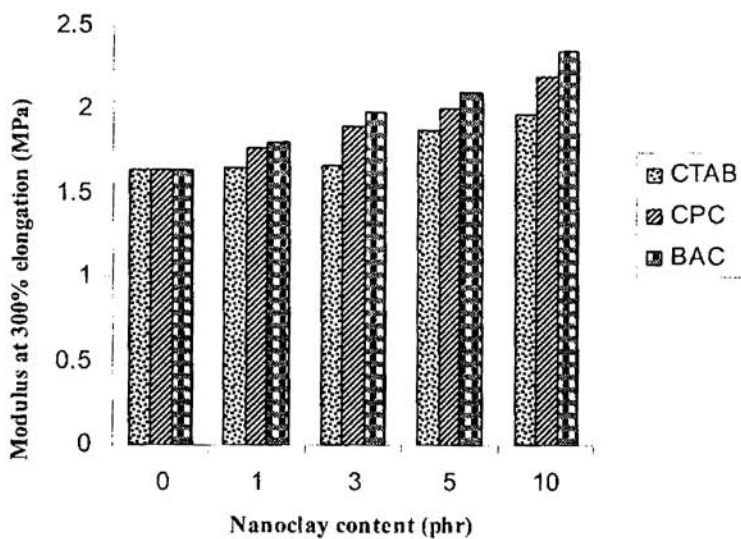


Figure 6.17 Tensile strength of nanocomposites





*Figure 6.18 Tear strength of nanocomposites*



*Figure 6.19 Modulus at 300% elongation of nanocomposites*

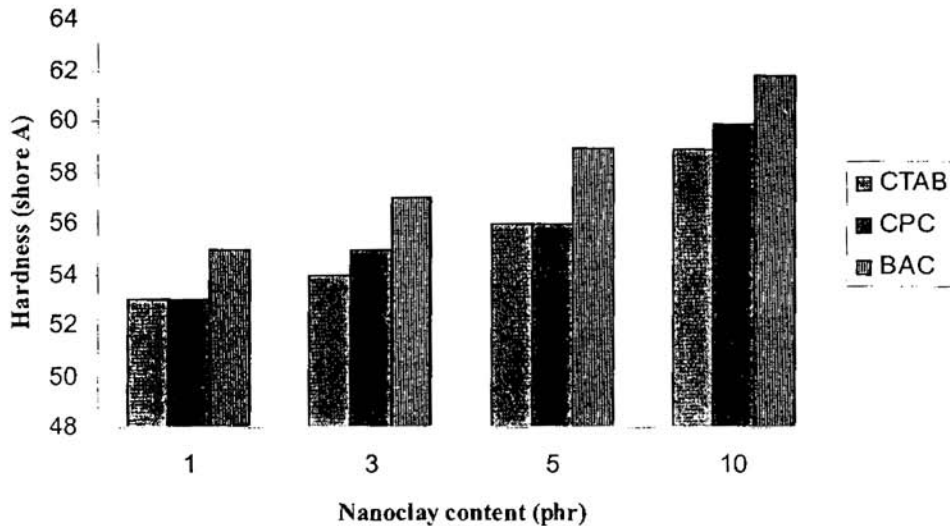


*Figure 6.20 Hardness of nanocomposites*

From these figures (6.17 to 6.20) it can be observed that properties like tensile strength, modulus at 300% elongation, hardness and tear strength of the composites increase with increase in nanoclay content. The largely increased reinforcement and the tear resistance of the nanocomposites should be ascribed to the dispersed structure of clay at the nano level, the high aspect ratio and the planar orientation of the silicate layers [14]. Tensile stress-strain measurements have been one of the standard methods for characterizing rubber vulcanisates [15]. Among the three organoclays used BAC modified clay imparts maximum improvement in mechanical properties for NBR vulcanisates. This is similar to the findings obtained for NR vulcanisates. The tensile strength of NBR – BAC clay nanocomposite exhibited 2.5 times higher value than that of conventional gum vulcanisates. This is followed by the nanocomposites obtained with CPC and CTAB modified clays. The organic part of the organoclay enables conversion of the hydrophilic interior clay surface to hydrophobic and increases the layer distance as well. Under this condition, the polymer chain is capable of diffusing easily into the clay galleries to increase the layer distance further.

### 6.2.4 Strain sweep studies

The complex modulus values of the nanocomposites with three different modified clays as a function of strain is plotted in figures 6.21 – 6.23. The complex modulus values are found to be increased with increase in nanoclay content. This trend is very distinct at lower strain; at higher strain the trend is not very clear. BAC modified clay nanocomposite possess higher storage modulus in all concentrations. The increase in storage modulus is due to the increase in cross linking density.

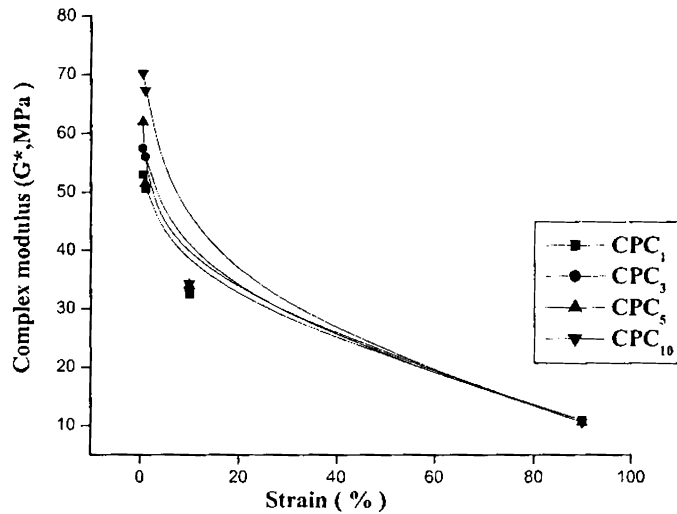


*Figure 6.21 Variation of complex modulus with clay content of CPC modified clay nanocomposites*

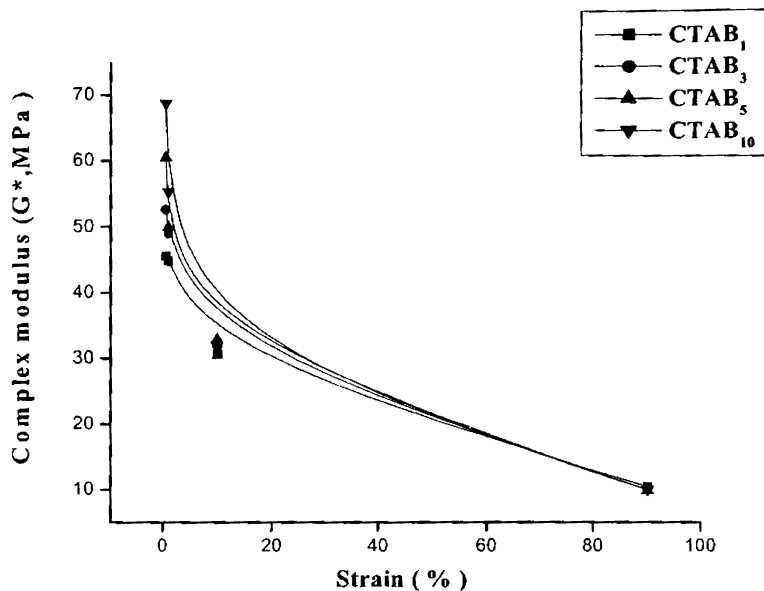


Figure 6.22 Variation of complex modulus with clay content of CTAB modified clay nanocomposites

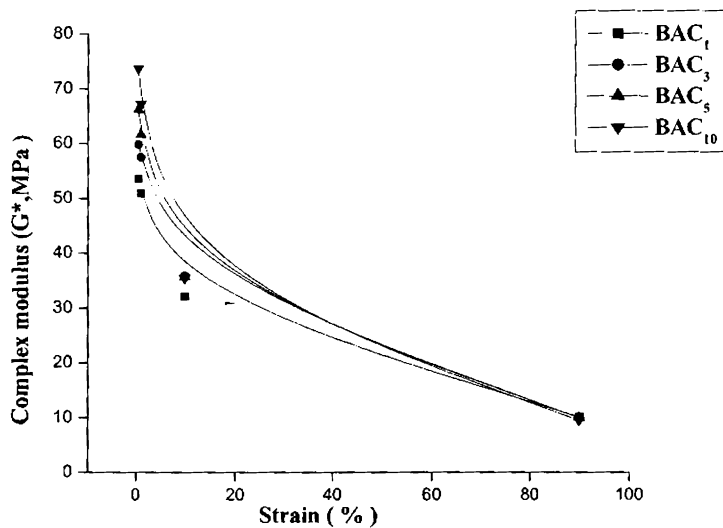


Figure 6.23 Variation of complex modulus with clay content of BAC modified clay nanocomposites

### 6.2.5 Swelling studies

Traditionally, the incorporation of nonporous fillers, such as metal oxides, silicas, or carbon blacks, into polymers reduces gas, solvents or vapor permeability. This decreased permeability is the result of a reduction in the amount of polymer through which transport may occur and an increase in the diffusion path length that penetrant molecules experience as they are forced to take a tortuous course around filler particles to traverse a film. From the figure 6.24, it is seen that at equilibrium swelling the maximum solvent uptake is higher for the gum vulcanisates than the nanocomposites. For NBR–organoclay nanocomposites, the swelling rate and swelling coefficient is decreased as the clay content increases as expected. This is because the solvent diffusion in the nanocomposite is impaired by the clay platelets and that these do not absorb solvent. It is also suggested that a significant clay – rubber adhesion, sufficient to limit rubber chain extension in the film plane in the presence of the solvent.

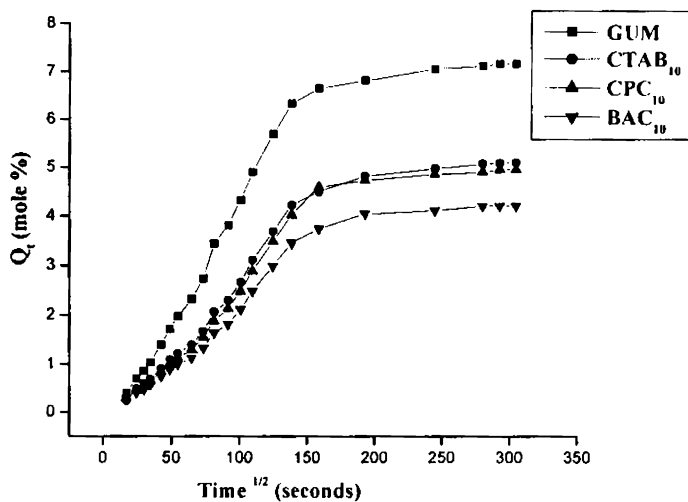


Figure 6.24 Sorption curves of the vulcanisates at 303K

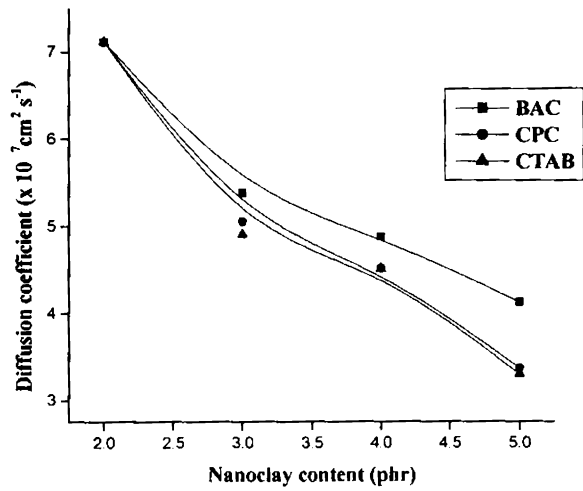


Figure 6.25 Variation of Diffusion coefficient with nanoclay loading

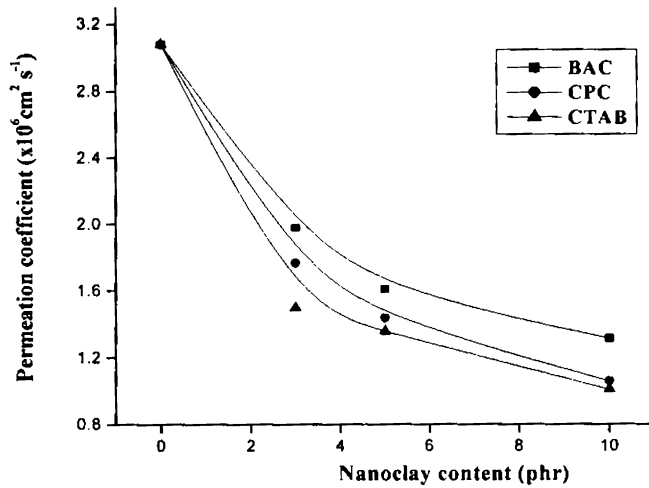


Figure 6.26 Variation of Permeation coefficient with nanoclay loading

From the figures 6.25 and 6.26 it is seen that the diffusion coefficient and permeation coefficient of the NBR vulcanisates is decreasing with increase in clay content. The coefficient of diffusion,  $D$ , may serve as an average (over a macro volume) rate of molecular transport. The local rate of moisture diffusion can substantially differ in the close vicinities of the clay particles, where molecular mobility is severely reduced because of intercalation of chains into galleries between platelets, and in the bulk, where mobility of chains is weakly affected by the presence of filler. This implies that the molecular transport in the nanocomposite becomes substantially heterogeneous as in the case of vinyl ester resin matrix-montmorillonite clay composites reported by Drozdov et al [16].

The degree of cross linking of nanocomposite is higher for BAC samples as suggested by the torque values. The amine groups facilitate the crosslink formation [17]. Both  $\Delta S$  and  $\Delta G$ , the thermodynamical parameters of the NBR clay nanocomposites are given in table 6.5. It should be noted that  $\Delta G$  values are higher for the nanocomposites. It is assumed that  $\Delta G$  is closely related to the elastic behaviour of the material, the nanocomposites shows better elasticity than the gum vulcanisate and it is higher for vulcanisate with 10phr of BAC modified clay. These results can be attributed to better compatibility between the silicate and rubber, the rubber molecules can penetrate into the galleries more easily giving rise to a process of exfoliation of the silicate layer. This exfoliation is responsible for the noticeable increase of entropy of the clay filled composites compared to gum vulcanisate.

**Table 6.5  $\Delta G$ ,  $\Delta S$  and Cross link density for gum and 10 phr of modified clay filled NBR vulcanisates**

Sample code	gum	CTAB <sub>10</sub>	CPC <sub>10</sub>	BAC <sub>10</sub>
Crosslink density ( $\nu$ ) $\times 10^4$ (moles gm <sup>-1</sup> )	1.37	1.69	1.77	1.85
$\Delta G$ (J mol <sup>-1</sup> )	-27.84	-35.64	-37.77	-39.76
$\Delta S \times 10^2$ (J mol <sup>-1</sup> )	0.91	1.17	1.24	1.31

### 6.3 Conclusion

Nitrile rubber-clay nanocomposites were prepared by shear mixing process and characterized by XRD for interlayer spacing. Effect of interlayer distance of the layered nanoclays in modifying the mechanical properties and swelling characteristics of the nitrile rubber based nanocomposites was studied. The tensile strength increases by more than 440% for 10phr cloisite 15A clay filled vulcanisate compared to the gum vulcanisate with a slight variation on the elongation at break. The large improvement in the ultimate properties of the composite is the result of nanolevel dispersed structure of the clay and the planar orientation of the silicate layers in the NBR matrix. The intercalated structure with maximum d-spacing presented the highest tortuosity leading to the lowest permeability for the solvent molecules.

Three different types of organoclays prepared by adopting the procedure mentioned in section 5.1 were used with nitrile rubber, and their nanocomposites were found to be intercalated. The scorch time of the nanocomposites were reduced due to cure acceleration by organic modifier present in the modified clays. Among the three organoclays used BAC modified clay imparts better improvement in mechanical properties for NBR based nanocomposites. This is similar to the findings observed for NR-organoclay nanocomposites.



## References

1. Blackley, D. C., Polymer lattices Science and technology, 2, Chapman and Hall, London, UK, 1997.
2. Zhang, W., Chen, D., Zhao, Q., Fang, Y., Polymer, 44, 7953, 2003.
3. Kojima, Y., Fukumori, K., Usuki, A., Okada, A. and Kurauchi, T., J. Mater. Sci. Lett., 12, 889, 1993.
4. Wu, Y., Jia, Q., Yu, D. and Zhang, L., J. Appl. Polym. Sci., 89, 3855, 2003.
5. Kim, J., Oh, T. and Lee, D., Polym. Int., 52, 1058, 2003.
6. Karger Kocsis, J. and Wu, C. M., Polym Eng Sci., 44, 1083, 2004.
7. Giannelis, E. P., Krishnamoorti, R. and Manias, E., Adv. Polym. Sci., 138, 107, 1999.
8. LeBaron, P. C., Wang, Z. and Pinnavaia, T. J., Appl. Clay Sci., 15, 11, 1999.
9. Yano, K., Usuki, A., Okada, A., Kuruachi, T. and Kamigaito, O., J. Polym. Sci., Part A, 31, 2493, 1993.
10. Yano, K., Usuki, A. and Okada, A., J. Polym. Sci., Part A, 35, 2289, 1997.
11. Giannelis, E. P. Adv. Mater., 8, 29, 1996.
12. Strawhecker, K. E. and Manias, E., Chem. Mater., 12, 2943, 2000.
13. Mousa, A. and Karger-Kocsis, J., Macromol. Mater. Eng., 286, 260, 2001.
14. Wu, Y.P., Jia, Q. X., Yu, D.S. and Zhang, L.Q., J Appl Polym Sci., 89, 3855, 2003.
15. ASTM D 412-83. American Chemical Society for Testing and Materials, Philadelphia, P A
16. Drozdov, A. D., Christiansen, J. Dec., Gupta, R. K., Shah, A. P., Journal of Polymer Science: Part B: Polymer Physics, Vol. 41, 476, 2003.

17. Konstantinos, G. Gatos and József Karger-Kocsis, *Polymer*, Vol.46(9), 3069, 2005

## *Chapter 7*

---

### *Conclusion*

This chapter provides a glimpse of the conclusions drawn from the research work carried out on rubber layered clay nanocomposites and the scope for the future work on polymer nanocomposites

Nanocomposites play a major role in the science and technology of the present day. Polymer nanocomposites especially rubber based nanocomposites is one of the many composite materials in which scientists and engineers are interested and find scope for possible exploitation of commercial applications.

Composites that exhibit a change in composition and structure over a nanometer scale have shown remarkable property enhancements relative to conventional composites. Because of their nanometer size, rubber clay nanocomposites exhibit markedly improved properties when compared to the pure polymers or their traditional composites. Most notable properties are increased tensile strength, tear strength, modulus, gas barrier properties, heat distortion temperature, resistance to small molecule permeation, ablative characteristics, resistance to atomic oxygen and retention in impact strength.

As the distance between the clay layers is less than 1nm it does not allow the penetration of the polymer molecules therein. So the space between the platelets or layered galleries of the silicate should be made accessible for the polymer chains. To support intercalation and exfoliation the interlayer distance should be greater than 1.5 nm and the layered structure should be broken down. Thus the polymer intercalation might be made more effective by increasing the interlayer distance.

Modification of the clay using organic surfactants improves the compatibility between filler and polymer matrix. The morphology and properties of nanocomposites are often greatly influenced by the properties of the modifying group. Thus an effort is made to find whether the surfactants containing different functional groups viz., an aliphatic, an aromatic and a heterocyclic group provided the best performance of the nanocomposite in natural rubber matrix, both in latex stage and dry rubber.

Preparation of rubber nanocomposites from latex is simple. The barrier properties of latex films have a prominent role in dipped goods. It is reported that quaternary ammonium salts possessing at least one substituent alkyl chain with minimum eight carbon atoms are able to kill micro-organisms such as bacteria and fungi. This area of the use of nanoclays in latex has been investigated in order to find the effect on antibacterial properties, tensile strength, modulus and elongation at break of natural rubber latex films.

Rubber-clay nanocomposite technology has been extended to synthetic rubbers besides natural rubber. The polarity of the polymer chains and the basal spacing of the clay are important for the structure of the polymer-clay nanocomposites. Thus the effect of the interlayer distance and the modifying groups of nanoclays in nitrile rubber matrix is evaluated.

This study mainly focused on the preparation and characterisation of rubber layered clay nanocomposites. Effect of interlayer distance of the layered clays on the cure characteristics, mechanical properties and transport properties of natural rubber nanocomposites were investigated. Maximum torque of the nanocomposite increased and a reduction in cure time was obtained, which shows the accelerating effect of organoclays in the curing of NR. This reduction in cure time is slightly boosted with the increase in interlayer distance of the clay. It is seen that the nanocomposite with the clay having higher interlayer distance shows the better mechanical properties. As the interlayer distance increases, polymer chains could penetrate more easily into the clay layers, which results in the formation of an intercalated structure.

Organosilane coupling agents improve the dispersion of clay platelets within the rubber organic phase and the clay-rubber interactions. Thus the organoclays, treated with the silane coupling agent behaved as an effective reinforcement agent for NR and showed a stronger reinforcing potential while retaining the elasticity of the rubber

Furthermore, the effects of carbon black on NR-clay nanocomposites were investigated. While carbon black alone offered improvement in the mechanical properties of the rubber, the synergism of organoclays and carbon black brought similar property enhancements. Incorporation of a small amount of nanoclay (1 phr) along with 30 phr carbon black in natural rubber shows an improvement in mechanical properties much greater than 40 phr of carbon black alone. Also, NR nanocomposites with a combination of nanoclay and carbon black had good barrier properties and better reduction in heat build up in comparison with compound containing carbon black alone.

Transport properties of natural rubber latex-clay nanocomposites with low level filler loading were studied in detail. A considerable decrease in diffusion, permeation and sorption coefficients were observed for the nanocomposites. About 70% reduction in diffusion coefficient with 3 phr nanoclay is obtained. It was observed that the decreasing value of the permeability of the nanocomposites was largely dominated by the diffusion phenomenon. The permeation resistance of the nanocomposite was confirmed by the gas permeability testing and it fits with the Nielson's model, which describes the tortousity effect of plate like particulates on gas permeability of polymer composite structures. Oxygen permeability of the natural rubber latex film is decreased by 66% with 1 phr loading of nanoclay. A 100% increase in modulus at 300% elongation and 65% increase in tensile strength were obtained for the nanocomposite with 3 phr clay loading compared to the gum vulcanisate. This also directs to the better reinforcement of clay layers in the rubber matrix. The thermodynamic parameters,  $\Delta S$  and  $\Delta G$  direct the formation of a better elastic and

exfoliated nanocomposite. As the barrier properties of latex films have a prominent role in dipped goods, it has high potential for commercialization.

Montmorillonite (MMT) clay functionalized with three different types of surfactant, an aliphatic, an aromatic and a heterocyclic group was prepared. Organophilic modification of the clays was confirmed from the XRD, TGA curves and IR spectrum. In the case of NR-organoclay nanocomposites, the chain length of the surfactant and functional groups determines the dispersion of clay nanolayers in the rubber matrix and the overall properties of the nanocomposites. Due to the better interaction between the rubber molecules and the surfactant used for the clay modification, clay modified with bulky surfactant shows better property improvement both in latex and dry stage. Permeation resistance reduced from 22.5 to 5.3 cm<sup>2</sup> s<sup>-1</sup> for the BAC modified natural rubber latex nanocomposite compared to gum vulcanisate.

Antibacterial activity of the three different organoclays-NR latex nanocomposites was determined against Gram positive bacteria, *Bacillus cereus* and Gram negative bacteria, *E.coli* using halo ring method. When the antibacterial property was determined, all the three organoclays-natural rubber latex nanocomposites possess antibacterial property against both Gram positive and Gram negative bacteria. The positively charged quaternary ammonium groups on the interlayer of clay surface could interact with the anionic molecule on the cell surface. This interaction could change the permeability of the cell membrane of the microorganisms, resulting in a leakage of intercellular components and then caused the death of the cell. This findings will help in the production of antibacterial polymeric products suitable as urethral catheters, gloves or the like, and the development of a process for preparing moulded product having the antibacterial properties. The urethral catheter can not be kept aseptic because of penetration of bacteria from outside or inside, outside of the catheter passageway is responsible for the development of infectious diseases such as urethritis, cystitis, pyelonephritis or the like. Consequently there is now a demand for improvements in urethral catheters which are having the antibacterial characteristics.

Further, a need has arisen for antibacterial gloves such as gloves for medical use in operations or inspection or for food-processing purposes in order to prevent the contamination of infectious diseases or to improve the hygienic conditions.

Nitrile rubber (NBR) was also used in the synthesis of rubber/clay nanocomposites. As in the case of natural rubber better physical properties were obtained for NBR based nanocomposites prepared with clay having higher interlayer distance. The tensile strength increases by more than 440% for 10 phr cloisite15A clay filled vulcanisate compared to the gum vulcanisate with a slight reduction in elongation at break. Better reinforcement potential of the modified clays is obtained for that with bulky surfactants as evident from the improvement in properties.

Systematic investigation into the various aspects of the antibacterial and antivirus properties of dipped goods meant for medical applications, based on natural rubber latex and organically modified nanoclays is a worthwhile research proposition that can be pursued further.

There is ample scope for carrying out extensive investigations on nanocomposites, based on synthetic rubber other than NBR and with various layered clays. Various intrincating phenomena taking place at the interface of the polymer and filler, polymer-polymer and filler-filler interfaces need to be understood properly. At increased surface to volume ratio, these interactions play a very dominant role in determining the overall properties of the composites. It would be interesting to carry out a similar study delving into the interactions taking place at the interface in these nanocomposites. This assumes importance from a theoretical perspective. Though it has been found that layered silicate becomes reinforcing in NR and NBR matrix and shows synergism with carbon black, much light could not be shed on the synergistic effect of these nanoclays with other reinforcing fillers like silica. This is a fit case for a systematic study.

## List of Abbreviations

ACN	Acrylonitrile
ASTM	American Society for Testing and Materials
BAC	Benzalkonium chloride
BIS	Bureau of Indian Standards
CB	Carbon Black
CBS	N- cyclohexyl-2-benzothiazole sulphenamide
CEC	Cation Exchange Capacity
cm	Centimetre
CPC	Cetyl pyridinium chloride
cP	Centi poise
CR	Chloroprene Rubber
CSBR	Carboxylated Styrene Butadiene Rubber
CTAB	Cetyl trimethyl ammonium bBromide
D	Diffusion coefficient
2M2HT	Dimethyl dihydrogenated tallow
2MBHT	Dimethyl benzyl hydrogenated tallow
DMA	Dynamic Mechanical Analysis
DRC	Dry Rubber Content
EB	Elongation at break
ENR	Epoxidized Natural Rubber
FEF	Fast Extrusion Furnace
FTIR	Fourier Transform Infrared Spectroscopy
GPF	General Purpose Furnace
HA	High Ammonia
HAF	High Abrasion Furnace
Hz	Hertz
ISAF	Intermediate Super Abrasion Furnace
ISNR	Indian Standard Natural Rubber
KOH number	Potassium Hydroxide number



LA	Low Ammonia
MMA	Methyl methacrylate
MMT	Montmorillonite
MPa	Mega pascal
MST	Mechanical Stability Time
NBR	Acrylonitrile Butadiene Rubber
nm	Nano meter
NMR	Nuclear magnetic Resonance
NR	Natural Rubber
NRL	Natural Rubber Latex
P	Permeation coefficient
PCN	Polymer clay nanocomposites
PET	Polyethylene terephthalate
phr	Parts per hundred rubber
PRI	Plasticity Retention Index
R	Universal gas constant
RPA	Rubber Process Analyzer
S	Sorption coefficient
SAF	Super Abrasion Furnace
SAXS	Small angle X-ray diffraction
SBR	Styrene Butadiene Rubber
SEM	Scanning Electron Microscopy
Si69	Bis- ( triethoxy silyl propyl) tetrasulphide
SPP	Sodium pentachlorophenolate
SRF	Semi Reinforcing Furnace
TEM	Transmission Electron Microscopy
TGA	Thermo Gravimetric Analysis
TMTD	Tetra methyl thiuram disulfide
TSC	Total Solid Content
UTM	Universal Testing Machine
VFA number	Volatile Fatty Acid number

WAXD

XRD

ZDC

Wide angle X-ray diffraction

X-Ray Diffraction

Zinc diethyldithio carbamate

## List of Symbols

T	Absolute temperature
Å	Angstrom
G*	Complex modulus
°C	Degree Celsius
$\rho_p$	Density of polymer
$\rho_s$	Density of solvent
$\Delta S$	Entropy change
$\alpha_\phi$	Filler specific constant
$\Delta G$	Change in Gibbs free energy
$\beta$	Lattice Constant
g	Gram
Tan $\delta$	Loss factor
G''	Loss modulus
M <sub>H</sub>	Maximum torque
m	Metre
$\mu\text{m}$	Micrometre
M <sub>L</sub>	Minimum torque
meq	Milliequivalent
M <sub>c</sub>	Molar mass between crosslinks
V <sub>s</sub>	Molar volume of the solvent
t <sub>90</sub>	Optimum cure time
t <sub>10</sub>	Scorch time
$\delta_p$	Solubility parameters of polymer
$\delta_s$	Solubility parameters of solvent
A <sub>0</sub>	Solvent uptake of the polymer
G'	Storage modulus
V <sub>r</sub>	Volume fraction of swollen polymer
$\phi_\phi$	Volume fraction of the clay in the polymer sample
$\lambda$	Wave length of X-ray
W <sub>s</sub>	Weight of the solvent at equilibrium swelling

## **List of Publications**

1. **Ansu Jacob**, Philip Kurian, Abi Santhosh Aprem, Transport properties of natural rubber latex layered silicate nanocomposites, *Journal of Applied Polymer Science*, 108, 4, 2623-2629, 2008.
2. **Ansu Jacob**, Philip Kurian, Abi Santhosh Aprem, Preparation and characterisation of natural rubber organoclay nanocomposites, *Journal of Polymeric Materials* 56, 593-604, 2007.
3. **Ansu Jacob**, Philip Kurian, Antimicrobial studies of natural rubber latex layered clay nanocomposites, *Polymer*, Elsevier (communicated).
4. **Ansu Jacob**, Philip Kurian, Effect of modifying groups on natural rubber based nanocomposites, *European Polymer Journal*, (communicated).

## **Conference Papers**

1. **Ansu Jacob**, Philip Kurian, Abi Santhosh Aprem, Effect of interlayer distance of nanoclays on mechanical and cure characteristics of natural rubber based nanocomposites, Kerala Science Congress, 17th-19th, January, 2006, Akkulam, Trivandrum.
2. **Ansu Jacob**, Philip Kurian, Mechanical Properties and swelling characteristics of nitrile rubber based clay nanocomposites, Kerala Science Congress, 2007, 29th-31th January, 2007, Kannur.
3. **Ansu Jacob**, Philip Kurian, Effect of nanoclay on carbon black filled NR composites ICMSRN – 2008, 27th – 29th February, 2008, Mother Teresa Women's University, Kodaikanal, Tamil Nadu.